Università degli Studi di Padova
Dipartimento di Farmacologia ed Anestesiologia

Scuola di Dottorato in Scienze Farmacologiche
Indirizzo Farmacologia Molecolare e Cellulare
XXIV Ciclo

Analysis of the molecular mechanisms of the antineoplastic effect of ouabain

Direttore della Scuola: Ch.mo Prof. Pietro Giusti
Dipartimento di Farmacologia ed Anestesiologia
Università degli Studi di Padova

Coordinatore d'indirizzo: Ch.mo Prof. Pietro Giusti
Dipartimento di Farmacologia ed Anestesiologia
Università degli Studi di Padova

Supervisore: Dott.ssa Lucia Trevisi
Dipartimento di Farmacologia ed Anestesiologia
Università degli Studi di Padova

Dottorando : Annalisa Trenti

To Luca

Index

Abstract

Ouabain is a cardiac glycoside whose primary action is inhibition of Na/K ATPase activity, a ubiquitous enzyme responsible for translocating Na and K ions across the cell membrane using ATP as the driving force. It has been demonstrated that the Na/K ATPase also functions as a classical receptor, capable of converting cardiac glycodise binding into activation of various protein kinase cascades (Liu and Xie, 2010). Also, recent studies have shown that cardiac glycosides selectively inhibit cell proliferation and/or induce apoptosis in several cancer cell lines (Schoner and Sheiner-Bobis, 2007). These *in vitro* studies are supported by epidemiological data reporting a protection from several types of cancer in patients who were on cardiac glycoside treatment (Stenkvist, 1999; Haux 1999; Haux *et al*, 2001).

To elucidate the cellular and molecular mechanisms underlying cardiac glycoside effect against cancer cells, we studied the effect of ouabain (1-100 nM) on two cancer cell lines, Jurkat (human T cell lymphoblast-like cell line) and A549 (human lung adenocarcinoma epithelial cell line). Ouabain (1-20 nM) induced a concentration-dependent decrease in proliferation of both cell lines. At higher concentrations (50-100 nM) ouabain was cytotoxic for the two cancer cell lines, as demonstrated by the increase in Annexin V/propidium iodide binding. At the same concentrations, ouabain did not affect cell viability of peripheral blood mononuclear cells (PBMC) and, as previously shown in our laboratory, protected from apoptosis human umbilical vein endothelial cells (HUVEC) (Trevisi L *et al.*, 2004).

Ouabain increased Src and ERK1/2 phosphorylation in A549 and Jurkat thus demonstrating the activation of the known signaling pathways triggered by Na/K ATPase signalosome. However, pharmacological inhibition of Src or MEK did not abolish the cytotoxic activity of ouabain. In both cell lines ouabain caused a decrease of phospho-Akt levels.

Decrease of Bcl-2 protein levels and mitochondrial membrane potential were early events of ouabain treatment in both cell lines. However, only in Jurkat cells were observed caspase 3/7 activation, DNA ladder fragmentation and inhibition of cell death by the *pan*

caspase inhibitor Z-VAD-fmk, hallmarks of caspase-dependent apoptosis. On the other hand, a marker of autophagy, i.e. conversion of LC3-I to LC3-II isoform, was observed in ouabain-treated A549. Moreover, ouabain enhanced the autophagic flux in A549 as demonstrated by increase of p62 degradation and increase of punctate pattern of LC3 after co-incubation with chloroquine, a drug that blocks fusion of autophagosomes with lysosomes. Furthermore, cell death induced by ouabain was completely blocked by treatment with an inhibitor of autophagy such as 3-methyladenine. It has been suggested that decrease of Bcl-2 levels could induce autophagy since Bcl-2 interacts with the autophagic protein Beclin 1, inhibiting the formation of the autophagy initiation complex (Pattingre S *et al*., 2005). This interaction is regulated by JNK because JNK-dependent phosphorylation of Bcl-2 causes Bcl-2 degradation and disruption of Bcl-2/Beclin1 complex. In A549 treated with ouabain the levels of Beclin 1 were manteined costant. However, inhibition of JNK with SP600125 blocked cell death induced by ouabain only in A549. We speculate that JNK activation by ouabain in A549 reduces Bcl-2 levels thus releasing Beclin 1 and inducing autophagy. Further studies will be required to confirm this hypothesis.

Finally, to ascertain whether differences in sensitivity to ouabain among normal and cancer cells are related to a specific pattern of Na/K ATPase α subunit isoform expression, western blotting analysis of α isoforms was performed in Jurkat and A549 cells and compared to the expression pattern of two normal cell lines: HUVEC and PBMC. We found that α1 isoform is ubiquitous, α2 isoform is not expressed only in PBMC and that α3 isoform is expressed exclusively in the two cancer cell lines. These data suggest that α3 subunit could be critical for ouabain cytotoxic effect.

Riassunto

L'ouabaina é un glicoside cardioattivo la cui azione più nota è l'inibizione della Na/K ATPasi, enzima ubiquitario della membrana plasmatica responsabile del trasporto di ioni Na e K attraveso le membrane utilizzando ATP come forza motrice. È stato dimostrato che la Na/K ATPasi, oltre alla sua funzione di pompa, é in grado di agire come recettore, attivando varie cascate di segnale (Liu and Xie, 2010). Studi recenti hanno dimostrato che i glicosidi cardioattivi inibiscono in maniera selettiva la proliferazione e/o inducono apoptosi in diverse linee di cellule tumorali (Schoner and Sheiner-Bobis, 2007). Questi studi *in vitro* sono supportati da dati epidemiologici che evidenziano una protezione da vari tipi di cancro in pazienti trattati con glicosidi cardioattivi (Stenkvist, 1999; Haux 1999; Haux *et al*, 2001).

Al fine di chiarire il meccanismo molecolare e cellulare alla base dell'effetto citotossico dei glicosidi cardioattivi sulle cellule tumorali, abbiamo studiato gli effetti dell'ouabaina (1-100 nM) nei confronti di due linee cellulari tumorali, le Jurkat (una linea proveniente da un linfoma a cellule T) e le A549 (linea ottenuta da carcinoma bronchiolo-alveolare). Il trattamento con ouabaina (1-20 nM) provocava una diminuzione della proliferazione cellulare concentrazione dipendente in entrambe le linee cellulari. Alle concentrazioni più elevate (50-100 nM) l'ouabaina era citotossica per le due linee cellulari testate, come dimostrato dall'aumento di cellule Annessina V/propidio positive. Alle stesse concentrazioni l'ouabaina non alterava la vitalità delle cellule mononucleate estratte da sangue periferico umano (PBMC) e, come già dimostrato nel nostro laboratorio, proteggeva dall'apoptosi le cellule endoteliali della vena ombelicale umana (HUVEC) (Trevisi L *et al.*, 2004).

Il trattamento con ouabaina induceva l'attivazione delle chinasi Src ed ERK1/2 in entrambe le linee cellulari, confermando così la stimolazione della nota cascata di segnale innescata dala Na/K ATPasi. Tuttavia, l'inibizione farmacologica della Src o della MEK non contrastava l'effetto citotossico dell'ouabaina. In entrambe le linee cellulari il trattamento con ouabaina induceva una diminuzione della fosforilazione di Akt.

In entrambe le linee cellulari, la diminuzione della proteina antiapoptotica Bcl-2 e del

potenziale di membrana mitocondriale costituivano gli eventi iniziali a seguito del trattamento con ouabaina. Tuttavia, solo nelle Jurkat sono stati riscontrati alcune marcatori dell'apoptosi caspasi-dipendente quali l'attivazione delle caspasi 3/7, la tipica frammentazione del DNA (*DNA ladder*) e l'inibizione della morte cellulare indotta dall'inibitore *pan* caspasico Z-VAD-fmk. Al contrario nelle A549 sono stati riscontrati i classici marcatori di autofagia come la conversione di LC3 dalla forma LC3-I alla isoforma LC3-II. Inoltre l'ouabaina aumentava il flusso autofagico nelle A549, come dimostrato dall'aumento della degradazione di p62 e dall'aumento delle forme puntate di LC3 in caso di co-incubazione con clorochina, un inibitore della fusione lisosomi-autofagosomi. Infine la morte cellulare indotta da ouabaina era bloccata dal trattamento con l'inibitore dell'autofagia 3-metiladenina. È stato ipotizzato che la diminuzione della Bcl-2 induca autofagia in quanto la Bcl-2 interagisce con Beclin 1 prevenendo così la formazione del complesso di iniziazione (Pattingre S *et al*., 2005). Tale interazione è regolata da JNK, la quale fosforilando Bcl-2, causa la sua degradazione e la rottura del complesso Bcl-2/Beclin 1. Nelle A549 trattate con ouabaina i livelli di Beclin 1 erano costanti, ma l'inibizione di JNK con SP600125 bloccava la morte cellulare. Noi ipotizziamo che l'attivazione di JNK da parte dell'ouabaina nelle A549 riduca i livelli di Bcl-2 permettendo il rilascio di Beclin 1 e di conseguenza attivi il processo di autofagia. Ulteriori studi saranno necessari per chiarire questo punto.

Infine, attraverso l'analisi western blotting è stata studiata l'espressione delle varie isoforme della subunità α della Na/K ATPase nelle due linee tumorali studiate (A549 e Jurkat) e paragonata a quella di due linee normali (HUVEC e PBMC), allo scopo di verificare se le differenze nella sensibilità all'ouabaina fra cellule normali e tumorali possano essere ascritte ad uno specifico tipo di espressione della varie isoforme della subunità α. I nostri risultati indicano che l'isoforma α1 è ubiquitaria, l'isoforma α2 non è espressa solo nei PBMC mentre l'isoforma α3 è espressa solo nelle due linee cellulari tumorali. Questo dato suggerisce che la subunità α3 possa essere determinante per gli effetti citotossici dei glicosidi cardioattivi nei confronti delle cellule tumorali.

List of Abbreviations

3 MA	3-methyladenine
4NQO	4-nitroquinoline-N-oxide
ACTH	adrenocorticotropic hormone
AIF	apoptosis inducing factor
Akt	protein kinase B
AMPK	AMP activated protein kinase
AP-1	Activator Protein-1
Apaf-1	Apoptotic Protein Activating Factor-1
ATG	autophagy related genes
ATP	Adenosine triphosphate
Bad	Bcl-2 associated death
Bcl	B-cell lymphoma
BECN1	Beclin 1
BH	Bcl-2 Homology
Bid	Bcl-2 interacting domain
Ca	calcium
CAD	caspase-activated DNase
cDNA	complementary DNA
CMB	caveolin binding motif
CM-H_2DCFDA	chloromethyl-dichlorodihydrofluoresceindiacetate
CTS	cardiac glycosides
DAP1	death-associated protein 1
DAPK	death-associated protein kinase
DD	death domain
DEPC	diethylpyrocarbonate
DIABLO	direct IAP binding protein with low pI
DISC	death-inducing signaling somplex
DMBA	7,12-dimethylbenz[a]anthracene
DMEM	Dublecco’s modified Eagle medium
DMSO	dimetilsulfoxide
DNA	deoxyribonucleic acid
dNTP	deoxiribonucleotide
DRAM	damage regulated autophagy modulator
dsDNA	double-stranded DNA
EDTA	ethylene-diamine-tetraacetic acid
EGFR	endothelial growth factor receptor
ERK	extracellular regulated kinases

FADD	Fas-Associated protein with Death Domain
FasL	Fas ligand
FBS	fetal bovine serum
FGF2	fibroblast growth factor 2
FKHR	Forkhead transcription factors
FLIP	FLICE-Inhibitory Protein
FOXO	hepatocite nuclear factor 3
GAPDH	glyceraldehyde 3-phosphate dehydrogenase
GC	guanine cysteine
GPCR	G-protein coupled receptor
Grb2	growth factor receptor-bound protein 2
GSK	glycogen shyntase kinase
HNF3A	hepatocite nuclear factor 3
HOXB13	homeobox protein Hox-B13
HRP	horseradish peroxidase
HUVEC	human umbilical endothelial cell
IAP	inhibitor of Apoptotic Proteases
ICAD	inhibitor of CAD
IL	interleukin
IP3	inositol-1,4,5-trisphosphate
IP3R	IP 3 receptor
JNK	C Jun N-terminal Kinase
K	potassium
K_d	dissociation constant
LAMP	lysosomal-associated membrane proteins
LC3	light chain 3
MAPK	mitogen-activated protein kinase
MEK	extracellular signal-regulated kinase
mRNA	messanger RNA
mTOR	mammalian target of rapamyacin
mTORC1	mTOR complex 1
MTT	3-(4,5-dimethylthiazol-2-yl)-2,5-diphenyltetrazolium bromide
MβCD	methylcyclodextrin
Na	sodium
NAC	N-acetylcystein
NCX	Na^+/Ca^{2+} exchange system
NF- κB	nuclear factor κB
NSCLC	non small cell lung cancer
OMM	outer mitochondrial membrane
PARP-	poly(ADP)ribose polymerase
PAS	preautophagosomal structure
PBMC	peripheral blood mononuclear cells
PBS	hosphate buffer saline
PCR	polimerase chain reaction

PE	phosphotidylethanolamine
PI	ropidium iodide
PI3K	phosphatidylinositide 3 kinase
PKA	protein kinase A
PKC	protein kinase C
PLC	phospho-lipase C
PP2	amino-5-(4-chlorophenyl)-7-(t-butyl)pyrazolo[3,4-d]pyrimidine
PS	phosphatidylserine
PST-2238	rostafuroxin
RNA	ribonucleic acid
ROS	reactive oxygen species
RTK	tirosin-kinases-receptors
RT-PCR	reverse transcriptase PCR
SE	tandard error
siRNA	small interfering RNAs
Smac	second mitochondrial activator of caspases;
TAE	tris-acetate-EDTA
TCA	tricarboxylic acid cycle
TMRM	tetramethylrhodamine methyl ester
TNF	tumor necrosis factor
TNFR	NF receptor
TPA	12-O-tetradecanoylphorbol-13-acetate
TRADD	TNF-R type 1-Associated Death Domain protein
ULK	unc-51-like kinase
UNBS1450	2"-oxovoruscharin
UTR	untraslated region
UVRAG	ultraviolet radiation resistance-associated gene
Z-VAD-fmk	Benzyloxycarbonyl-Val-Ala Asp(OMe)fluoromethylketone

Introduction

1.1 The sodium pump: Na/K ATPase

The sodium pump is found in the cells of all higher eukaryotes and is responsible for translocating sodium and potassium ions across the cell membrane utilising ATP as the driving force (Lingrel and Kuntzeiler, 1994; Horisberger, 2004). The existence of an ATP hydrolysing enzyme that requires the presence of sodium and potassium for activity was first demonstrated conclusively in crab nerve by Jens Christian Skou (Skou, 1957). In 1997 Jens Christian Skou was awarded with the Nobel Prize for his outstanding contribution to the field of Na/K ATPase research.

The Na/K ATPase belongs to the family of P-type ATPases, enzymes that become autophosphorylated by the γ phosphate group of the ATP molecule that they hydrolyse. For every molecule of ATP hydrolysed, three Na^+ ions from the intracellular space and two K^+ ions from the external medium are exchanged. The Na/K ATPase has two conformational states, E1 and E2. Na/K ATPase binds Na+ and ATP in the E1 conformational state and is phosphorylated at an aspartate residue. This leads to the occlusion of three Na+ ions and then to their release on the extracellular side. This new conformational state (E2-P) binds K+ with high affinity. Binding of K+ leads to dephosphorylation of the enzyme and to the occlusion of two K+ cations. K+ is then released to the cytosol after ATP binds to the enzyme with low affinity. Thus, the sodium pump contributes substantially to the maintenance of the membrane potential of the cell, provides the basis for neuronal communication and muscle contractility and contributes to the osmotic regulation of the cell volume. In addition, the electrochemical Na+ gradient is the driving force behind secondary transport systems (Horisberger, 2004; Scheiner-Bobis, 2002).

1.1.1 The structure of Na/K ATPase

The sodium pump is composed of two subunits in equimolar ratios: (i) the α catalytic subunit which is a multipass transmembrane protein containing the binding sites for Na^+, K^+, ATP and cardiac glycoside, and (ii) the β regulatory subunit, a transmembrane protein with several glycosylation sites, required for the biogenesis and activity of the enzyme complex. There are four different α and three β subunit isoforms identified that are selectively expressed in various tissues (Lingrel and Kuntzweiler, 1994; Blanco *et al*, 1999; Blanco, 2005). All possible α,β combinations result in catalytically competent enzymes, indicating that multiple Na/K ATPase isozymes can operate in the cell (Horisberger, 2004; Blanco, 2005a; Blanco *et al, 1995;* Blanco *et al,* 1997, Blanco and Mercer, 1998, Yu *et al,* 1997*;* Crambert *et al*., 2000). In certain cells and tissues a third subunit type has been found to be associated with functional Na/K ATPase (Geering, 2005; Geering, 2006). The members of this third type of subunit are regulatory single span (except for FXYD3: which is double span) type I transmembrane proteins from the FXYD family, that are able to modify sodium pump transport properties in a tissue- and isoform-specific manner (figure 1). To date seven members (FXYD1–7) of this family have been described. Li et al. (Li *et al*, 2004) have shown that FXYD2 (first discovered and named the γ subunit), FXYD4 and FXYD7 interact with α subunit TM9 segment. Co-expressing FXYD5 with the α1 and β1 subunits of Na/K ATPase in Xenopus oocytes elicited a more than 2-fold increase in pump activity (Lubarski *et al*, 2005). FXYD1, FXYD2 and FXYD3 decrease but FXYD4 increases sodium affinity, while FXYD2 increases ATP affinity. Additionally, FXYD7 decreases the apparent K^+ affinity of α1β1 and α2β1 but not of α3β1 isozymes (Beguin *et al*, 2002). Increasing numbers of publications emphasize the role, structure and functions of these proteins, revealing them to be fine regulators of sodium pump functions.

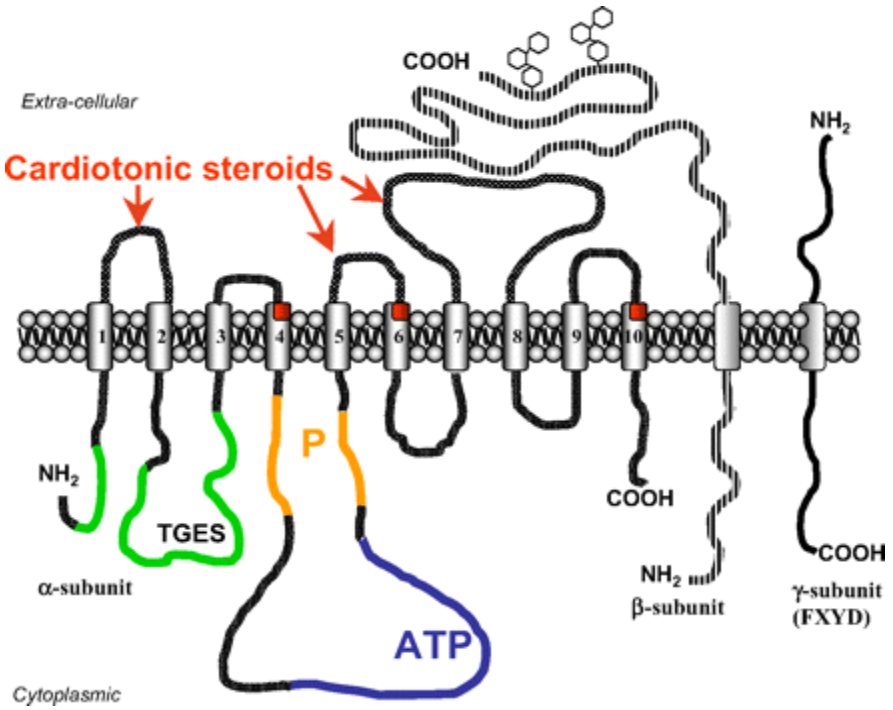

Figure 1. *Structure of Na+/K+-ATPase.* Na+/K+-ATPase consists of two α and β polypeptides in equimolar ratios. The α catalytic subunit has 10 transmembrane segments, schematically presented in an "unfolded" disposition; in fact, there is a bungle around M4, M5, and M6 transmembrane segments. The extracellular segments of α subunit form a binding site for CTS (shown in red), which include TM1–TM2, TM5–TM6, and TM7–TM8 loops and several amino acids from the transmembrane regions M4, M6, and M10. The binding site for ATP is located on the intracellular loop TM4–TM5 (shown in blue), which forms the "pocket" for this nucleotide. The phosphorylation domain (P; shown in orange) is located on the proximal and distal parts of intracellular loop TM4–TM5. The actuator domain, specifically its TGES motif, is responsible for the dephosphorylation step; it is constituted by the cytoplasmic NH2-terminal and TM2–TM3 intracellular loop (shown in green). The regulatory β glycoprotein subunit is a single-transmembrane protein with a several glycosylation sites (two are shown). The extracellular part of β subunit interacts with a conserved motif SYGQ on the extracellular loop TM7–TM8 of α subunit. The αβ-subunit complex of Na+/K+-ATPase associates with third subunit, which contains the conserved motif FXYD identical for all seven proteins from this family. FXYD2 protein is known as the earlier described γ subunit of Na+/K+-ATPase. These proteins, including the γ subunit, are not an integral part of sodium pump, but they are associated with specific domains of αβ-subunit complex and modulate catalytic properties of the Na+/K+-ATPase. From Bagrov *et al*, 2009

Na/K ATPase under normal conditions operates at a low percentage of its maximum pumping capacity (Lytton *et al*, 1985, Skou, 1992; Walters *et al*, 1999). Several reports have suggested that basal Na/K ATPase activity in intact cells is one third of its maximum capacity (Skou, 1992). In fact, α1 containing isozymes pump at half their maximum capacity (Walters *et al*, 1999) and α2 containing isozymes pump at 1/20 of their maximum (Lytton *et al*, 1985). Therefore, the Na/K ATPase appears to have an important reserve capacity thought to be sufficient to maintain normal ion transport even in pathological conditions associated with down-regulation of its expression and/or activity. Thus harnessing this reserve capacity represents a mechanism by which cellular Na/K ATPase activity can be rapidly upregulated.

1.1.2 Na/K ATPase expression and regulation

Studies on Na/K ATPase isozyme/subunit expression have demonstrated a tissue-specific expression pattern (Blanco *et al*, 2005a; Blanco *et al*, 2005b; Mobasheri *et al*, 2000). Among the sodium pump isozymes, α1β1 is the most widely expressed in nearly every tissue and is often the major form of the enzyme, while other α and β subunit combinations exhibit a much more restricted pattern of expression (Blanco *et al*, 2005a; Blanco *et al*, 2005b; Mobasheri *et al*, 2000). The distribution of the α1 isoform is ubiquitous (Blanco and Mercer, 1998). The α2 isoform is expressed in adult heart (Zahler *et al.*, 1992; Shamraj *et al*., 1993), vascular smooth muscle (Zhang *et al*., 2005), skeletal muscle (Hundal *et al*., 1992), brain (Urayama *et al*., 1989; McGrail *et al*., 1991), adipocytes (Lytton *et al*., 1985), and cartilage and bone (Mobasheri *et al*., 2000). The expression of the α2 isoform is also insulin-dependent (Russo and Sweadner, 1993). The α3 isozyme is expressed mostly in excitable tissues (Urayama *et al*., 1989), being most abundant in the central and peripheral nervous tissues (Hieber *et al*., 1991; McGrail *et al*., 1991) and in the conductive system of the heart (Zahler *et al*., 1992). It is noteworthy that the α4 isoform seems to be testis-specific (Shamraj and Lingrel, 1994). The expression of β1 is also ubiquitous. The β2 and β3 isoforms are expressed in brain, cartilage, and erythrocytes, whereas β2 can also be found in cardiac tissues and β3 can be observed in lung tissues. Studies of the artificial expression of different combinations of α and β isoforms in heterologous cells have revealed that the α subunit isozymes are responsible

for substrate and cardiac glycoside affinities of human Na/K ATPase (Mueller-Ehmsen *et al*., 2001) and also demonstrated an important function of the β subunit (Blanco *et al*., 1995; Blanco and Mercer, 1998; Pierre *et al*., 2008).

Overall, Na/K ATPase is most abundantly expressed in ion-transporting epithelia (e.g. kidney) and in excitable tissues such as the brain, skeletal muscle and cardiac muscle (Ernst and Mills, 1980; Sweadner, 1989; Lingrel *et al*, 1990; Katzmarzyk *et al*, 1999; James *et al*, 1999; Jaitovich and Bertorello 2006). Tissue-dependent variation in Na/K ATPase expression can reach differences of 160,000 fold (erythrocytes vs. brain cortex), while vascular smooth muscle with 400,000–700,000 pumps/cell has 100 times lower levels than heart muscle, as evaluated by means of ^{3}H-ouabain binding (Kjeldsen *et al*, 1988; Aydemir-Koksoy and Allen, 2001; Aydemir-Koksoy, 2002). Besides this tissue-specific expression pattern under normal physiological conditions, sodium pump isoform expression is specifically altered in a tissue-specific manner in diseases such as hyper- and hypothyroidism, hypokalemia, hypertension, heart failure (Magyar *et al*, 1995; McDonough *et al*, 1996; Kim *et al*, 1994; Schwinger *et al*, 1999) and also in cancer cells and tissues (Espineda *et al*, 2003; Sakai *et al*, 2004; Rajasekaran *et al*, 1999; Mijatovic *et al*, 2007; Espineda *et al*, 2004; Blok *et al*, 2004; Akopyanz *et al*, 1991; Boukerche *et al*, 2004). Additionally, certain FXYD proteins are expressed or over-expressed in cancer. Sodium pump isoform expression is also developmentally regulated; in fact rat fetal heart expresses α1 and α3, while rat adult heart expresses α1 and α2 (Blanco *et al*, 2005; Blanco, 2005a; Mobasheri *et al*, 2000). It is interesting to note that in vitro culture conditions can significantly influence sodium pump isoform expression. Rat cardiomyocytes cultured in serum-free medium display a neonatal Na/K ATPase isoform composition of α1 and α3. In contrast, those cultured in serum-supplemented medium revealed a gradual decline in α3 and the appearance of α2 Na/K ATPase isoforms, albeit at a relatively low level (Arystarkhova and Sweadner, 1997; Sharabani-Yosef *et al*, 1999).

Sodium pump subunit expression and activity are regulated in a timely manner. Short-term regulation of Na/K ATPase function can be achieved by changes in: (i) intracellular sodium concentration; (ii) the number of enzyme molecules in the cell plasma membrane (increases in plasma membrane sodium pump proteins due to trafficking of heterodimers from intracellular pools); (iii) the catalytic property of the enzyme already present in the

plasma membrane and (iv) the PKA- and PKC- mediated phosphorylation of α subunits, as certain phosphorylations can inhibit enzyme activity by reducing transport activity or by inducing clathrin-mediated enzyme internalisation (Mobasheri *et al*, 2000; Sznajder *et al*, 2002; Ewart and Klip 1995; Bertorello *et al*, 1991; Aperia *et al*, 1994). Adrenergic agonists increase the pump's affinity for Na+ and recruit sodium pump subunits to the basolateral plasma membrane of COS 7 cells from intracellular endosomal compartments (Feraille *et al*, 2000). In lung alveolar epithelial cells, activation of G protein-coupled receptors, via either dopaminergic or adrenergic stimuli, rapidly (30 s to 15 min) increases Na/K ATPase activity by insertion of sodium pump proteins from intracellular compartments into the plasma membrane (Barnard *et al*, 1999; Lecuona *et al*, 2000; Ridge *et al*, 2002; Suzuki *et al*, 1995; Ridge *et al*, 2003; Minakata *et al*, 1998). These effects are dependent on a dynamic interaction between protein-transporting vesicles, microtubulae and the actin cytoskeleton, since pre-treatment with colchicine, brefeldine or phallacidin prevents this recruitment.

Long-term regulation of Na/K ATPase occurs via transcriptional and post-transcriptional mechanisms, including changes in transcription rate and mRNA stability, translation, protein degradation, and in membrane enzyme-specific activity (reviewed in Bertorello and Katz, 1995; Ingbar, 1998; Therien and Blostein, 2000). Transcriptional regulation of sodium pump subunit genes is an important component of the multifaceted response to hormonal stimulation, hyperoxia and cellular stress. Because the subunit genes are on different chromosomes, transcription may be independently regulated. Increased transcription of the Na/K ATPase subunit genes in the lung may be mediated by compounds and hormones such as dexamethasone, insulin and aldosterone (Ingbar, 1998). Aldosterone increases both transcription and plasma membrane insertion of pre-formed pump molecules (Ewart and Klip, 1995; Olivera *et al*, 2000). Both functional enzyme activity and gene transcription are increased by low intracellular K+ or high Na+ concentrations or by various hormones, including thyroid hormone (McDonough *et al*, 1990). A recent study reported that adrenergic stimulation of serum-starved alveolar epithelial cells regulated Na/K ATPase translation via extracellular regulated kinase-rapamycin pathways independent of changes in Na/K ATPase transcription (Pesce *et al*, 2000). Translation of Na/K ATPase mRNA is an important locus of regulation in a variety of settings. For example, similar increases in steady-state levels of mRNA result

in different activity levels of the sodium pump, indicating that post-transcriptional steps play a role in the regulation of Na/K ATPase (Pesce *et al*, 2000; Gick *et al*,1993). In vitro studies of translation demonstrated that untranslated mRNA regions (UTRs) could affect subunit translation. The mRNA for α1 is translated less efficiently than that for β1 because of α1 mRNA's 3UTR region being extremely GC rich and folded in a complex fashion and because translational efficiency may be altered by glucocorticoids (Devarajan *et al*, 1992). Besides being the regulators of sodium pump activity, cardiac glycosides are also potent regulators of sodium pump expression. Rosen et al. (Rosen *et al*, 2004) reported that cardiac glycoside lead to the appearance of cytoplasmic vacuoles containing membrane components including sodium pumps, decreasing thus the number of pumps at the cell surface.

1.2 Cardioactive glycosides

Cardiac glycosides are a class of natural products that are traditionally used to increase cardiac contractile force in patients with congestive heart failure and cardiac arrhythmias (first described by William Withering in 1785; Evans, 1996; Abarquez, 2001). These glycosides are found as secondary metabolites in a diverse group of plants including Strophanthus spp. (ouabain), *Digitalis lanata* and *Digitalis purpurea* (digoxin, digitoxin), *Scilla maritima* (proscillaridin A), *Nerium oleander* (oleandrin, oleandrigenin) but also in frogs (some frog-poisons contain bufadienolides like bufalin, marinobufagenin). Plants containing cardiac steroids have been used as heart drugs at least since 1500 B.C. Throughout history these plants or their extracts have been variously used as arrow poisons, emetics, diuretics, and heart tonics (Evans, 1996; Wade, 1986, Kinne-Saffran, 2002). Cardiac glycosides represent a class of compounds that share a common structure consisting of a steroid (cyclopentanoperhydrophenanthrene) ring, substituted in position 3-OH with a sugar moiety and in position 17β with an unsaturated lactone ring (figure 2). The lactone at the C17 position defines the subgroups of cardiac glycosides (cardenolides and bufadienolides). The cardenolides have an unsaturated butyrolactone ring (5-membered unsaturated lactone) whereas the bufadienolides have a pyrone ring (6-membered unsaturated lactone) (Evans, 1996; Haensel, 1999, Beltz *et al*., 2001). One to four sugars are found to be present in most cardiac glycosides attached to the 3β-OH

group. The sugars most commonly found include L-rhamnose, D-glucose, D-digitoxose, and D-digitalose. One of the most widely used cardiac glycosides is digitalis, a powdered extract of *Digitalis purpurea* (foxglove) or *Digitalis lanata*. Digitalis itself consists of two major specific cardiac glycosides digoxin and digitoxin. The structural difference between digitoxin and digoxin is just an extra hydroxyl group on digoxin, which changes the pharmacokinetics and pharmacodynamics of these substances. Digitoxin is more lipophilic, is mainly metabolized in the liver and has a longer half-life than digoxin (Beltz *et al*., 2001).

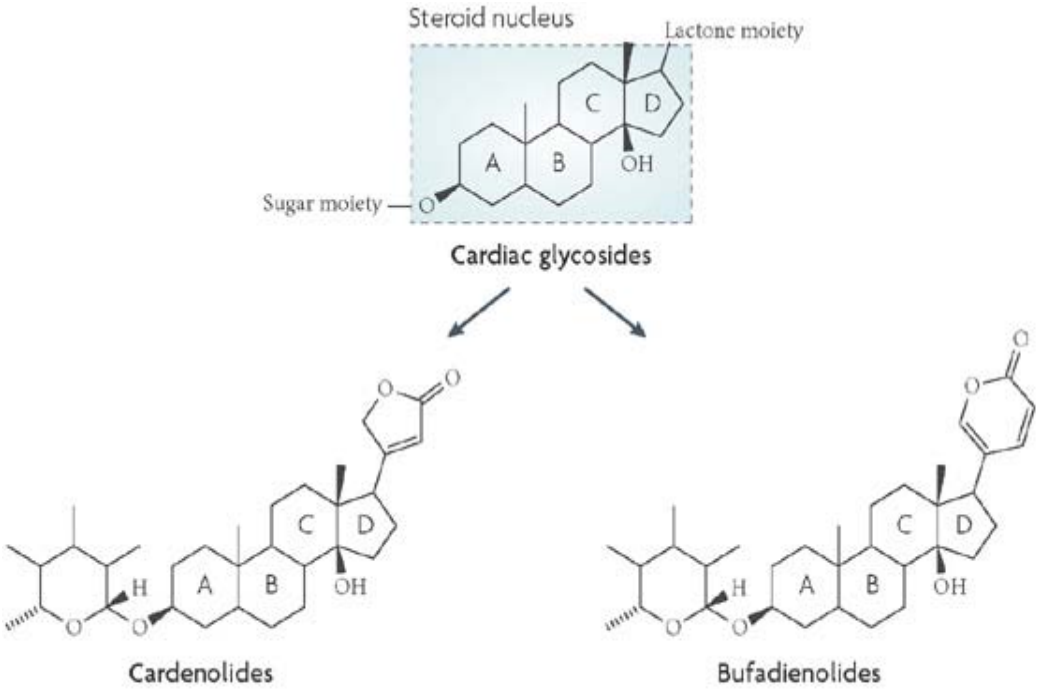

Figure 2. *Structure of cardiac glycoside.* Each molecule of this family consist of three distinct structural motifs: a steroid nucleus, a sugar moiety and a lactone moiety. The lactone moiety defines the functional class of each compound. Cardenolides contain a five-membered unsaturated burylactone ring, whereas bufadienolodes contain a six-membered unsaturated pyrone ring. From Prassas and Diamandis, 2008

The therapeutic effect of cardiac glycosides is mostly explained by the hypothesis that inhibition of Na/K ATPase acytivity causes accumulation of sodium in cardiac cells which are enforced to promote the sodium-calcium exchange system in the cell membrane, thus leading to a higher level of intracellular and myocardial calcium

concentration (figure 3) (Beltz *et al.*, 2001). The elevated intracellular calcium concentration results in increased inotropism, accentuating the force of myocardial contraction by increasing the velocity and extent of sarcomere shortening, thus translating into increased stroke work for a given filling volume of pressure

Na/K ATPase has an evolutionarily conserved cardiac glycoside binding site. Cardiac glycoside bind to Na/K ATPase at a site formed in the extracellular part of the catalytic α-subunit by the H1-H2, H3-H4, and H5-H6 loops. K_d values of the cardiac glycoside for α1-, α2-, and α3-human isoforms range from 10^{-8} to 10^{-9} mol/l, whereas rodents exhibit an ouabain-insensitive α1-isozyme. In the actively pumping Na+ pump, cardiac glycoside are fixed by tight binding in the E2 conformational state, a process leading to the enzyme's inactivation. Since the E2-phosphoenzyme-cardiac glycoside complex formed is almost irreversible, it is likely that, under cellular conditions, the cardiac glycoside-pump complex is internalized and degraded (Schoner and Scheiner-Bobis, 2007).

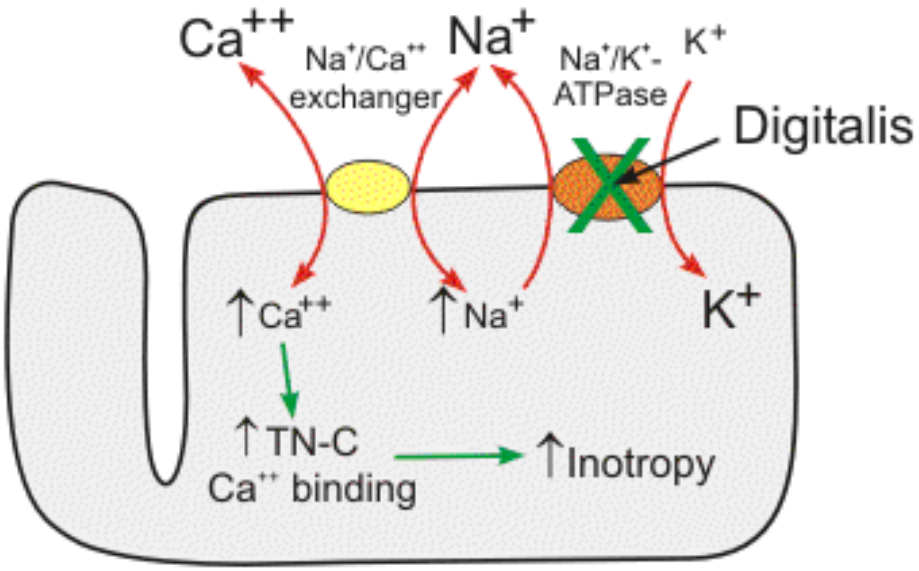

Figure3. *Mechanism of action of cardiac glycoside*

1.2.1 Ouabain

Ouabain is a cardiotonic glycoside extracted from the seeds of *Strophantus gratus*; it contains a steroid nucleus with a lactone ring containing 5 carbons, unsaturated in 17° position and with a rhamnose in 3° position of nucleus (figure 4).

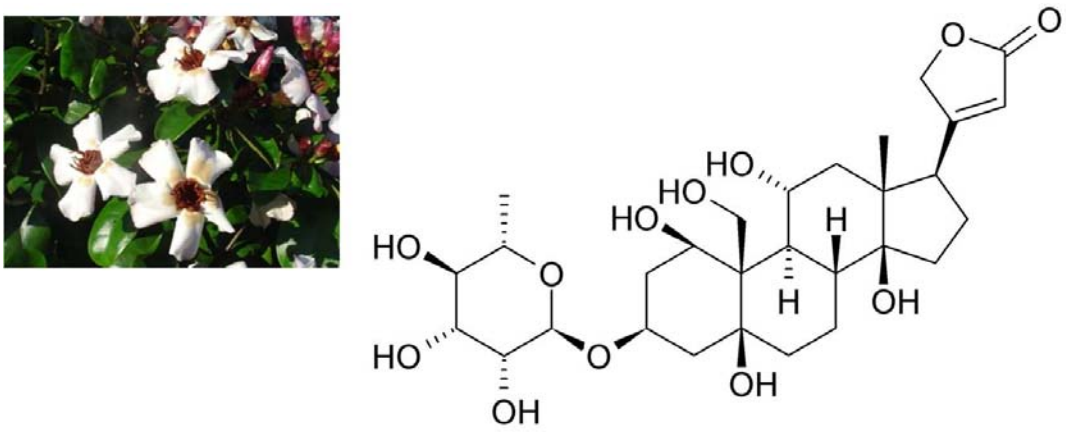

Figure 4. *Ouabain chemical structure and a photo of Strofantus gratus.*

1.2.2 Endogenous Ouabain

A preliminary report of Blaustein and coworkers showed that a circulating sodium pump inhibitor was directly correlated with blood pressure in normotensive and hypertensive subjects (Hamlyn *et al*., 1982). Intensive research for an endogenous Na+/K+ATPase inhibitor culminated in 1991 with the paper of Hamlym et al. reporting that this compound was ouabain (an identical molecule to the plant compound or a stereoisomer) (Hamlyn *et al*., 1991).

There is now much evidence that ouabain is a steroid hormone of the adrenal cortex and the hypothalamus (Schoner and Scheiner-Bobis, 2005). Ouabain-like immunoreactivity has been found in almost all tissues, including plasma, but the highest concentrations have been observed in adrenal cortex, hypophysis and hypothalamus (Hamlyn *et al*., 1998; Hamlyn *et al.*, 1991; Li *et al*., 1995). Ouabain is apparently synthesized in the adrenals and released upon hormonal stimulation. De novo synthesis of ouabain from

pregnenolone and progesterone has been demonstrated in tissue culture experiments (Schoner and Scheiner-Bobis, 2005).

Although endogenous ouabain was isolated in the search for a natriuretic hormone, the link between salt and endogenous ouabain in the homeostatic regulation of blood pressure is not yet resolved. A recent study has demonstrated that chronic salt intake augments endogenous ouabain levels in normal men and, as such, provides support for the hypothesis that increased circulating endogenous ouabain could be an early event linking salt intake with hypertension (Manunta *et al*. 2006).

Based on the evidence that plasma concentrations of ouabain correlate with systolic and mean arterial blood pressure (Manunta and Ferrandi, 2004; Wang *et al.,* 2003; Manunta *et al.,* 1999; Pierdomenico *et al*., 2001), it has been suggested that ouabain is a blood-pressure modulating factor that could play a key role in some forms of hypertension (Schoner and Scheiner-Bobis, 2005; Blaustein *et al*., 2006). In fact, elevated levels of endogenous ouabain have been observed in about 40% of patients with untreated essential hypertension, in patients with primary aldosteronism and in those with ACTH-induced hypertension (Rossi *et al*., 1995; Goto and Yamada, 2000; Goto *et al*., 1996). In a study of Manunta and colleagues it was observed that the concentration of plasma endogenous ouabain was of 253±53 pmol/L in normotensives while in patients with essential hypertension, half showed normal levels of ouabain and the other half elevated levels of plasma endogenous ouabain (540±197 pmol/L) (Manunta *et al*., 1999). Another evidence of the relationship between ouabain levels and blood pressure comes from the fact that an ouabain antagonist that does not itself inhibit Na+/K+ATPase, rostafuroxin (PST-2238), decreases blood pressure in ouabain-induced and salt-dependent hypertension in rats. In early Phase II clinical trials, rostafuroxin lowered blood pressure in nearly half of the tested human subjects with essential hypertension (Ferrari *et al.,* 2006).

Elevated plasma concentrations of endogenous ouabain have been also directly correlated with blood pressure in several animal models of hypertension (Blaustein *et al*, 2006). Furthermore, various studies demonstrate that prolonged administration of ouabain itself produces hypertension in the rat (Yuan *et al*., 1993; Pamnani *et al*., 1994; Manunta *et al*., 1994; Manunta *et al.,* 2000; Ferrari *et al*., 2006; Rossoni *et al*., 2002). Nevertheless, other investigations have shown that chronic ouabain treatment does not increase blood pressure (Cargnelli *et al*., 2000; Ceolotto *et al*., 2003; Neri *et al*., 2006; Li *et al*., 1995;

Pidgeon *et al*., 1996).

1.3 Na+/K+ATPase as a signal transducer

Since endogenous ouabain circulates in blood plasma of humans in the picomolar-to-nanomolar concentration range, even under pathological conditions (Schoner and Scheiner-Bobis, 2007) an important point is how low concentrations of endogenous ouabain, producing slight or no inhibition of Na+/K+ATPase activity, could influence the cardiovascular function and elevate blood pressure. In addition, it has been reported that noninhibitory subnanomolar concentrations of ouabain stimulate the proliferation of smooth muscle (Abramowiz *et al*, 2003; Aydemir-Kokosoy *et al*, 2001), endothelial (Saunders and Scheiner-Bobis, 2004), and kidney tubule cells in culture (Dmitrieva and Doris, 2003; Khundmiri *et al*, 2006). These evidences have prompted many laboratories to investigate whether Na/K ATPase, following ouabain binding, can generate secondary messages independent of its pumping function. Subsequently, several mechanisms and pathways by which Na/K ATPase transmits the ouabain signal to different intracellular compartments have been discovered and different mechanisms of signal transduction have been proposed.

1) The PlasmERosome Hypothesis

This hypothesis, postulated by Blaustein and coworkers, assumes that a partial inhibition of the sodium pump by cardiac glycosides leads to a transient increase of $[Na^+]_i$, which in turn increases $[Ca^{2+}]_i$ via the Na^+/Ca^{2+} exchange system (NCX1) running in a reverse mode. In cardiac and vascular smooth muscle cells, this exchanger is thought to contribute to Ca^{2+} extrusion from the cytosol in the relaxation process (Blaustein and Lederer, 1999). In smooth muscle cells, astrocytes and hippocampal neurons of rodents, minimal inhibitory effects of cardiac glycoside on the Na+/K+ ATPase seem to be amplified by a special arrangement of the α-isoforms that makes it possible for low concentrations of ouabain to provoke calcium signaling. Immunochemical studies in rat arteries showed that NCX1 and the ouabain sensitive α2- and α3-isoforms (but not the rather insensitive α1-isoform) of Na+/K+ ATPase are closely juxtaposed to the underlying sarc(endo)plasmic reticulum. Within these domains, called plasmERosomes, sodium pumps and the Na^+/Ca^{2+} exchanger may function cooperatively, producing a

localized calcium increase and, consequently, a rise in the calcium content of the sarc(endo)plasmic reticulum (Blaustein *et al*., 2006).

The Blaustein's plasmERosome hypothesis may explain, at least in part, the development of arterial hypertension at sustained elevated concentrations of endogenous ouabain. Other mechanisms must exist as well, since, especially at subnanomolar ouabain concentrations, Na/K ATPase activity and cell proliferation are stimulated (Schoner and Scheiner–Bobis, 2007). Furthermore, there is no strict correlation between the hypertensive action of cardiac glycosides and inhibition of Na/K ATPase (Manunta *et al*, 2006).

In heart muscle cells, a functional Na^+/Ca^{2+} exchanger seems to be necessary for an acute inotropic effect of cardiac glycosides (Altamirano *et al*, 2006; Reuter *et al*, 2002). However, even though α1-, α2-, and α3-isoforms of Na/K ATPase are found there is no evidence for a plasmERosome like mechanism in cardiac cells. In contrast to a plasmERosome mechanism, in the heart muscle the α1-isoform of Na/K ATPase regulates cardiac contractility and functionally interacts and colocalizes with the Na^+/Ca^{2+} exchanger of the heart (Dostanic *et al*, 2005). Furthermore in humans, cardiac glycoside affinities of all α-isoforms of Na/K ATPase are very similar suggesting that in heart muscle, no cardiac glycoside-amplification mechanism is necessary to achieve inotropy. (Schoner and Scheiner-Bobis, 2007)

2) Interaction of Na+/K+ ATPase with the IP3 receptor

Recent studies from Aperia's laboratory have identified another important calcium-signaling microdomain involving the interaction between the Na/K ATPase and sarc(endo)plasmic reticulum in renal epithelial cells, the IP3 receptor (IP3R). IP3R belongs to a family of Ca2+ release channels predominately localized in the endoplasmic reticulum membrane, and mainly regulated by IP3 generation and changes in cytoplasmic Ca^{2+}. The IP3R can interact and regulate ion channels, protein kinase/phosphatases, and structural proteins. Activation of G protein-coupled-receptors (GPCRs) or tirosin-kinases-receptors (RTKs) can activate/recruit PLC-β or PLC-γ to the plasma membrane, resulting in an increase in IP3 production and the opening of IP3R (Patterson *et al*., 2004; Rebecchi e*t al*., 2000). Interaction between Na+/K+ ATPase and IP3R generates low-frequency calcium oscillations that activate NF-κB pathway and protect renal epithelial cells from serum deprivation-induced apoptosis (Zhang *et al.*, 2006). These calcium oscillations are

independent of intracellular Na^+ concentration, PLC activation and IP3 generation. A three aminoacid sequence (LKK) at the α1 N-terminus is essential for binding to IP3R and ouabain-induced calcium oscillations (Zhang *et al.*, 2006).

3) Na/K ATPase signalosome

A large number of experiments support the hypothesis that Na/K ATPase inhibition is not necessary for the inotropic effect of cardiac glycosides in the myocardium. In the mid-1990s Xie, Askari and collaborators unveiled in a series of experiments with cardiac myocytes in culture that ouabain, at subnanomolar concentrations, lead to increased inotropy of cardiac muscle and to hypertension, proliferation, differentiation, and altered cell life span (Peng *et al.*, 1996; Kometiani *et al.*, 1998; Xie *et al.*, 1999). The Na/K ATPase signalosome uses all α-isoforms to transduce the information of ouabain's binding from the Na^+ pump to the cell interior and nucleus (Schoner and Scheiner-Bobis, 2007). The Na/K ATPase signalosome is located in caveolar structures and may transfer signals to the cell interior, even when the pump is unable to work (Liang *et al*., 2006), and affect membrane recycling and trafficking, as well as cell-cell interactions (figure 5). Interaction of endogenous and exogenous cardiac glycosides with Na+/K+-ATPase, even at nanomolar concentrations of the drug, may lead to conformational changes that are recognized by neighboring proteins assembled into the caveolae (Xie and Asaki, 2002).

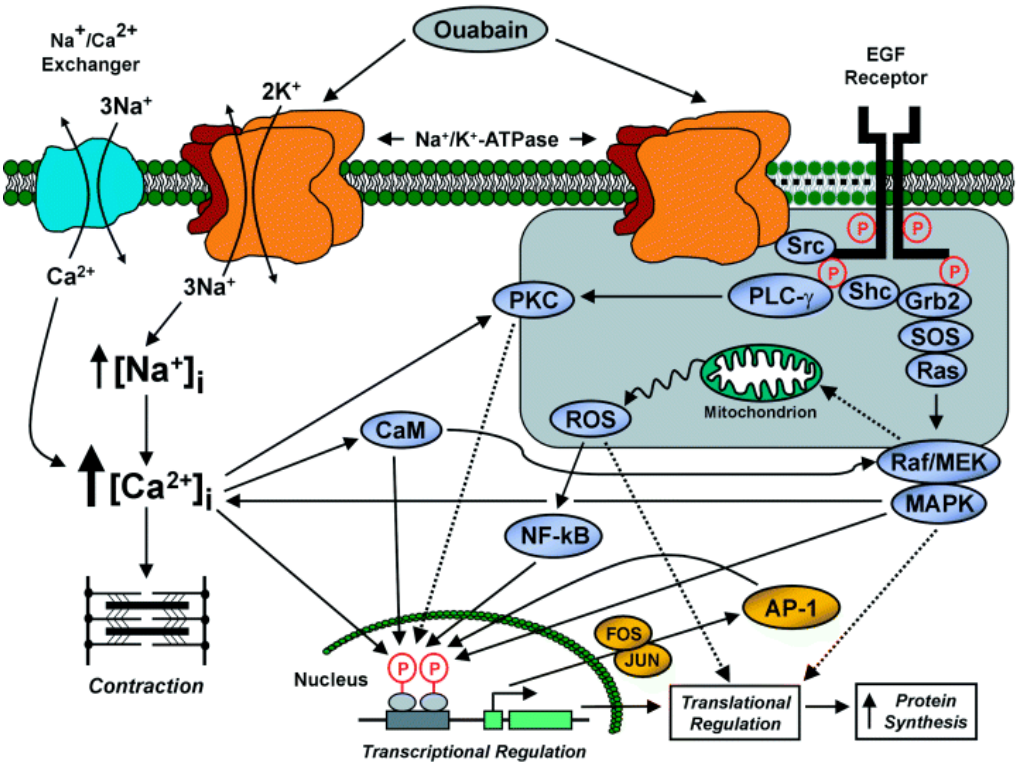

Figure 5. *The signal transducing function of Na/K ATPase and its consequences in cardiac myocytes* . Two pools of the enzyme, one pumping ions and the other interacting with neighboring proteins are suggested by the data. The partial inhibition of the pump by ouabain causes a modest change, if any, in [Na+]i and [K+]i, but a significant change in [Ca2+]i due to the presence of the Na+/Ca2+-exchanger. Ouabain interaction with the other pool alters protein–protein interactions to activate the indicated signaling pathways. The events placed in the grey box have been shown to be independent of changes in [Na+]i, [K+]i, and [Ca2+]i that may occur. These activated pathways, the resulting increase in ROS, and the concomitant increase in [Ca2+]i lead to activations of NF-kB and AP-1, transcriptional regulation of early response genes (c-fos, c-jun), and cardiac growth-related genes (those of atrial natriuretic factor, skeletal β-actin, and the α3 subunit of Na/K ATPase), stimulation of protein synthesis, and myocyte hypertrophy. The solid arrows indicate experimentally supported events induced by ouabain in myocytes, and the broken arrows indicate those with limited or indirect support. In several cell types other than cardiac myocytes, some of the same signaling events are induced by ouabain, but there are also significant cell-specific differences between the ouabain-induced pathways and the down-stream consequences. From Xie and Askari, 2002.

Caveolae were first identified as flask-shaped vesicular invaginations of plasma membrane enriched in cholesterol, glycosphingolipids, and sphingomyelin. Caveolins are 21–24 kDa membrane-associated scaffolding proteins that serve as a protein marker of caveolae (Razani *et al.*, 2002). Three caveolin genes have been identified and the expression of the different isoforms is tissue-specific. Caveolins directly interact with many signaling proteins via the scaffolding domain's binding to CBM (caveolin-binding motif) of target proteins. The mammalian Na/K-ATPase α1 subunit contains two potential CBMs (Wang *et al.*, 2004): one locates in the cytosolic N-terminal domain near the first transmembrane helix (M1) and the other resides at the extracellular side of M10. The appearance of the N-terminal CBM correlates well with the occurrence of the domain for ouabain binding (Bagrov *et al.*, 2009). Disruption of caveolar structure by depletion of either cholesterol by methylcyclodextrin (MβCD) or caveolin-1 by siRNA redistributes the Na/K-ATPase and Src (see below) from the caveolae to other compartments, resulting in the inhibition of CTS-induced signaling (Liu and Xie, 2010). Confocal imaging and immunoprecipitation studies have confirmed that Na/K-ATPase co-localized with caveolin and concentrated in caveolae in many different cells including cardiac myocytes, smooth muscle and renal epithelial cells (Liu and Xie, 2010).

Signal transduction pathways activated by the Na/K ATPase signalosome can be divided into three main groups:

A) SRC-EGFR-RAS-RAF-ERK CASCADE. Ouabain binding to the Na/K ATPase stimulates Src kinase, which in turn phosphorylates the EGFR, leading to activation of the Ras-Raf-MEK-ERK pathway (figure 6). Fluorescence resonance energy transfer studies revealed a close proximity of Na/K ATPase to Src at the plasma membrane (Tian *et al.*, 2006). Binding of Src to Na/K ATPase is independent of the Na+/K+-ATPase's catalytic activity (Liang *et al.*, 2006) and the binding of the SH2 domain of Src to cytosolic domains 2 and 3 of the Na/K ATPase α-subunit inhibits Src activity if no cardiac glycoside is bound to the Na/K ATPase (Tian *et al.*, 2006). As a consequence of ouabain-induced conformational change of the Na+/K+-ATPase, Src is released from the Na+/K+-ATPase-Src complex and activated by phosphorylation at Tyr418 (Tian *et al.*, 2006) and this leads to an increased tyrosine phosphorylation of EGFR and to recruitment and phosphorylation of the adaptor protein Shc. This results in binding of the adaptor protein

Grb2 to the Src-EGFR complex and, subsequently, activation of Ras (Kometani *et al.*,1998).

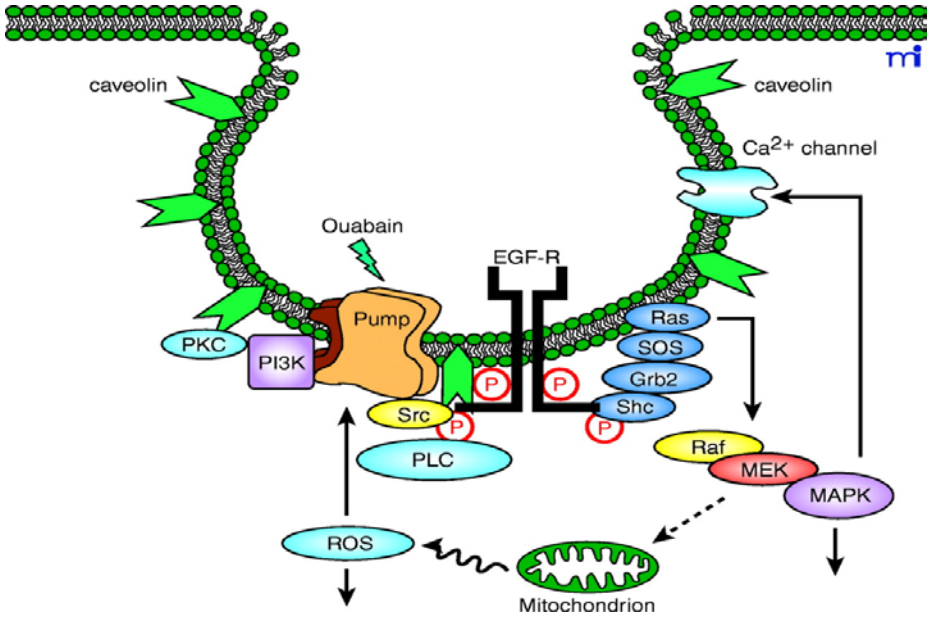

Figure 6. *Schematic presentation of Na/K ATPase signalosome.* The Na/K ATPase (pump) is preassembled with its partners in caveolae; ouabain binding to the pump activates the signalosome, and transduces signals via multiple pathways. From Xie and Cai, 2003.

Ras activation leads to further activation of three different branches of the signal transduction cascades. One of the pathways communicates with the mitochondria: Ras induces an increase in $[Ca^{2+}]_i$ that results in opening of mitochondrial ATP-sensitive K^+ channels (Tian *et al.*, 2003) and generation of mitochondrial reactive oxygen species (ROS) (Tian *et al.*,2001). ROS production by mitochondria is an essential second messenger for many of the downstream events that are linked to Na+/K+ATPase. In cardiac myocytes, this results in the stimulation of downstream events that include activation of the transcription factors AP-1 and NF-κB, induction of early response proto-oncogenes, increase of protein synthesis and myocyte hypertrophy (Xie and Askari, 2002). The second pathway, the Ras-Raf-MEK-ERK1/2 cascade, leads to gene activation when ERK1/2 is activated in cooperation with PLC in the presence of Ca^{2+} and ROS (Schoner and Scheiner-Bobis, 2007) In addition JNK might be a substrate of ERK (Kometani *et al.*, 2005), as well as the JNK kinase SEK1 (Li and Wattenberg, 1998). A

third pathway of ouabain dependent Ras activation in muscle cells results in activation of p90 ribosomal S6 kinase and inactivation of glycogen synthase kinase (GSK-3α/β), a process that stimulates glycogen synthesis (Kotova *et al*., 2006). Since GSK-3 is a master switch regulating cell-fate specificity and tumorigenesis, inhibition or suppression of GSK-3 may also affect transcription factors (Schoner and Scheiner-Bobis, 2007).

B) CALCIUM AS SECOND MESSENGER The rise of $[Ca^{2+}]_i$ caused by nanomolar concentrations of ouabain may result from a direct interaction of Na/K ATPase with the IP3R of the endo(sarco)plasmic reticulum (see above). $[Ca^{2+}]_i$ increase can be also accomplished by Src-dependent PLC-γ1 activation, that may increase IP3 formation, which in turn enhances Ca^{2+} release from intracellular stores (Schoner and Scheiner Bobis, 2007). Additionally, activation of PLC-γ1 stimulates diacylglycerol formation and, thus, PKC activity (Gotoh *et al*., 1993). Activation of PKC and Ca^{2+}-calmodulin kinase may activate the expression of early-response genes, such as *c-fos* and *c-jun*, leading to formation of the transcription factor AP-1 (Peng *et al*., 1996).

C) ACTIVATION OF PHOSPHATIDYLINOSITIDE 3'-KINASE AND AKT. The NH2-terminal end of the catalytic α-subunit of Na/K ATPase contains a binding motif for PI3K (Yudowski *et al*., 2000). Ouabain-induced conformational change was shown to activate cell proliferation in kidney proximal tubule cells via a Ca^{2+}-dependent phosphorylation of Akt (Khundmiri SJ *et al*., 2006). In the heart, this conformational change may lead to cardiac hypertrophy and metabolic alterations (Schoner and Scheiner-Bobis, 2007). Ouabain-induced activation of Akt was reported to show an antiapoptotic action (Trevisi *et al*., 2004). Hence, Akt plays an important role in ouabain-induced signal transduction

1.4 Effect of cardiac glycosides on cell survival and proliferation of normal and cancer cells

As described above, the interaction of ouabain with Na+/K+ATPase activates signalling cascades involved in the regulation of cell survival, growth and proliferation. In cardiac myocytes ouabain stimulates hypertrophic growth while in other cell types, ouabain produces an increase of cell proliferation. Exposure of vascular smooth muscle cells (from human, canine and rat origin) to ouabain concentrations that cause no detectable inhibition of pump activity promotes the signalling function of Na+/K+ATPase and

stimulates proliferation. (Aydemir-Koksoy *et al*., 2001; Allen *et al*., 2003; Abramowitz *et al.*, 2003). Also in endothelial cells from the human umbilical artery ouabain induces an increase of cell proliferation (Saunders and Scheiner-Bobis, 2004). Nanomolar concentrations of ouabain protect from apoptosis induced by serum starvation and actinomycin D treatment in renal epithelial cells (Li *et al*, 2006; Zhou *et al.*, 2001). Also human umbilical endothelial cells are protected from apoptosis induced by serum starvation and staurosporine treatment by nanomolar concentrations of ouabain (Trevisi *et al*, 2004).

On the contrary, non-toxic concentrations of ouabain and other cardiotonic steroids can induce apoptosis in different malignat cell lines (Watabe *et al*., 1997; Watabe *et al*., 1998; Kawazoe *et al*., 1999; McConkey *et al.*, 2000; Chueh *et al*., 2001; Akiyama *et al*., 1999; Xiao *et al*., 2002). Numerous other reports have confirmed the antiproliferative and apoptotic effects of these compounds in several cancer cell lines, including breast, prostate, melanoma, pancreatic, lung, leukaemia, neuroblastoma and renal adenocarcinoma. In breast cancer cell lines (MDA-MB-435s) ouabain (at nanomolar concentration) caused the activation Src/EGFR/ERK1/2 pathway, resulting in a increased level of cell cycle inhibitor p21Cip1 and growth arrest (Kometiani *et al*., 2005). In another study Haux and coworkers assessed the susceptibility to digoxin and digitoxin of several cancer prostate cell lines (LNCaP, PC-3, TSU-pr1, DU-145); digoxin, in clinically relevant concentrations, induced minor inhibition of viability, whereas digitoxin potently inhibited all four cell lines, inducing apoptosis by the elevation in intracellular Ca^{2+} (Haux *et al*., 2000). Treatment of myeloid leukemia U937, cervical carcinoma HeLa, and breast carcinoma MCF-7 cells with oleandrin facilitated nuclear translocation of FKHR by dephosphorylating Akt; it also activated MAPK and JNK and induced expression of FasL leading to apoptosis (Raghavendra *et al*., 2007). In another study using the neuroblastoma cell line SH-SY5Y, Scheiner-Bobis and collaborator demonstrated that ouabain induced a reduction in the abundance of the anti-apoptotic proteins Bcl-XL and Bcl-2 and caused cytochrome c release into the cytosol and caspase-3 activation, events that point towards the stimulation of apoptotic pathways (Kulikov *et al*., 2007). Further effects of cardiac glycoside against cancer cell lines are summarized in Table 1 (adapted from Newman *et al*., 2008 and Schoner and Scheiner-Bobis, 2007).

Table 1. *In vitro citotoxic effects of cardiac glycosides in cancer cells*

Cancer type	Compound tested	Cell lines	Mechanism of action	Reference
Breast	Digitoxin, digoxin, proscillaridin, ouabain	MCF-7, MDA-MD-435	Inhibition of topoisomerases I and II;	Bielawski K. *et al*, 2006; Lopez-Lazaro *et al*., 2006
Prostate	Oleandrin, ouabain, digoxin, bufalin, cinobufagenin	PC-3, LNCaP, DU145	Increased Ca2+ uptake; Increased ROS production, oxidative injury and mitochondrial injury; Caspase activation	McConkey *et al*., 2000; Huang 2004; Yeh *et al*., 2003
Melanoma,	Digoxin, oleandrin, digitoxin, proscillaridin A, ouabain, digitonin	UACC-62, BRO	Inhibition of topoisomerases I and II; Increased ROS production, oxidative injury, and mitochondrial injury	Lopez-Lazaro *et al*., 2006; Newman *et al*., 2006
Lung	Digitoxin, digoxin, ouabain, oleandrin	NCI-H-358, Calu1, Sklu1, NCI-H6, H69AR	Initiates Apo2L/TRAIL apoptosis via increased expression of death receptors 4 and 5	Frese *et al*, 2006; Johansson *et al*., 2001
Leukaemia,	Bufalin, oleandrin, digitoxin, proscillaridin A, ouabain	HL60, U-937, CCRF-CEM, CEM-VM-1	Inhibition of topoisomerases I and II; Increased activation of MAPKs; Downregulation of cyclin A, Bcl-2 and Bcl-xL; Increased expression of p21 and Bax	Lopez-Lazaro *et al*., 2006; Kawazoe *et al*., 1999; Watabe *et al*., 1997
Renal,	Digitoxin, digoxin, proscillaridin A, ouabain	TK-10, ACHN 78,93	Inhibition of topoisomerases I; Increased activation of MAPKs	Lopez-Lazaro *et al*., 2006; Johansson *et al*., 2001
Myeloma	Digitoxin, digoxin, proscillaridin A, ouabain,	8226-S, 8226-LR5, 8226-DOX-40	Increased expression of FasL; Increased cytochrome *c* release; Caspase activation	Raghavendra *et al*., 2007; Johansson *et al*., 2001
Pancreatic	Oleandrin	PANC-1	Decreased phosphorylation of Akt; Mitochondrial injury; Increased activation of MAPKs	Newman *et al*., 2007

Variation in the effects of cardiac glycosides on cell growth is certainly due to differences in the gene expression of normal versus cancer cells. Among the most common perturbations in malignant, transformed cells is the overexpression and/or mutation of growth factor tyrosine kinase receptors, leading to an increased phosphorylation of ERK and constitutive NF-κB activation, which enable malignant cells to escape apoptosis (Schoner and Scheiner-Bobis, 2007). However, there are unifying themes that link mechanisms involving proapoptotic action of cardiac glycosides, including: activation of ERK1/2; increased expression of the cell cycle inhibitor p21Cip1 and consequent inhibition of cell cycle progression (through decreased expression of cyclin proteins); inhibition of transcription factors, such as NF-κB and AP-1; inhibition of Akt and related critical components of the PI3K pathway; initiation of death receptor–mediated apoptosis; sustained ROS production with consequent mitochondrial injury; inhibition of topoisomerases and reduction in expression of anti-apoptotic proteins, such as Bcl-xL and Bcl-2. The exact mechanisms underlying these effects of cardiac glycosides are not yet fully elucidated, more studies are necessary to clarified this point.

Interestingly, marked differences characterize the potencies of these structurally similar compounds. For instance, Johansson and colleagues evaluated the cytotoxic profile (IC_{50}) of seven cardiac glycosides in primary cultures of tumour cells from patients and in a panel of human cell lines (Johansson *et al*, 2001). They found that proscillaridin A was the most potent, followed by digitoxin, ouabain, digoxin, lanatoside C, digitoxigenin and digitonin (Johansson *et al*, 2001). Furthermore, Van Quaquebeke et al. (Van Quaquebeke *et al*, 2007) semi-synthesized a library of 27 novel cardenolides and studied their structure–activity profile against a panel of 57 cancer cell lines. One of these compounds, UNBS1450 (see below), displayed better antitumour properties in vitro compared with commonly used chemotherapeutic drugs, and was best tolerated in vivo by mice compared with digitoxin and ouabain (Van Quequebeke *et al*, 2007). Such structure–activity relationship analyses highlight the structural characteristics that are important for the activity of these compounds and lay the foundations for the development of novel, more active compounds with higher in vivo tolerance and improved therapeutic potential as anticancer agents.

In parallel, several recent publications highlight the effects of cardiac glycosides in the regulation of the gene-expression profiles of many cancer cells. Johnson and coworkers

screened 9,000 compounds for their ability to simultaneously inhibit expression of six commonly overexpressed genes in prostate cancer cells (Johnson *et al*, 2002). Interestingly, digitoxin and ouabain were the only compounds that could confer significant inhibition in the expression of four of the target genes, including transcription factors HOXB13, PDEF (also known as SPDEF), hepatocyte nuclear factor 3 (HNF3A; also known as FOXOA1) and the apoptosis inhibitor survivin. Moreover, oleandrin was shown to inhibit export of fibroblast growth factor 2 (FGF2) from PC-3 and DU145 prostate cancer cells in a concentration-dependent and time-dependent manner (Smith *et al*, 2001). In another study it has been found that oleandrin inhibits interleukin 8 (IL8)-mediated biological responses by altering the plasma-membrane fluidity (Manna *et al*, 2006). IL8 is highly expressed in many cancers, where it acts as a chemoattractant and is a principal angiogenic stimulus for neovascularization.

1.5 Evidence of the anticancer effect of cardiac glycosides

1.5.1 *Ex vivo* and *in vivo* data

More than a decade ago, Inada and coworkers (Inada *et al*, 1993) first reported the ability of digitoxin to inhibit tumour formation in a two-stage carcinogenesis model of mouse skin papillomas induced by 7,12-dimethylbenz[a]anthracene (DMBA) and 12-O-tetradecanoylphorbol-13-acetate (TPA), and in a mouse pulmonary tumour model induced by 4-nitroquinoline-N-oxide (4NQO) and glycerol. In agreement with this, a study investigating the tumour growth-inhibitory effects of oleandrin after TPA induction of skin carcinogenesis, found that topical application of oleandrin (2 mg per mouse) half an hour before TPA induction significantly inhibited skin carcinogenesis in a time-dependent manner (Afaq *et al*, 2004). Furthermore, it has been demonstrated that digoxin is a specific neuroblastoma growth inhibitor in mice grafted with the human neuroblastoma cell lines SH-SY5Y and Neuro-2a (Svensson *et al*, 2005). Moreover, the antitumour activity of bufalin has been suggested in an orthotropic transplantation tumour model of human hepatocellular carcinoma in nude mice, where non-toxic concentrations of bufalin can induce specific apoptosis of transplanted tumour cells (Han *et al*, 2007).

1.5.2 Epidemiological data

Epidemiological data have indicated lower mortality rates in cancer patients who were on digitalis at time of first diagnosis, compared to patients not on digitalis therapy (Stenkvist, 1999; Haux 1999). Stenkvist and coworkers reported that the tumour cell populations from breast cancer patients on digitalis medication for cardiac problems have a lower proliferative capacity than tumour cells from patients not on digitalis treatment (Stenkvist *et al*, 1978; Stenkvist *et al*, 1980). In a 5-year follow-up study, they observed that the recurrence rate of breast cancer in patients not on digitalis was 9.6 times higher than in patients treated with digitalis (Stenkvist *et al*, 1982). After a 20-year follow-up, the death rate from breast carcinoma (excluding other causes of death and confounding factors) was 6% (2 of 32) among patients on digitalis compared with 34% (48 of 143) among patients not on digitalis ($p = 0.002$) (Stenkvist 1999). Goldin and Safa confirmed Stenkvist's results by conducting a retrospective study of 127 cancer patients in their records (Goldin and Safa, 1984). Among 21 deaths they found only one cancer death among those who had taken digitalis. Additionally, a study with 9271 patients showed a relationship between high plasma concentrations of digitoxin and a lower risk for leukaemia/lymphoma (Haux *et al*, 2001). It should be noted that these studies were not specifically designed to explore the relationship between the cardiac glycoside treatment and cancer..

1.6 Clinical trials with glycoside-based anticancer drugs

Based on epidemiological data and on in vitro studies demonstrating the antiproliferative and cytotoxic activity of cardiac glycosides against cancer cells, some clinical trials using a single cardenolide or a chemical derived compound have been undertaken.

In April 2000, the US Food and Drug Administration (FDA) approved a Phase I study of Anvirzel in patients with advanced solid tumours. Anvirzel is an aqueous extract of the plant *Nerium oleander*. It contains a variety of compounds including polysaccharides, proteins, sugars and cardiac glycosides, mainly oleandrin and its aglycone oleandrigenin. It has been demonstrated that Anvirzel inhibits the export of FGF2 from prostate cancer cells through sodium-pump inhibition by oleandrin (Smith *et al*, 2001). Furthermore,

Pathak and coworkers have investigated the mechanisms of Anvirzel-induced cancer cell death in various cancer cell lines of human, murine and canine origin and found that human cells are more susceptible to the effects of this drug (Pathak *et al*, 2000). The results of Phase I trials show that Anvirzel can be safely administered to patients with solid tumours. Overall, this agent appears to be well tolerated as patients in the trial experienced only mild-to-moderate side effects. No evidence of significant antitumour activity was detected, but this might be due to the fact that the patient group consisted exclusively of individuals who had refractory cancers or because the limited time of exposure to the product and intramuscular route of administration limited the total volume of extract that could be administered on a daily basis. A longer time of exposure and a different route of administration may impact response. Also, no dose-limiting toxicities were found. The product known as PBI-05204 was produced in response to the need for a formulation and route of administration suitable for adequately exploring the anticancer potential of an oleander extract. PBI-05204 is a modified supercritical CO_2 extract of organically grown *Nerium oleander* that has been especially formulated for oral administration to humans. An IND for evaluation of PBI-05204 as a "botanical drug" was obtained from the FDA in September, 2007, and a Phase I clinical trial in patients with solid tumors has now been initiated at the University of Texas M.D. Anderson Cancer Center.

UNBS1450, a semi-synthetic derivative of the novel cardenolide 2"-oxovoruscharin, entered Phase I clinical trials in Belgium in 2006. This promising novel cardenolide has been shown to deactivate NF-κB-mediated cytoprotective effects in human non-small-cell lung cancer cells (Mijatovic *et al*, 2006a; Mijatovic *et al*, 2006b). The modifications induced by UNBS1450 led to a decrease in both the DNA-binding capacity of the p65 subunit and the NF-κB transcriptional activity (Mijatovic *et al*, 2006a; Mijatovic *et al*, 2006b). UNBS1450 was as potent as taxol and SN38 (the active metabolite of irinotecan) in reducing the overall growth levels of the human A549 non small cell lung cancer cell line, and was more efficient than platin derivatives, including cisplatin, carboplatin and oxaliplatin (Mijatovic *et al*, 2006a; Mijatovic *et al*, 2006b).

1.7 The sodium pump as a new target in anti-cancer therapy

Numerous studies have dealt with changes in the transmembrane transport of cations during the course of malignant cell transformation, due to increases in Na/K ATPase activity (Weidemann 2005, Kaplan, 1978; Shen *et al*, 1978). There is evidence that these kinetic changes in Na/K ATPase activity are already present at the very early stages of tumorigenesis, even before morphological evidence of tumour appearance (Gonta-Gabriec *et al*, 1986; Davies *et al*, 1991). Interestingly, in contrast to the increase in Na/K ATPase activity in cancer cells referred to in several studies (Weidemann, 2005; Kaplan, 1978; Shen *et al*, 1978), Davies and coworkers. (Davies *et al*, 1991) have reported a inhibition of Na/K ATPase activity in a mice model of induction of experimental colon cancer. During the development of large bowel cancer, they observed alterations in the ion transport of colon epithelial, some of which resulted in altered intracellular ionic composition. They also demonstrated that changes occur in Na/K ATPase activity in premalignant mucosa, months before gross tumours develop, and these changes may partially explain the altered levels of Na+ and K+ in the cytoplasm of pre-malignant and malignant colonocytes. These differences are furthermore emphasized by the presence of specific cancer-related FXYD proteins affecting the function of the sodium pump, like FXYD3 (Mat-8: a mammary tumour marker which mediates the decrease in apparent Na+ and K+ affinity of the sodium pump) which is highly up-regulated in breast and prostate tumours and FXYD5 (related to ion channels) which is expressed in several cancer tissues but in only a few normal cell types (Greering, 2005, Geering 2006).

Also, not only does the activity of Na/K ATPase differ between normal and malignant cells, but also their sensitivity towards cardiotonic steroids. This may be due to an altered density of Na/K ATPase at the plasma cell membrane of tumour cells, as well as differences in isozyme expression. In line with this, it has been widely reported that the Na/K ATPase β1 subunit is very frequently down-regulated in human epithelial cancer cells and down-regulation of the β1 subunit seems essential for epithelial cancer cells to be able to become individually invasive (Espineda *et al*, 2003; Rajasekaran *et al*, 1999; Espineda *et al*, 2004; Blok *et al*, 1999; Akopyanz *et al*, 1991). In contrast, Na/K ATPase α subunits seem to be up-regulated in some malignant cells (Sakai *et al*, 2004; Mijatovic *et al*, 2007; Boukerche *et al*, 2004), a phenomenon which has been quite poorly

investigated to date. Except for bladder cancer, investigated by means of tissue microarray involving samples from 167 different patients (Espineda *et al*, 2003) and non small cell lung cancer, investigated by means of immunohistochemistry involving 94 samples (Mijatovic *et al*, 2007), other reported studies have relied merely on the use of cell lines (usually one per type) or a very limited number of tissue samples. Sakai et al. (Sakai *et al*, 2004) reported that the α3 subunit was over-expressed in colon cancer cells compared to normal colon cells, while α1 subunit expression was reduced. Further large-scale investigation should bring more evidence in support of the proposal that over-expressed sodium pump subunits could be suitable new targets in anti-cancer therapeutics.

In a recent review, Chen at al. (Chen *et al*, 2006) put forward several pieces of evidence to support the novel concept that Na/K ATPase could be a potentially important target for the development of promising anti-breast cancer drugs: (i) the sodium pump is a key player in cell adhesion and is involved in cancer progression; (ii) it serves as a versatile signal transducer and is a target for a number of hormones including oestrogens and (iii) its aberrant expression and activity are implicated in the development and progression of breast cancer.

Collectively, the data from the literature strongly suggest that targeting Na/K ATPase could represent a novel means to combat a growing number of malignancies. The question is how to optimally target the sodium pump in order to combat cancer. It should be borne in mind that cardiac glycoside are the natural ligands and inhibitors of the sodium pump and this fact supports the possibility of their potential development as anti-cancer agents targeting over-expressed Na/K ATPase subunits, notably α subunits.

1.8 Programmed cell death

Cell death can be classified according to the morphological appearance of the lethal process (that may be apoptotic, necrotic, autophagic or associated with mitosis), enzymological criteria (with and without the involvement of nucleases or distinct classes of proteases, like caspases or cathepsins), functional aspects (programmed or accidental, physiological or pathological) or immunological characteristics (immunogenic or non-immunogenic). Thanks to the advancing comprehension of cellular demise, it has become clear that the textbook equation 'programmed cell death=apoptosis=caspase activation=non-immunogenic cell death', although applicable to some instances of cell death, constitutes an incorrect generalization, at several levels. Thus, necrosis can be programmed both in its course and its occurrence. Apoptosis can be lethal without caspase activation, and caspase activation does not necessarily cause cell death. Finally, cell death with an apoptotic appearance can be immunogenic, in which case the immunogenicity is caspase-dependent.

Since the first descriptions of programmed cell death mechanisms, which date back to the mid-1960s (Lockshin and Williams, 1964) several attempts have been made to classify cell death subroutines based on morphological characteristics. Even though deep insights into the molecular pathways that regulate and execute cell death have been gained and biochemical assays for monitoring cell death-related phenomena have become laboratory routine, the scientific community has not yet adopted a systematic classification of cell death modalities based on biochemical rather than morphological criteria. Nonetheless, there has been a tendency to dichotomize cell death events into either of two mutually exclusive groups. Thus, caspase-dependent, tolerogenic, programmed and physiological cell death instances have been contrasted to their caspase-independent, immunogenic, accidental and pathological counterparts, respectively. In 2005, the Nomenclature Committee on Cell Death proposed a functional classification of cell death subroutines that applies to both *in vitro* and *in vivo* settings and included apoptosis, regulated necrosis, autophagic cell death and mitotic catastrophe. In the last year, they proposed a new classification of lethal signaling pathways based on biochemical and functional considerations. (Galluzzi *et al*., 2012)

1.9 Apoptosis

Apoptosis (from the Greek words από = from and πτωσις = falling) is one of the main types of programmed cell death. In contrast to necrosis, which is a form of cell death that results from acute cellular injury, apoptosis is carried out in an ordered process that generally confers advantages during an organism's life cycle. Apoptosis playes a critical role in controlling the number of cells in development and throughout an organism's life by the removal of cells at the appropriate time. It is an important biological process for the elimination of unwanted cells such as those with potentially harmful genomic mutations, autoreactive lymphocytes, or virally infected cells. Alterations of this normal process can result in the disruption of the delicate balance between cell proliferation and cell death and can lead to a variety of diseases (Galluzzi *et al*., 2012). For example, in many forms of cancer, key proapoptotic proteins are mutated or antiapoptotic proteins are upregulated, leading to the accumulation of cells and the inability to respond to harmful mutations, DNA damage, or chemotherapeutic agents.

1.9.1 Mechanism of apoptosis

In the last few years, much has been learned about the signal transduction pathways of programmed cell death, providing us with insight into how programmed cell death works and how dysregulation of apoptosis contributes to disease. The overall process of programmed cell death occurs in several stages. In the first step, the apoptotic pathway is triggered, which can be accomplished by a wide variety of stimuli, including DNA damage, growth factor withdrawal, toxins, and radiation. Once activated, the signal is transduced by a series of protein–protein interactions that involve a conserved set of signaling modules. In the next stage, cell death is executed by the activation of specific proteases called caspases that cleave multiple substrates, leading to changes characteristic of apoptotic cells such as DNA fragmentation, chromatin condensation, cell shrinkage, and membrane blebbing.

Caspases are a family of cysteine proteases that cleave their target proteins next to aspartate amino acids (thus the name "caspase": "c" for cysteine protease and "asp" for the strong aspartate preference) (Alnemri, 1996). They are constitutively present in most

mammalian cells and reside in the cytosol as single chain proenzymes. In fact the caspases are all expressed as proenzymes (30 to 50 kD) that contain three domains: an NH_2-terminal domain, a large subunit (~20 kD), and a small subunit (~10 kD). During activation, procaspases are cleaved to generate the large and small subunits of the active enzymes, typically liberating an N-terminal prodomain from the processed polypeptide chain. The active enzymes consist of heterotetramers composed of two large and two small subunits, with two active sites per molecule (Thornberry and Lazebnik, 1998; Cryns and Yuan, 1999) (figure 7).

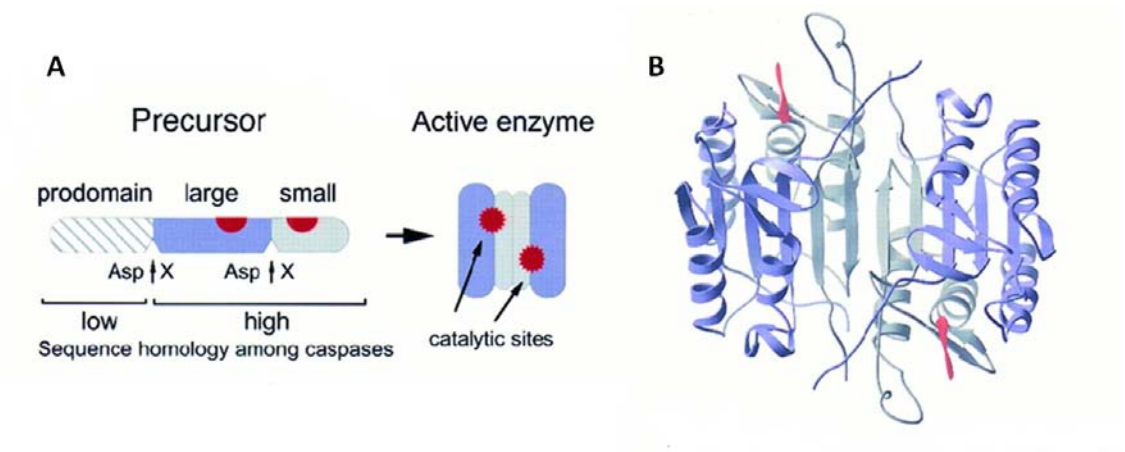

Figure 7. *Proposed caspase structure. A)* In common with other proteases, caspases are synthesized as precursors that undergo proteolytic maturation. The NH_2-terminal domain, which is highly variable in length (23 to 216 amino acids) and sequence, is involved in regulation of these enzymes. *B)* Shown is the crystal structure of caspase-3 in complex with a tetrapeptide aldehyde inhibitor (red). The active enzyme is composed of a large (20 kD, lavender) and small (10 kD, gray) subunit, each of which contributes amino acids to the active site. In the two crystal structures that are available, two heterodimers associate to form a tetramer. From Thornberry and Lazebnik, 1998

There are two types of caspases, upstream caspases called initiator caspases (e.g., caspases-8, -9, and -10), and their downstream targets known as effector or executioner caspases (e.g., caspases-3, -6, and -7) (Salvesen and Dixit, 1997).

Several components comprise the “caspase-centric” effector model of apoptosis and there

are two pathways associated with caspase activation, involving either the mitochondria or death receptors (figure 8) (Budihardjo *et al.*, 1999).

The mitochondrial pathway (named also intrinsic apoptotic pathway), is driven by various stimuli, e.g. DNA damaging agents, oxidative stress, hypoxia and growth factor deprivation, converging on mitochondria, the sensing organelles of this apoptotic pathway. The key event of the cascade is represented by mitochondrial outer membrane permeabilization. Following mitochondria permeabilization, the electron transport chain intermediate cytochrome c translocates from the intermembrane space of mitochondia to the cytosol where, togheter with dATP, can bind to Apoptotic Protein Activating Factor-1 (Apaf-1), allowing the formation of a multi-protein platform called the apoptosome, a seven-spoked, wheel shaped complex essential for the recruitment and subsequent activation of caspase-9 (Fadeel *et al*., 2008). Upon activation, caspase-9 in turn activates caspase-3 and caspase 7, thus promoting the execution of apoptosis.

The death receptor pathway (or extrinsic pathway) is promoted by soluble molecules belonging to the Tumor Necrosis Factor (TNF) family, normally secreted as homotrimers, which can bind to plasma membrane receptors of the TNF-Receptor (TNF-R) family (such as TNFR1, Fas, DR-3, DR-4, or DR-5), causing their trimerization and subsequent activation. TNF-Rs possess a Death Domain (DD) (Lahm *et al*., 2003) that is responsible for the recruitment of other DD-containing proteins, such as TNF-R type 1-Associated Death Domain protein (TRADD) and Fas-Associated protein with Death Domain (FADD). Procaspase-8 is then recruited, via the adaptor protein FADD (or TRADD), this promotes its homodimerization and activation by autocatalysis. The complex formed by TNF-R, FADD (and eventually TRADD) and caspases-8 and -10 is referred as Death-Inducing Signaling Complex (DISC) (Chaigne-Delalande *et al*., 2008; Pennarun *et al*., 2010). Upon activation, caspases-8 and -10 cleave the effector caspases-3, and -7, which are in charge of cellular dismantling during the final step of apoptosis (Chowdhury *et al*., 2008).

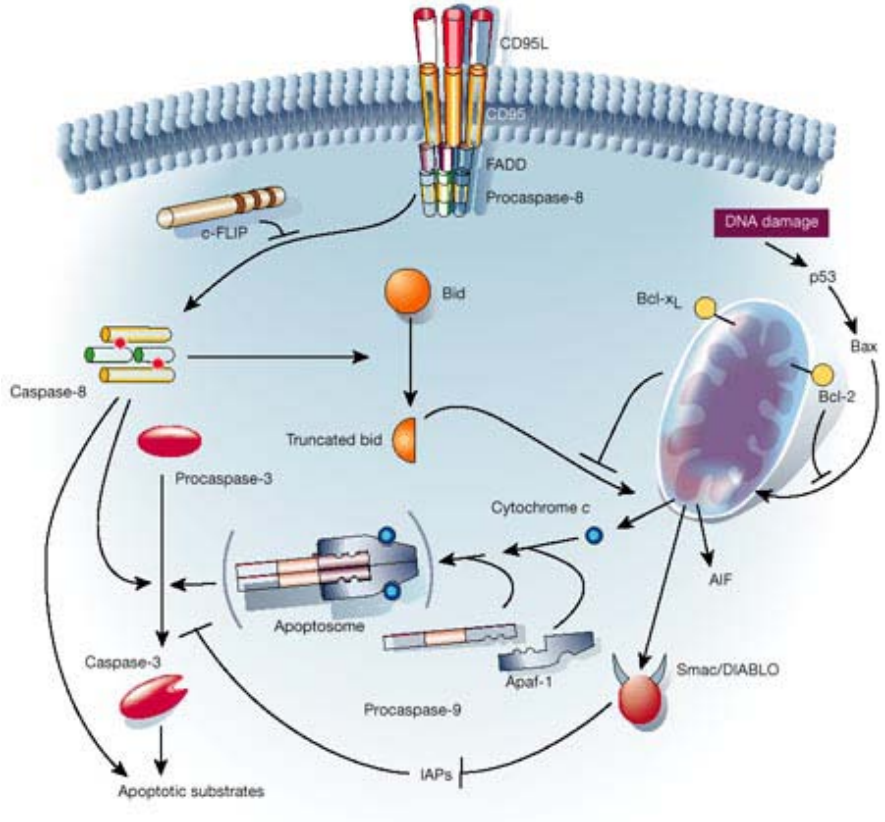

Figure 8. *Two major apoptotic pathways in mammalian cells.* The regulation of the intrinsic and extrinsic pathways of caspase activation during apoptosis. (Hengartern, 2000).

Activation of death receptors has also been shown to activate the intrinsic pathway, which appears to be required to execute apoptosis in certain cell types. In fact another notable target of caspase-8 is Bid (see Bcl-2 proteins family section). Thus, the recruitment of the intrinsic pathway of apoptosis by caspase-8 activation can serve to initiate and/or amplify intracellular signals to trigger apoptosis (Wang *et al*., 2005; Arnoult *et al*., 2003; Lu *et al*., 2003; Fu *et al*., 2002)

Caspases are controlled by specific cellular inhibitors called Inhibitor of Apoptotic Proteases (IAP), which can bind to them, thus blocking their function (Srinivasula and Ashwell, 208; Altieri, 2010). To counteract IAP function, Smac/DIABLO and HtrA2/Omi are released from mitochondria in order to bind to or cleave IAPs, respectively (Martinez-

Ruiz *et al*., 2008; Vande Walle *et al*., 2008). The last step of the apoptotic program is DNA degradation which is carried out by various nucleases (Scovassi and Torriglia, 2003), including Endonuclease G, which is released from mitochondria to the nucleus, where it cleaves DNA. DNA fragmentation occurs also during caspase-independent apoptosis, where it is mainly operated by L-DNase-II (Torriglia *et al*., 2000; Altairac *et al*., 2003*;* Brossas *et al*., 2004; Torriglia and Lepretre, 2009), and in parthanatos, which is characterized by PARP-1 activation and AIF translocation from mitochondria to the nucleus (Wang *et al.*, 2009). Once the cell has been committed to death and the apoptotic program is activated, cellular fragments are engulfed by professional or amateur phagocytes near the apoptotic cell, thus avoiding inflammatory response (Savill and Fadok, 2000).

At the heart of this mechanism, in addition to the caspase family, lies another family of proteins that control the process, the Bcl-2 extended family.. The Bcl-2 family is so called because of the relationship of its members to the B-cell lymphoma oncogene whose discovery led eventually to the identification of most of the other family members (Borner *et al*., 1994), but at the molecular level this family is remarkably diverse (Borner, 2003).

1.9.2 Bcl-2 proteins family

As one might imagine, apoptosis is highly regulated. One class of regulators is the Bcl-2 family of proteins that are subdivided into three groups on the basis of their pro- or antiapoptotic action and the Bcl-2 Homology (BH) domains they possess (Figure) (Schinzel *et al*., 2004; Youle and Strasser, 2008). Antiapoptotic Bcl-2-like proteins (e.g., Bcl-2, Bcl-xL, Bcl-w, Mcl-1, and A1/Bfl-1) and proapoptotic Bax-like proteins (e.g., Bax, Bak, and Bok/Mtd) display four BH domains (Kvansakul *et al.*, 2008). The proapoptotic BH3-only proteins (e.g., Bid, Bim/Bod, Bad, Bmf, Bik/Nbk, Blk, Noxa, Puma/Bbc3, and Hrk/DP5), on the other hand, possess only a short motif called the BH3 domain as their name indicates. The proapoptotic class is thus comprised of 2 groups, according to its content of Bcl-2 homology (BH) domains (figure 9).

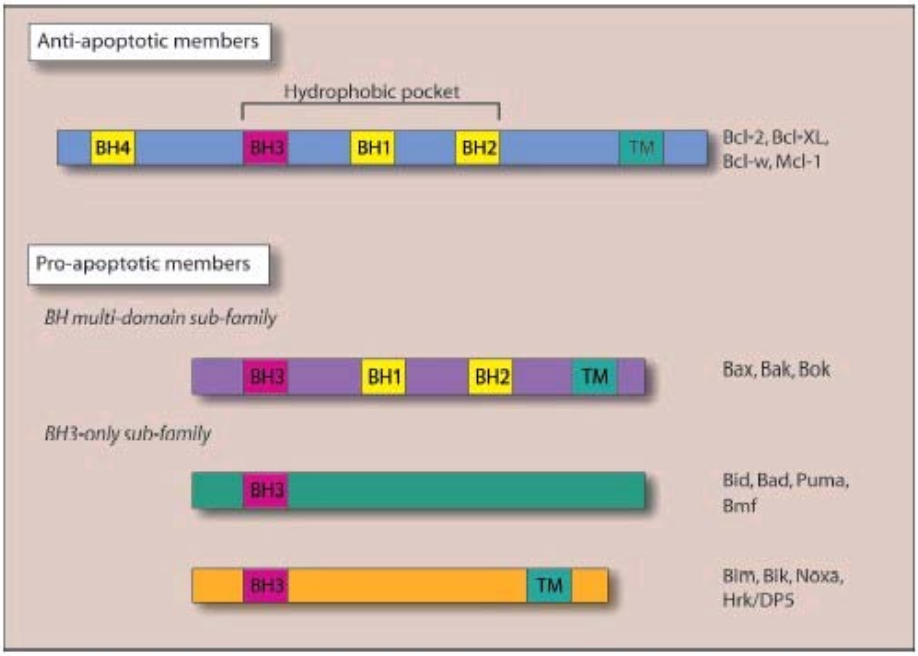

Figure 9. *Summary of anti-apoptotic and pro-apoptotic BCL-2 members.* BCL-2 homology regions (BH1-4) are denoted as the carboxy-terminal hydrophobic (TM) domain (Bras *et al.*, 2005).

The four BH domains contained by antiapoptotic members are absolutely required for their survival functions. The BH1–BH3 domains form a hydrophobic groove and the N-terminal BH4 domain stabilizes this structure. These domains do not have any enzymatic activity but mediate the interaction of Bcl-2 with other protein partners. For example Bcl-xL complexed with the BH3 domain of the death factors Bak or Bad (Borner, 2003). In this way Bcl-2-like survival factors act as membrane bound scavengers for BH3-containing death factors and other proapoptotic molecules.

The antiapoptotic proteins are tail-anchored in several intracellular membranes (mitochondria, nuclear/ER membranes) and perform their function in a monomeric state without any major change in conformation or subcellular localization. Removal of the C-terminal transmembrane tail leads to a cytoplasmic localization of these proteins where they are still partially active as survival factors.

The proapoptotic members like Bax and Bak contain BH domains 1–3 that form a hydrophobic pocket as in Bcl-2 and Bcl-xL. In contrast to Bcl-2-like survival factors, Bax-like factors either form channels or interact with channel forming proteins to increase

the permeability of the outer mitochondrial membrane promoting the release of the proapoptotic factors as cytochrome c, Smac/DIABLO (Smac: second mitochondrial activator of caspases; DIABLO: direct IAP binding protein with low pI) and Htr2A/Omi which stimulate the formation of the Apaf-1/caspase-9 apoptosome.

Another group of proapoptotic proteins contain only BH domain 3 (BH3) (e.g., Bid, Bad, Bim, Bik, PUMA, NOXA, etc.). BH3-only proteins, are activated by post-translational modifications. For example inactive Bad is phosphorylated at several serine residues and this allows its sequestration in the cytoplasm by binding to 14-3-3 scaffold proteins. The phosphorylation has been attributed to different kinases, such as Akt/PKB (a transducer of the survival signal of growth factors within the PI-3-kinase pathway), Raf (which links growth factor receptors to the MAPK cascade) and PKA. If growth factors or extracellular matrix are withdrawn, Bad is dephosphorylated and released from 14-3-3 thus becoming free to interact with Bcl-2-like survival factors (Zha *et al.*, 1996) and to promote the apoptotic machinery. BH3-only proteins can also be activated by proteolysis, a mechanism responsible for Bid activation in response to death receptor stimulation. In this case, death receptors activate caspase-8 which cleaves the inactive cytosolic form of Bid into a truncated fragment (tBid) that translocates to mitochondria (Li *et al.*, 1998; Luo *et al.*, 1998). The active form of Bid increases mitochondrial permeability by releasing Bax-like factors from Bcl-2, as well as by stimulating the oligomerization and membrane insertion of Bax or Bak. Moreover, recent evidence has been found showing that Bid can form membrane pores on mitochondria and can change lipid composition of the outer mitochondrial membrane making it more permeable during apoptosis (figure 10).

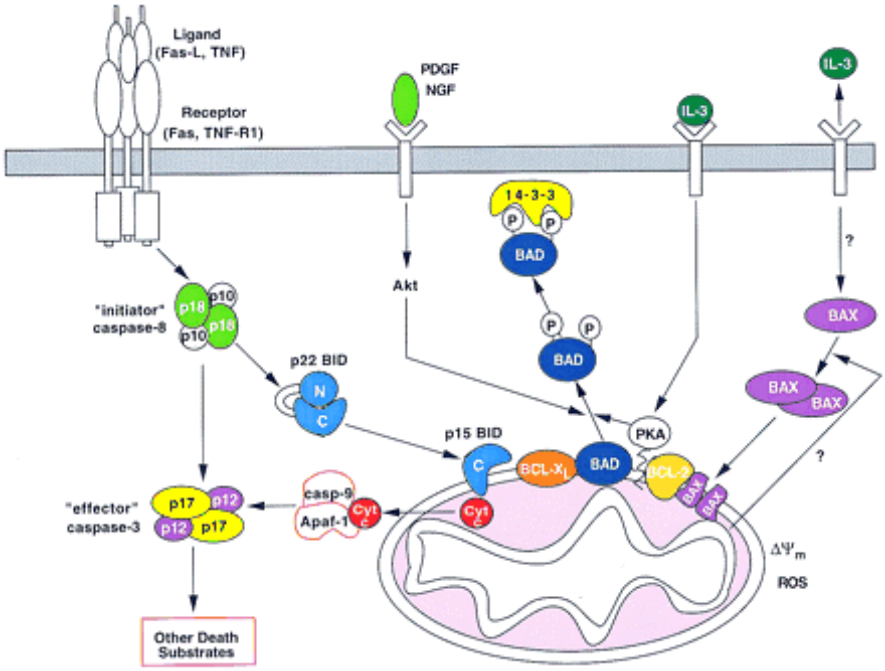

Figure 10. *Model of apoptotic and survival signaling pathways involving the Bcl-2 members.* (Left) Activation of the TNFα/Fas cell surface receptor leads to activation of caspase-8. Caspase-8 cleaves cytosolic p22 Bid generating a p15 carboxy-terminal fragment that translocates to the mitochondria resulting in the release of cytochrome c. Released cytochrome c activates Apaf-1, which in turn activates a downstream caspase program. (Right) A death stimulus (IL-3 deprivation) induces the translocation of Bax to the mitochondria where it is integral membrane and cross-linkable as a homodimer. (Center) Activation of the NGF or PDGF receptors mediates the activation of Akt, resulting in the phosphorylation of Bad at Ser-136. Activation of the IL-3 receptor mediates the activation of the mitochondrial-based PKA holoenzyme, resulting in the phosphorylation of Bad at Ser-112. Phosphorylated Bad is sequestered to the cytosol by the phosphoserine-binding protein 14-3-3 (Gross *et al.*, 1999).

1.10 Autophagy

The term autophagy comes from the Greek words αύτος (autos), which means self, and φαγέω (fageo), which means eat; it is a self-degradative process which ensures the regular turnover of cellular components by sequestering damaged organelles and misfolded proteins, targeting them for lysosomal degradation (Mizushima and Levine, 2010). Since its discovery, autophagy was considered a kind of disposal mechanism aimed at recycling of cellular components (Yang and Klionsky, 2010), but now it is clear that it is much more than a recycle bin, being involved in many cellular and physiological pathways, including development and differentiation (Mizushima and Levine, 2010).

Autophagy is activated as an adaptive catabolic process in response to different forms of metabolic stress, including nutrient deprivation, growth factor depletion, and hypoxia. This bulk form of degradation generates free amino and fatty acids that can be recycled in a cell-autonomous fashion or delivered systemically to distant sites within the organism. Presumably, the amino acids generated are used for the de novo synthesis of proteins that are essential for stress adaptation. The molecular basis for the recycling function of autophagy has only recently begun to be defined with the identification of yeast ATG22 as a vacuolar permease required for the efflux of amino acids resulting from autophagic degradation (Mizushima and Klionsky, 2007). It is presumed that the recycling function of autophagy is conserved in mammals and other higher organisms, although direct data proving this concept are lacking.

The amino acids liberated from autophagic degradation can be further processed and, together with the fatty acids, used by the tricarboxylic acid cycle (TCA) to maintain cellular ATP production. This role of autophagy in maintaining macromolecular synthesis and ATP production is likely a critical mechanism underlying its evolutionarily conserved prosurvival function. Thus, a critical physiological role of autophagy appears to be the mobilization of intracellular energy resources to meet cellular and organismal demands for metabolic substrates. The requirement for this function of autophagy is not limited to settings of nutrient starvation. Because growth factors are often required for nutrient uptake, loss of growth factor signaling can result in reduced intracellular metabolite concentrations and activation of autophagy-dependent survival mechanisms (Lum *et al.*,

2005). It is also possible that in certain settings, especially when cells suddenly have high metabolic needs, autophagy may be needed in a cell-autonomous fashion to generate sufficient intracellular metabolic substrates to maintain cellular energy homeostasis. This hypothesis may explain why there are high levels of autophagy in the mouse heart and diaphragm immediately following birth (Kuma *et al.*, 2004).

Moreover autophagy has been shown to mediate physiological cell death *in vivo*, during the developmental program of *D. melanogaster* and appears to be responsible for the death of some cancer cells (especially when they lack essential apoptotic modulators like BAX and BAK or caspases) that respond to a selected panel of chemotherapeutic agents *in vitro* (Galluzzi *et al*., 2012). Nonetheless, in most known cases, autophagy constitutes a cytoprotective response activated by dying cells in the attempt to cope with stress, and its inhibition accelerates, rather than prevents, cell death (Boya *et al*., 2005).

1.10.1 The process of autophagy

Autophagy is ubiquitous in eukaryotic cells and is a multi-step process involving initiation, autophagosome formation, maturation, and degradation controlled by a set of autophagy-related genes (ATG) (Mizushima, 2007). The process starts with the activation of the unc-51-like kinase (ULK), a serine/threonine kinase complex that includes ATG13 and FIP200. This complex is regulated by the mammalian target of rapamyacin (mTOR) which senses nutrient levels in the environment: under high-nutrient conditions inhibits autophagy by phosphorylation of ULK1/2; during periods of nutrient deprivation mTOR dissociates from the ULK1/2 complex and this allows dephosphorylation of ULK1/2 which, in turn, phosporylates and activates ATG13 and FIP200 (Xie and Klionsky, 2007, Rosenfeldt and Ryan, 2009 and Roy and Debnath, 2010). The initiation of autophagy is completed with the accumulation of the ULK1/2-ATG13-FIP200 complex, resulting in a site for development of the isolation membrane, also known as the phagophore (Jung *et al.*, 2009).

Like mTOR, AMP activated protein kinase (AMPK) is also a key sensor for cellular energy that is involved in the initiation of autophagy. During glucose starvation, AMPK inhibits mTOR, but it also directly interacts with ULK1, phosphorylating serines to activate autophagy. Interestingly, under amino acid starvation or pharmacologic

inhibition of mTOR with agents such as rapamycin, ULK1 is activated in an AMPK-independent manner (Kim *et al.*, 2011). AMPK phosphorylation of ULK1 and ULK2 is also associated with cellular mitophagy (autophagy that specifically targets mitochondria) and a loss of AMPK or ULK1 results in impaired autophagy and defective mitophagy (Egan *et al*., 2011).

Recent evidence has also identified a direct substrate of mTOR that negatively regulates autophagy. Death-associated protein 1 (DAP1) is inhibited by mTOR phosphorylation in nutrient rich conditions. Under starvation stress and loss of mTOR function, DAP1 is released from phosphorylation inhibition and suppresses autophagy. The exact mechanism through which DAP1 is able to suppress autophagy is unclear, though early evidence points towards an effect occurring between the mTOR complex and the LC3 conjugation systems. By activating and suppressing autophagy at the same time, this may create a counter-balance, or "gas and brake" method, to prevent over-activation of autophagy during starvation stress (Koren *et al.*, 2010a and Koren *et al.*, 2010b).

The development of the autophagosome (an intracytoplasmic vacuole containing elements of a cell's own cytoplasm that fuses with a lysosome and the contents are subjected to enzymatic digestion) is dependent on a class III phosphoinositide 3-kinase (PI3K) complex involving the proteins Vps-34, beclin1, and p150 (Simonsen and Tooze, 2009). This complex localizes to the phagophore and recruits further ATGs to allow for elongation and completion of the autophagosome. Studies have found that positive regulators binding to Beclin1 include ATG14 (Itakura *et al.*, 2008), ultraviolet radiation resistance-associated gene (UVRAG) (Liang *et al*., 2006) and Ambra (Fimia *et al*., 2007). The Rubicon molecule has been identified as a negative regulator, binding to beclin1 and reducing Vps34 activity and impairing autophagosome formation (Zhong *et al.*, 2009). Another significant negative regulator of autophagy is Bcl-2, which works by binding to the Beclin1 BH3 domain. While the Beclin1/Bcl-2 interaction does not necessarily alter the anti-apoptotic function of Bcl-2 (although this may vary depending upon the sub-cellular location of the Bcl-2 protein), it does influence the ability of Beclin1 to stimulate autophagy (Kang *et al.*, 2011). Bcl-2 binds Beclin1, stabilizing it in a dimer, blocking its ability to interact with Vps-34 and decreasing Beclin1-associated class III PI3K activity (Pattingre *et al*., 2005 and Noble *et al*., 2008).

Once the PI3K complex is activated, elongation of the phagophore is controlled by two

ubiquitin-like conjugation systems involving ATG12 and ATG8 (Ohsumi and Mizushima, 2004). In the first system, the E1-like ATG7 and E2-like ATG10 conjugate ATG12 to ATG5. This allows ATG12-ATG5 to bind with ATG16, creating a complex that localizes to the outer surface of the membrane. The second system involves ATG8 or its mammalian ortholog microtuble-associated protein light chain 3 (LC3). ATG8 is cleaved at the C-terminus by ATG4 (LC3-I) and then conjugated to phosphotidylethanolamine (PE) via ATG7 and E2-like ATG3. The ATG8-PE complex (LC3-II) binds to both the inner and outer membrane of the autophagosomes (Geng and Klionsky, 2008). Interaction between the two conjugation systems is essential to autophagy as the ATG16L complex targets LC3-1 to the phagophore membrane and accelerates its conjugation to PE (Fujita *et al*., 2008).

Once the autophagosome is created, maturation is completed by fusion with a lysosome to form an autophagolysosome. This process involves lysosomal-associated membrane proteins (LAMP) LAMP1 and LAMP2 as well as UVRAG and the GTPase Rab7. In addition to its binding to beclin1 to up-regulate phagophore formation, UVRAG interacts with class C Vps proteins and stimulates Rab7 and autophagosome/lysosome fusion and delivery of cargo for degradation (Liang *et al*., 2008). The final autophagolysosome is a single membrane acidic vesicle wherein lysosomal hydrolases such as cathepsins degrade intravesicular material into amino acids and other components, which are released and used for energy and as building blocks for cellular macromolecules (figure 11)

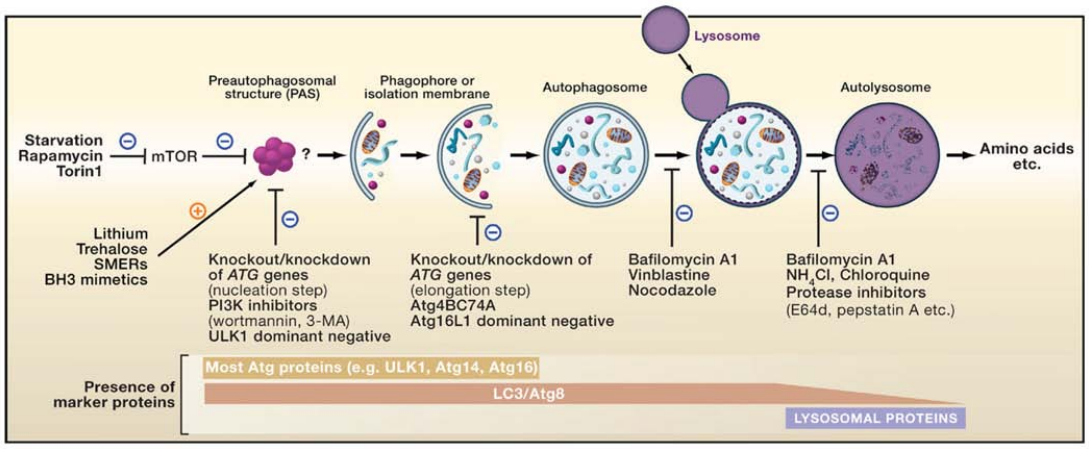

Figure 11. *The Process of Autophagy* A portion of cytoplasm, including organelles, is enclosed by a phagophore or isolation membrane to form an autophagosome. The outer membrane of the autophagosome subsequently fuses with the lysosome, and the internal material is degraded in the autolysosome. In yeast, autophagosomes are generated from the preautophagosomal structure (PAS), which has not yet been identified in mammalian cells. A partial list of treatments and reagents that modulate autophagy are indicated. Notably, lithium may also inhibit autophagy through mTOR activation. Atg proteins that have thus far been identified on isolation membranes include ULK1/2, Atg5, Beclin 1, LC3, Atg12, Atg13, Atg14, Atg16L1, FIP200, and Atg101. From Da Mizushima *et al*., 2010.

1.10.2 Autophagy in Life and Death Decisions of the Cell

Under most circumstances, autophagy constitutes a stress adaptation pathway that promotes cell survival. An apparent paradox is that autophagy is also considered a form of nonapoptotic programmed cell death called “type II” or “autophagic” cell death. This type of cell death has been historically defined by morphological criteria, but it is now clear that the mere presence of autophagosomes in dying cells is insufficient to distinguish “cell death with autophagy” from “cell death by autophagy.” The knockdown of ATG genes has recently defined whether autophagy functions in the execution of cell death in different settings (reviewed in Maiuri *et al*., 2007a).

It is not yet understood which factors determine whether autophagy is cytoprotective or cytotoxic and whether cytotoxicity occurs as the result of self-cannibalism, the specific

degradation of cytoprotective factors, or other as of yet undefined mechanisms (Maiuri *et al.*, 2007a). The most intuitive mechanism is self-cannibalism. However, cells subjected to prolonged growth factor deprivation or shortage of glucose and oxygen can lose the majority of their mass via autophagy and fully recover when placed in optimal culture conditions (Degenhardt *et al*., 2006; Lum *et al*., 2005), suggesting that cell death via autophagy may not be simply a matter of crossing a quantitative threshold of self-digestion. Although autophagy can independently influence life and death decisions of the cell (by being cytoprotective or self-destructive), it is also intricately linked to apoptotic death pathways. Factors that may control the cellular "decision" between the two responses include potentially variable thresholds for each process, molecular links that coordinately regulate apoptosis and autophagy, and mutual inhibition or activation of each pathway by the other (Maiuri *et al.*, 2007a).

1.10.3 Autophagic cell death and apoptosis

The morphological and biochemical features of autophagic cell death and apoptosis are generally distinct (Gozuacik and Kimchi, 2004; Bursch *et al*., 2000; Bursch, 2001). In autophagic cell death, unlike apoptotic cell death, caspases are not activated, and neither DNA degradation (measured by DNA laddering assays) or nuclear fragmentation are apparent. Instead, autophagic cell death is characterized by degradation of the Golgi apparatus, polyribosomes and endoplasmic reticulum before nuclear destruction — these organelles are preserved in apoptosis. Therefore, the occurrence of caspase-independent cell death, together with an increased number of autophagic vesicles, might be a hallmark of autophagic cell death (Gozuacik and Kimchi, 2004).

Although tumour cells have been observed to undergo both apoptosis and autophagic cell death in response to therapy, little is known about the connection between these two. Apoptosis and autophagy are not always separate, there can be crosstalk between the two pathways. In many cases, inhibition of apoptosis causes autophagy, and inhibition of autophagy triggers apoptosis. For example, when apoptosis was inhibited by defects in the function of the pro-apoptotic proteins BAX and BAK, autophagic cell death was triggered in MEFs and bone marrow-derived immortalized cells (Shimizu *et al*., 2004; Lum *et al*., 2005). When apoptosis was inhibited in mouse fibroblasts by a caspase-8

inhibitor, autophagic cell death, dependent on ATG7 and BECN1 activity, was induced, and autophagy inhibitors decreased the amount of cell death (Yu *et al*., 2004). Conversely, the use of autophagy inhibitors such as 3-MA, or inhibition of autophagy by small interfering RNAs (siRNAs) targeted against autophagy-associated genes, induced apoptosis in HeLa cells (Boya *et al*., 2005). In other settings, autophagy induction delayed sulindac sulphide (a non-steroidal anti-inflammatory drug)-induced apoptosis in colon cancer cells by sequestering mitochondrial death-promoting factors such as cytochrome c (Bauvy *et al*., 2001)). Inhibition of autophagy by the H^+-ATPase inhibitor bafilomycin A1 increased apoptotic cell death in various cancer cells treated by irradiation or chemotherapy (Kanzawa *et al*., 2004; Paglin *et al*., 2001; Kanzawa *et al*., 2003). Also, a same stimulus could promote apotosis or autophagy depending on the cell type, thus demostrating an interconnection between this two mechanisms of programmed cell death (Kanzawa *et al*., 2003; Pelicano *et al*., 2003)

1.10.4 Apoptosis and autophagy cross talk: crucial factors

The active search for common regulators of apoptosis and autophagy led to the discovery that Bcl-2 family members play a double (and opposite) role (reviewed in Zhou *et al*., 2011). Indeed, Bcl-2 and Bcl-XL bind to and inhibit Beclin 1 through the Beclin 1 BH3 domain (Maiuri *et al*., 2007). Under nutrient excess conditions, when autophagy is not necessary, the association between Bcl-2 and Beclin 1 is maximal, while decreases after cell starvation, i.e. when autophagy is essential to guarantee cell survival (Pattingre *et al*., 2005). The relevance of a finely tuned regulation of Beclin 1/Bcl-2 binding was further demonstrated by the evidence that Death-Associated Protein Kinase (DAPK) phosphorylates Beclin 1 on Thr119, thus promoting its dissociation from Bcl-2, and autophagy activation (Zalckvar *et al*., 2009). Of note, DAPK also participates in apoptotic bleb formation thanks to its interplay with cytoskeletal factors (Bovellan *et al*., 2010).

The existence of cross talk between autophagy and apoptosis is also supported by the double role of ATG5, which, in addition to the promotion of autophagy, enhances susceptibility to apoptotic stimuli. Overexpression of ATG5 sensitizes tumor cells to chemotherapy (Yousefi *et al*., 2006); by contrast, silencing of this gene results in partial resistance to anticancer drugs. It was shown that during apoptosis ATG5 is cleaved by

calpains. This event allows ATG5 translocation to mitochondria, where it interacts with Bcl-XL and controls cytochrome c release, caspase activation and apoptosis; on the contrary, in the absence of ATG5 within mitochondria, autophagy takes place (Yousefi *et al*., 2006; Bhutia *et al*., 2010). Another autophagic factor, ATG3, is controlled by FLICE-Inhibitory Protein (FLIP), which is a negative regulator of the extrinsic apoptotic pathway (being able to recognize and bind FADD through specific DED domains). Remarkably, within these domains, non-overlapping sequences are in charge of apoptosis inhibition and recognition and binding of ATG3; the latter event blocks the conjugation to LC3 and, in turn, autophagy (Lee *et al*., 2009). This points out a double role of FLIP, which can control both apoptosis and autophagy at the same time.

Moreover, it has been shown that caspases can degrade autophagic proteins. Caspase-3 (Luo and Rubinsztein, 2010) and other caspases (Cho *et al*., 2009; Wirawan *et al*., 2010) are able to cleave and inactivate Beclin 1, thus inhibiting autophagy and consequently enhancing apoptosis progression (Djavaheri-Mergny *et al*., 2010). Of note, N- and C-terminal fragments of Beclin 1 generated after the cleavage relocate to the nucleus and mitochondria, respectively. Remarkably, Beclin 1 C-terminal, which lacks the BH3 domain, induces cytochrome c and HtrA2/Omi release from mitochondria and subsequent amplification of the apoptotic stimulus.

A further link between these processes is represented by p62, also called sequestosome, a multifunctional protein that targets proteins to proteasome degradation and autophagy; p62 is implicated in autophagy progression as well as in apoptosis induction and cancer development (Moscat and Diaz-Meco 2009). LC3-II binds p62 to regulate protein packaging and delivering to the autophagosome, thus facilitating the clearance of misfolded/damaged proteins and deformed organelles through the autophagic machinery (Pankiv *et al*., 2007; Nezis *et al*., 2008; Kirkin *et al*., 2009; Mathew *et al*., 2009). Accumulation of p62 was described in autophagy-defective cells, which suffer from proteasome inactivation and altered NF-κB regulation, and undergo tumorigenesis (Mathew *et al*., 2009). The recent observation of a p62 role in modulating LC3-II degradation by the proteasome indicates that p62 is a crucial factor in the interplay between autophagy and proteasome activity (Gao *et al*., 2010). In the apoptotic scenario, the evidence for an effect of p62 on caspase-8 was provided; in fact, the critical initiator of the extrinsic apoptotic pathway requires p62 for its efficient polyubiquitination,

aggregation and full activation (Jin *et al*., 2009).

Also p53 is involved in the cross talk between apoptosis and autophagy. On the one hand, p53 regulates positively apoptosis by activating Bax and inducing mitochondrial depolarization; on the other hand, it increases the synthesis of DRAM and mTOR, both involved in the control of autophagy with opposite effects (Crighton *et al*., 2006). It is worth noting that especially the cytoplasmic form of p53 seems to be responsible for inhibition of autophagy, which can be rescued by blocking p53 itself (Tasdemir *et al*., 2008; Galluzzi *et al*., 2011). On the contrary, p53 post-transcriptionally down-regulates LC3 levels in starved cells, thus allowing a fine control of the autophagic flux, avoiding the "autophagic burst" that could be dangerous for cells (Scherz-Shouval *et al*., 2010).

Altogether, these observations support the existence of a cross talk between apoptosis and autophagy; however, how the intricate interconnection functionally affects the final outcome, remains a mystery.

Aim

The sodium pump, Na/K ATPase, could be an important target for the development of anti-cancer drugs as it serves as a versatile signal transducer, it is a key player in cell adhesion and its aberrant expression and activity are implicated in the development and progression of different cancers. The class of steroid-like compounds designated cardiac glycosides, known ligands of the sodium pump, includes well-known drugs such as digoxin, digitoxin, and ouabain. Their continued efficacy in treatment of congestive heart failure and as anti-arrhythmic agents is well appreciated. Less well known, however, is the emerging role of this category of compounds in the prevention and/or treatment of proliferative diseases such as cancer. Early epidemiological evaluations and subsequent demonstration of anti-cancer activity in vitro and in vivo have indicated the possibility of developing this class of compound as chemotherapeutic agents in oncology. New findings within the past years have revealed these compounds to be involved in complex cell-signal transduction mechanisms, resulting in selective inhibition of human tumor but not normal cellular proliferation. As such, they represent a promising form of targeted cancer chemotherapy.

Two cancer cell lines (one from lymphoblast and the other from a lung adenocarcinoma) will be used as a model for testing the effect of nanomolar concentration of ouabain against tumoral cell lines. Characterization of the cytotoxic effect of ouabain will be done studying morphological changes, biochemical features and using pharmacological inhibitors to block lethal signaling pathways. Western blotting analysis will be used to assess the three main groups of signal transduction pathways activated by the Na/K ATPase signalosome. Finally, it will be investigated the ouabain effect on the growth of human cancer cells in relation to Na/K ATPase α subunits expression.

Materials and Methods

3.1 Chemicals

Cell culture media, FBS, glutamine, antibiotics, elecrophoresis reagents, ouabain, 3-methyladenine (3MA), crystal violet, trypan blue, SYBERGreen JumpStart Taq Ready Mix, diethylpyrocarbonate, primers, dNTP mix and agarose were purchased from Sigma. 4-Amino-5-(4-chlorophenyl)-7-(t-butyl)pyrazolo[3,4-d]pyrimidine (PP2) and UO126 were from Calbiochem. Pan caspase inhibitor (Z-VAD-fmk) was purchased from MBL International Corporation. Chloromethyl-dichlorodihydrofluoresceindiacetate (CM-H_2DCFDA) and tetramethylrhodamine methyl ester (TMRM) were from Molecular Probes. RNAqueous extraction kit was from Ambion. Deoxyribonuclease I, Random examers, RNase OUT and HotStartTaq DNA Polymerase were purchased from Invitrogen. Caspase-Glo® 3/7 Assay was from Promega. ATPlite kit was from Perkin Elmer. Annexin V-FITC kit was from Immunotech. Tissue culture plastic were obtained from Falcon. Flat bottom, white 96-well plate were obtained form Perkin Elmer. Monoclonal antibody against α-tubulin, human GAPDH and human Bcl-2, polyclonal antibody against AMPK and α2 subunit of Na/K ATPase were purchased from Santa Cruz. Monoclonal IgG2a antibody to phosphorylated ERKs (p-ERK-1 and p-ERK-2) and against phospho-AMPK, polyclonal antibody against pSRC, LC3, phosphorylated Akt and overall Akt was from Cell Signaling. Monoclonal antibody against p62 was from Sigma Aldrich. Polyclonal antibody against LAMP2 was from Hybridoma Bank. Monoclonal antibody agains α1 subunit of Na/K ATPase was from Millipore, monoclonal antibody agains α3 subunit of Na/K ATPase was purchased from Affinity Bioreagent. Horseradish peroxidase-conjugated anti-mouse, anti-rabbit and anti goat IgG were from Santa Cruz Biotechnology. AlexaFluor488 anti-rabbit and AlexaFluor488 anti mouse were from Molecular Probes. Binding of the second horseradish peroxidase-conjugated antibody was detected with enhanced chemiluminescent detection reagent (Lite Ablot Turbo, Euroclone)

UO126, PP2 and Z-VAD-fmk were dissolved in dimethylsulfoxide (DMSO) and maintained at -20 °C. 3MA was dissolved in cell culture media just prior use, ouabain was dissolved in water and maintained at 4 °C for four weeks.

3.2 Cell culture

The human leukemic T cell line Jurkat was from Department of Oncology and Surgical Sciences, University of Padova. Jurkat were grown in RPMI medium supplemented with 10% (v/v) FBS, 2 mM glutamine, 100 U /mL penicillin-G, 100 µg/mL streptomycin.

A549 (human lung adenocarcinoma epithelial cell line) were from Istituto Zooprofilattico Sperimentale (IZS) of Brescia (Italy). A549 cells were grown in DMEM containing 10% (v/v) FBS, 2 mM l-glutamine, 100 U /mL penicillin-G, 100 µg /mL streptomycin.

3.3 Purification of peripheral blood mononuclear cells

PBMCs were purified from peripheral blood of healthy donors using Ficoll–Hypaque density gradient. Subjects were regular blood donors at the Transfusion Center of the Hospital (Padua, Italy). They all gave informed consent for blood drawing and treatment of clinical and laboratory data.

Procedure:

1. Blood was diluted with an equal volume of RPMI medium,
2. Diluited blood was carefullied overlay on top of 15 ml of Ficoll Hypaque solution in a 50 ml conical tube
3. The tube was centrifuged at 600×g for 40 min at room temperature.
4. Resultant layers (figure 12) are from top to bottom: Plasma plus platelets - PBMC - Ficoll - red blood cells (with granulocytes).

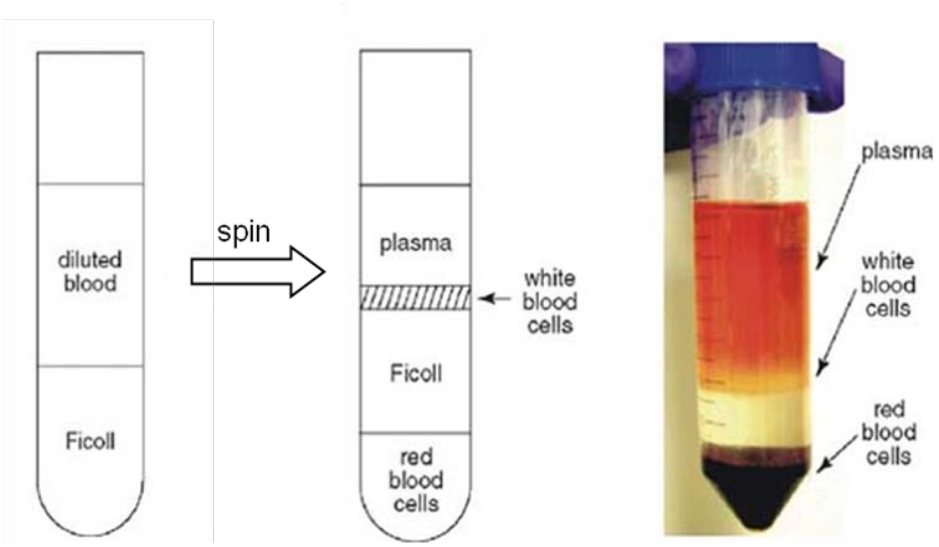

Figure 12 *Separation of PBMC using a Ficoll gradient*

5. The mononuclear cell layer was collected from interphase of RPMI/ Ficoll with a transfer pipette and transferred to a new 50 mL tube,
6. PBMC were washed with PBS and then centrifuged at 600×g for 15 min.
7. After discarding the supernatant, the pellet was washed twice with PBS and centrifuged at 300×g for 10 min.

PBMCs were counted using a hematocytometer with Trypan blue and maintained in RPMI 1640 medium supplemented with 10% FBS, 2 mM L-glutamine, 100 U/ml penicillin-G and 100 µg/ml streptomycin. Experiments were performed within seven days after purification.

Trypan blue solution

0,4% Trypan blue in PBS

3.4 Cell Viability Assays

3.4.1 Trypan blue exclusion assay

Trypan blue exclusion assay measures the percentage of viable cells in a suspension. The cells with an intact membrane are able to exclude trypan blue while cells without an intact membrane take up the coloring agent.

Procedure:

1. Cells were incubated with or without ouabain at the indicated concentrations for 24 h.
2. At the end of the treatment, cells were harvested and equal volume of cell suspension and Trypan blue were added to have a final concentration of 0.04%.
3. The counting chamber Burker hemocytometer was loaded with the diluition.

Cells excluding Trypan blue (viable cells) and cells permeable to Trypan blue (dead cells) were counted under the microscope.

Trypan blue solution

0.4% Trypan blue in PBS

3.4.2 MTT assay

MTT [3-(4,5-dimethylthiazol-2-yl)-2,5-diphenyltetrazolium bromide] assay, first described by Mosmann in 1983, is based on the ability of a mitochondrial dehydrogenase enzyme from viable cells to cleave the tetrazolium rings of the pale yellow MTT and form a dark blue formazan crystals which is largely impermeable to cell membranes, thus resulting in its accumulation within healthy cells. Lysis of the cells by the addition of a DMSO solution results in the liberation of the crystals which are solubilized. The number of surviving cells is directly proportional to the level of the formazan product created. The color can then be quantified using a multiwell scanning

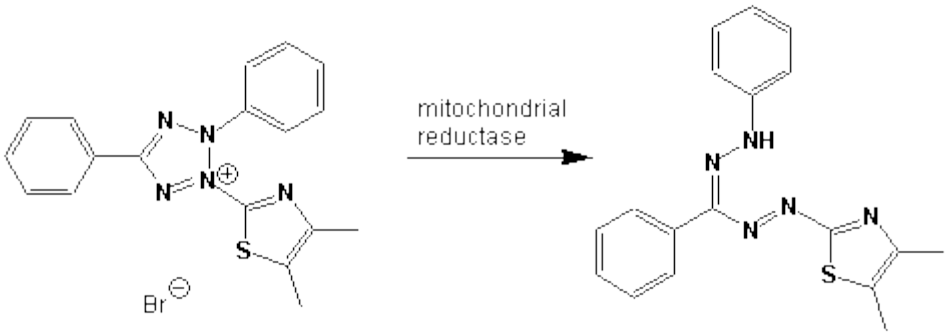

Figure 13. *Reduction of [3-(4,5-dimethylthiazol-2-yl)-2,5-diphenyltetrazolium bromide] (MTT) to formazan*

Procedure:

A549 cells:

1. A549 (1×10^4 cells/well) were plated in 200 µl media per well in a 96 well plate.
2. The cells were incubated (37°C, 5% CO_2) overnight to allow the attachment to the wells.
3. The day after, the cells were incuated with or without ouabain at the indicated concentrations for 24 hours.
4. Four hours before the end of the treatment 10 µl of stock solution of MTT was added to each well.
5. At the end of the treatment the incubation medium was removed and the formazan crystals were dissolved in 100 µl of DMSO.

Jurkat cells:

6. Jurkat were seeded in a 96-well plate (200 µl/well at the concentration of 2×10^5/ml) and incubated with or without ouabain at the indicated concentrations for 24 hours..
7. Four hours before the end of the treatment 10 µl of stock solution of MTT was added to each well.

8. At the end of the treatement the plate was centrifuged at 1800 rpm for 5 min, the supernatant discarded, and the formazan crystals were dissolved in 100 µl of solution of DMSO.

9. For both cell lines, MTT reduction was quantified by measuring the light absorbance with a multilabel plate counter (VICTOR^2 – Wallac) at 570 nm (with background subtraction at 630 nm). Absorbance from blank (media without cells) was subtracted. Quadruplicate wells were used for both control and treatment.

MTT solution 12 mM:

5 mg/ml of MTT was dissolved in PBS and filtered.

3.4.3 Clonogenic assay

A clonogenic assay is a technique for studying the effectiveness of specific agents on the survival and proliferation of cells.

Procedure

1. A549 (200 cells/well) were plated in a 6-well plate in complete medium.
2. The day after, the medium was carefully removed and cells were incubated with or without ouabain at the indicated concentrations for eight days.
3. At the end of the treatment colonies were washed with PBS, fixed with paraformaldehyde (4.0% v/v) for 10 minutes at room temperature, washed two times with PBS, stained with crystal violet (0.25% w/v) for 15 minutes at room temperature and counted using an inverted microscope. A colony is defined to consist of at least 50 cells.

Paraformaldehyde solution

1mL of Paraformaldehyde (36 %) in 9 mL of PBS

Crystal violet solution

0.25 g of crystal violet was dissolved in 90 mL methanol and 10 mL PBS

3.4.4 ATP Detection Assay

Adenosine triphosphate (ATP) is a marker for cell viability because it is present in all metabolically active cells and the concentration declines very rapidly when the cells undergo necrosis or apoptosis. Intracellular ATP content was detected using ATPlite 1step kit (Perkin Elmer). ATPlite 1step is a system based on the production of light caused by the reaction of ATP with added luciferase (of firefly *Photinus pyralis*) and D-luciferin. This is illustrated in the following reaction scheme:

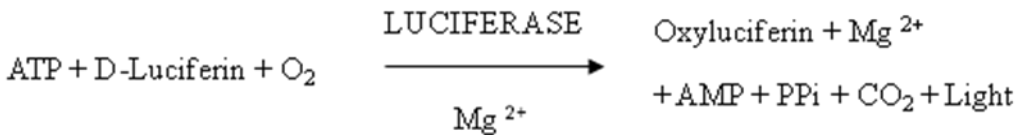

The emitted light is proportional to the ATP concentration.

Procedure:

1. A549 cells ($1x10^4$ cells/well) were seeded in 100 µL of culture medium in a flat-bottom, white 96-well plate and incubated with or without 100 µM Z-VAD-fmk in presence or absence of ouabain 100 nM for 24 hours.
2. 30 minutes before the end of the treatment the substrate vial and the buffer solution were equilibrate at room temperature and then reconstitute by adding the appropriate volume of buffer to the substrate vial. The contents of the vial were mixed by inversion and leave the solution to stand for 5 minutes.
3. At the end of the treatment an equal volume of reconstituted reagent was added to each wells and the plate was mixed briefly at 500 rpm on an orbital shaker for 60 second, shield from ambient light.
4. After incubation for 10 minutes at room temperature in the dark, the luminescence

of each sample was measured in a plate-reading luminometer (VICTOR^2 – Wallac). Quadruplicate wells were used for control and treatment, for blank and for negative control.

3.5 Apoptosis Assays

3.5.1 Caspase 3 assay

The Caspase-Glo® 3/7 Assay is a luminescent assay that measures caspase-3 and -7 activities. These members of the cysteine aspartic acid-specific protease (caspase) family play key effector roles in apoptosis in mammalian cells. The assay provides a luminogenic caspase-3/7 substrate, which contains the tetrapeptide sequence DEVD, in a reagent optimized for caspase activity. Luminescence is proportional to the amount of caspase activity present (figure 14).

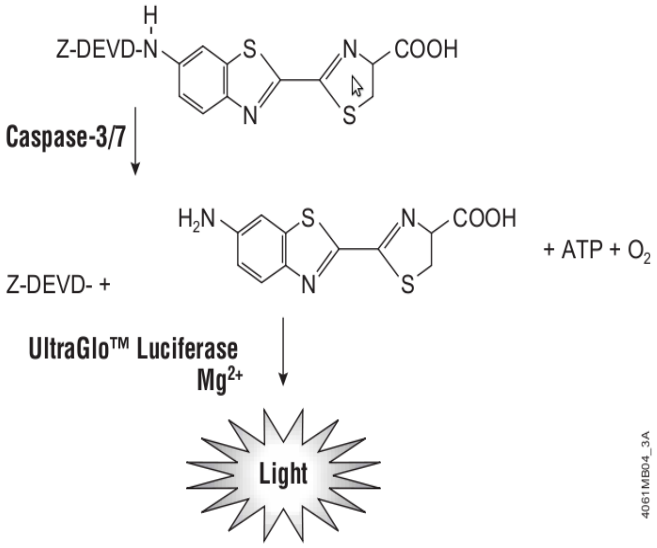

Figure 14: *Caspase-3/7 cleavage of the luminogenic substrate containing the DEVD sequence.* Following caspase cleavage, a substrate for luciferase (amino-luciferin) is released, resulting in the luciferase reaction and the production of light.

Procedure:

5. Cells ($1x10^4$ cells/well) were seeded in 100 µL of culture medium in a flat-bottom, white 96-well plate and incubated with or without ouabain at the indicated concentrations for the indicated time.
6. At the end of the treatment an equal volume of Caspase-Glo substrate was added to each well and the plate was mixed briefly at 500 rpm on an orbital shaker for 60 second, shield from ambient light.
7. After incubation for 30 minutes at room temperature in the dark, the luminescence of each sample was measured in a plate-reading luminometer ($VICTOR^2$ – Wallac). Quadruplicate wells were used for control and treatment, for blank and for negative control.

3.5.2 Flow cytometric analysis of annexin V and propidium binding

Annexin V, belonging to a family of proteins, the annexins, with anticoagulant properties, has proven to be a useful tool in detecting apoptotic cells since it preferentially binds to negatively charged phospholipids like phosphatidylserine (PS) in the presence of Ca^{2+} and shows minimal binding phosphatidylcholine. Changes in PS asymmetry, which is analyzed by measuring Annexin V binding to the cell membrane, were detected before morphological changes have occurred and before membrane integrity has been lost (figure 15). By conjugating FITC to Annexin V it is possible to identify and quantify apoptotic cells on a single-cell basis by flow cytometry. Staining cells simultaneously with Annexin V-FITC (green fluorescence) and the non-vital dye propidium iodide (PI) (red fluorescence) allows (bivariate analysis) the discrimination of intact cells (FITC-PI-), early apoptotic (FITC+PI-) and late apoptotic or necrotic cells (FITC+PI+ and PI+).

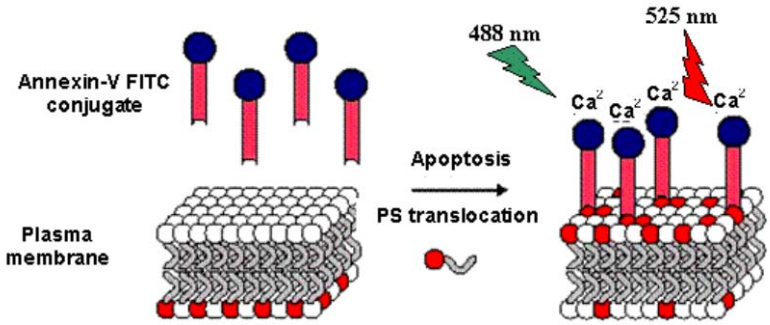

Figure 15. *Detection of early stage of apoptosis through binding of Annexin-V to phosphatidylserine.*

Procedure:

1. After the incubation with the drugs, A549 (1.5×10^5 cells/well) or Jurkat (5×10^5 cells/well) were harvested from 6-well or 12-well plates, respectively, and centrifuged at 1500 rpm for 10 minutes.
2. The cell pellet was resuspended in 100 µL of a binding buffer containing 0.125 µg/mL of Annexin V-FITC and 10 µM of propidium iodide.
3. The samples were incubated 15 min at room temperature in the dark.
4. The samples were diluted to 500 µL with binding buffer and analysed by flow cytometry (EPICS XL, Beckman Coulter). For each sample, 10,000 events were collected. Data acquisition and analysis were done using the EXPO^{TM} 32 ADC software (Beckman Coulter).

<u>Binding buffer:</u>

10 mM HEPES/NaOH (pH 7.4)

140 mM NaCl

2.5 mM $CaCl_2$

3.6 Mitochondial membrane potential

Mitochondrial membrane potential was measured using tetramethylrhodamine methyl ester (TMRM). TMRM is a cell-permeant, cationic, red-orange fluorescent dye that is readily sequestered by active mitochondria. Membrane potential-driven accumulation of TMRM within the inner membrane region of healthy functioning mitochondria results in a dramatic increase in TMRM-associated orange fluorescence.

Procedure:

1. A549 ($1.5x10^5$cells/well) were plated in a 6-well plate, Jurkat ($5x10^5$cells/well) were plated in a 12-well plate.
2. Cells were incubated with or without ouabain at the indicated concentrations for the indicated time.
3. 30 minutes before the end of the treatment, TMRM (200 nM) and cyclosporin H (4 μM) were added to each sample.
4. At the end of the treatment, cells were detached, centrifuged, suspended in PBS and analyzed at 575 nm by flow cytometry (EPICS XL, Beckman Coulter). For each sample 10,000 events were collected. Data acquisition and analysis were done using the EXPO^{TM} 32 ADC software (Beckman Coulter).

TMRM stock solution

100 μM in DMSO

cyclosporin H stock solution

4 mM in DMSO

3.7 ROS measurement

To determine intracellular ROS production, the fluorescent probe chloromethyl-dichlorodihydrofluorescein diacetate (CM-H_2DCFDA) was used. Diesterified probe can enter cells by simple diffusion across membranes. Once diffused in both cytoplasm and

different organelles, the ester moieties are hydrolyzed and the fluorescent dye is entrapped inside cells. Then, the probe can be oxidized, preferentially by hydrogen peroxide (H_2O_2), into the dehydrogenated form with excitation wavelength of 480 nm and emission wavelength of 530 nm (figure 16). Fluorescence signal is an index of intracellular ROS levels.

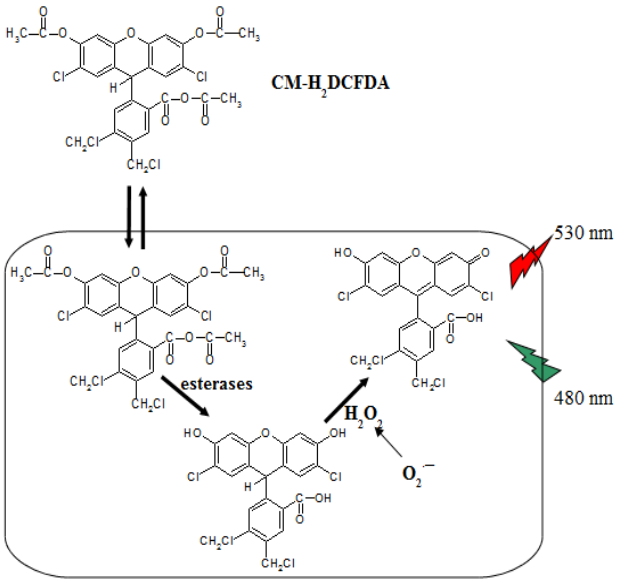

Figure 16 *Schematic representation of ROS detection with the fluorescent dye chloromethyl-dichlorodihydrofluorescein diacetate (CM-H_2D*CFDA)

Procedure

1. A549 (1.5x10^5cells/well) were plated in a 6-well plate, Jurkat (5x10^5cells/well) were plated in a 12-well plate.
2. Cells were incubated with or without ouabain at the indicated concentrations for the indicated time.
3. 30 minutes before the end of the treatment, CM-H_2DCFDA (5 µM) was added to each sample.
4. At the end of the treatment, cells were detached, centrifuged, suspended in PBS and analyzed at 575 nm by flow cytometry (EPICS XL, Beckman Coulter). For each sample 10,000 events were collected. Data acquisition and analysis were done using the EXPO^{TM} 32 ADC software (Beckman Coulter).

CM-H_2DCFDA stock solution

2.5 mM in DMSO

3.8 Immunocytochemistry

For immunocytochemistry, A549 cells were plated on a glass coverslip (previously sterilized with ethanol) and treated with 100 nM ouabain for the indicated time; Jurkat cells were treated with 100 nM ouabain for 6 hours then centrifuged, bound to a glass coverslip previously washed with hydrochloric acid and treated with poly-L-lysine to promote cell adhesion.

The procedure used for immunocytochemistry is divided into the below steps:

Fixation

At the end of the treatment, the cells were fixed in 4% paraformaldehyde in PBS pH 7.4 for 10 minutes at room temperature. The cells were then washed tree times with PBS to eliminate paraformaldehyde.

Permeabilization

To permeabilize cell membranes and improving the penetration of the antibody, cells were incubated for 10 minutes with PBS containing 0.1% Triton X-100 (Sigma).

Blocking and Incubation

Cells were incubated with 10% serum in PBS for 10 minutes to block non specific binding of the antibodies.

Primary antibodies (see Table 2), diluted in PBS with 5% serum, were applied for 1 hour in a humidified chamber at 37°C. Following washing with PBS 3x5 min, cells were incubated at room temperature for 1 h in the presence of the appropriate secondary antibody-fluorophore conjugate, diluted in PBS: goat anti-rabbit (1:500, AlexaFluor488, Molecular Probes), or goat anti-mouse (1:500, AlexaFluor488, Molecular Probes).

Following washing in PBS 3x5 min, samples were incubated at 37°C for 15 min with a solution of 100 ng/mL RNAse in PBS. Cells were washed three times with PBS.

Mounting and analysis

Coverslips were mounted with a drop of the mounting medium Mowiol (Sigma) in presence of 0,075% Propidium Iodide (Sigma).

Images were collected with a Nikon C1 confocal microscope and analysed using either Nikon EZ-C1 (version 2.1) or NIH ImageJ (version 1.32J) softwares.

Table 2. *Primary antibodies for Immunocytochemestry*

Protein	**Antibody**	**Dilution**
LC3 microtubule-associated protein1 light chain 3	Rabbit polyclonal	1:100
p62 polyubiquitin-binding protein	Rabbit monoclonal	1:100
LAMP 2 Lysosomal-Associated Membrane 2	Rabbit polyclonal	1:200
alpha 1 subunit of Na/K ATPase	Mouse monoclonal	1:50
alpha 3 subunit of Na/K ATPase	Mouse monoclonal	1:100

Poly-D-Lysine stock solution

Poly-D-Lysine (MW 30-70 kDa) was dissolved in PBS at 2 mg/mL and stored at 4°C.

Phosphate Buffered Saline with Triton (PBS-T) (100 ml):

0.1 mL Triton X100 in 99.9 mL PBS

Paraformaldehyde:

4% paraformaldehyde in PBS, pH 7.4

3.9 Western blotting Analysis

a) **Cell lysates of A549**: After treatment, the cells (2×10^6 cells/sample) were washed twice in the dish with ice-cold PBS and then PBS was drained off with a syringe. A549 were lysed in 100 μL of ice-cold lysis buffer with a rubber policeman and centrifuged at 10,000 g for 15 min at 4°C.

Protein content of cell lysates was determined by the BCA procedure using bovine serum

albumin as standard. The supernatant was heated for five minutes at 90°C. 30 µg of proteins were subjected to SDS-PAGE.

b) **Cell lysates of Jurkat**: After treatment 4×10^6 cells/sample were lysed in 200 µL of ice-cold lysis buffer and centrifuged at 10,000 g for 15 min at 4°C. Protein content of cell lysates was determined by the BCA procedure using bovine serum albumin as standard. The supernatant was heated for five minutes at 90°C. 30 µg of protein was subjected to SDS-PAGE.

Procedure:

1. Samples were loaded into gel and run in running buffer, for 1h at 40 mA (2002 power supply LKB Bromma). A molecular weights marker was used (PageRuler Prestained Protein Ladder, Fermentas).
2. Separated proteins were transferred to PDVF membrane (Hybond-P, Amersham), previously soaked in methanol. The gel was sandwiched together with the membrane between Whatman paper, two porous pads (all equilibrated in transfer buffer for few minutes) and two plastic supports. The blot sandwich was placed into the Mini-Transblot electrophoresis system (Bio-Rad) filled with transfer buffer, the membrane facing the anode. A constant current of 200 mA was applied for 4 h at 4°C.
3. Non specific binding sites were blocked by immersing the membrane in blocking solution, and shaking for 60 min at room temperature.
4. The membrane was exposed to the primary antibody (1:2500) in TBS/Tween-20 containing 2.5% (w/v) non fat-dried milk, overnight at 4°C.
5. After 3x15 min washes with TBS-Tween 20 at room temperature with gentle agitation, the membrane was incubated with horseradish peroxidase (HRP)-linked secondary antibody (1:50000) in TBS-Tween 20 for 1 hour at room temperature.
6. The membrane was washed 3x15 min with TBS-Tween 20.
7. The signal was detected by chemiluminescence using the enhanced chemiluminescent detection reagent (Lite Ablot Turbo, Euroclone). The

detection reagent was pipetted onto the membrane, which was placed with protein side up on a clean suitable surface. After 5 min of incubation at room temperature the chemioluminescent signal was detected using VersaDoc Imaging System (Bio-Rad). Molecular weight standards were used to identify appropiate antibody binding.

8. LC 3 protein was detected using a 15% Resolving gel; α subunits of Na/K ATPase were detected using a 8% Resolving gel; the others protein were detected using a 10% Resolving gel

Solution

Lysis buffer: PBS

1% Triton X100

0.5 mM phenylmethylsulfonyl fluoride

2 mM Na_3VO_4

10 μg/ml leupeptin

25 μg/ml aprotinin

1.25 mM NaF

1 mM Na-pyrophosphate

5X Laemmli buffer: 6.8 ml distilled water

2 ml 0.5 M Tris pH 6.8

3.2 ml glycerol

1.6 ml 20% SDS

0.8 ml β-mercaptoethanol

1.6 ml 1% bromophenol blue

8% Resolving gel**:** 2.82 ml distilled water

1.04 ml 40% acrylamide-N,N'-methylenebisacrylamide

1.3 ml 1.5 M Tris pH 8.8

50 µl 10% SDS

50 µl 10% ammonium persulfate ($(NH_4)_2S_2O_8$)

5 µl N,N,N',N'-Tetramethylethylenediamine (TEMED)

10% Resolving gel**:** 2.3 ml distilled water

1.3 ml 40% acrylamide-N,N'-methylenebisacrylamide

1.3 ml 1.5 M Tris pH 8.8

50 µl 10% SDS

50 µl 10% ammonium persulfate

5 µl N,N,N',N'-Tetramethylethylenediamine (TEMED)

15% Resolving gel**:** 1.65 ml distilled water

1.95 ml 40% acrylamide-N,N'-methylenebisacrylamide

1.3 ml 1.5 M Tris pH 8.8

50 µl 10% SDS

50 µl 10% ammonium persulfate

5 µl N,N,N',N'-Tetramethylethylenediamine (TEMED)

4% Stacking gel**:** 3.05 ml distilled water

0,65 ml 40% acrylamide-N,N'-methylenebisacrylamide

1.25 ml 0,5 M Tris pH 8.8

50 µl 10% SDS

50 µl 10% ammonium persulfate

5 µl N,N,N',N'-Tetramethylethylenediamine (TEMED)

Running Buffer: 25 mM Tris

125 mM Glycine

0,1 % SDS

Transfer Buffer: 25 mM Tris

192 mM Glycine

TBS-Tween 20: 50 mM Tris

150 mM NaCl

0,1 % Tween20

Blocking solution : 5 g non fat dry milk

100 ml TBS-Tween20

3.10 Protein Assay

Protein content of cell lysates was determined by Bicinchoninic Acid Protein Assay Kit (Sigma).

The principle of the bicinchoninic acid (BCA) assay is similar to the Lowry procedure, in that both rely on the formation of a Cu^{2+}-protein complex under alkaline conditions, followed by reduction of the Cu^{2+} to Cu^{+}. The amount of reduction is proportional to the protein present. It has been shown that cysteine, cystine, tryptophan, tyrosine, and the peptide bond are able to reduce Cu^{2+} to Cu^{+}. BCA forms a purple-blue complex with Cu^{+} in alkaline environments, thus providing a basis to monitor the reduction of alkaline Cu^{2+} by proteins.

Procedure

1. In a 96 wells plate 12.5 µL of protein sample were mixed with 100 µL of BCA Working Reagent (prepared by mixing 50 parts of Reagent A with 1 part of Reagent B)
2. The plate was incubated for 30 minutes at 37 °C. This allowed purplish color development with a peak of absorbance of 562 nm.
3. The absorbance of the sample at 570 nm was recorded using a plate reader (VICTOR2, Wallac) and the protein concentration was determined by comparison to a standard curve (using BSA).

3.11 DNA fragmentation analysis protocol

3.11.1 DNA extraction

The characteristic breakdown of the nucleus during apoptosis comprises collapse and fragmentation of the chromatin, degradation of the nuclear envelope and nuclear blebbing, resulting in the formation of micronuclei. Therefore, DNA fragmentation can be a useful tool for identifying a distinctive feature of apoptosis at the biochemical level. This method was used as a qualitative method for detecting apoptosis.

Procedure

1. A549 (15×10^6 cells/sample) were plated in complete medium. The day after, the cells were incubated with 100 nM ouabain for 24 hours.
2. Jurkat ($15x10^6$ cells/sample) were incubated with 100nM ouabain for 24 hours.
3. At the end of the treatment the culture medium was removed and centrifuged at 3000 × g for 5 min to collect detached cells.
4. Cells were lysed with 500 µL of hypertonic lysis buffer (400 mM NaCl, 10 mM tris-HCl pH 7.8, 1 mM EDTA, 0.1% NP40) and then pooled with pellets made of detached cells.
5. RNA was digested using RNase (0.1 mg/ml at 37 °C for 1 h) followed by

proteinase K treatment for 2 h at 50 °C.

6. DNA was extracted with a mixture of phenol, chloroform, and isoamyl alcohol (25:24:1).
7. DNA was precipitated by adding an equal volume of isopropyl alcohol, stored overnight at 20 °C, and centrifuged at 12,000 × g for 15 min at 4 °C.
8. The pellet was air-dried, resuspended in 20 μL tris acetate EDTA buffer supplemented with 2 μL of sample buffer (0.25% bromphenol blue, 30% glyceric acid, 0.62 mM Ficoll 400).

Tris-acetate-EDTA (TAE) (50X):

40 mM Tris-acetate

1 mM EDTA (pH 8.0)

3.11.2 DNA spectrophotometric quantification

Using the Beer-Lambert law it is possible to relate the amount of light absorbed to the concentration of the absorbing molecule (in our case, DNA). At a wavelength of 260 nm, the extinction coefficient for double-stranded DNA is 50 $(\mu g/ml)^{-1} cm^{-1}$. Thus, an optical density (or "OD") of 1 corresponds to 50 μg/ml for double-stranded DNA. The absorbance of DNA samples at 260 nm and 280 nm, diluted in sterile distilled water, was used to evaluate DNA concentration and protein contamination (A260/A280 ratio). The concentration of DNA was calculated by the following equation:

$$[DNA] \text{ in } \mu g/\mu L = (A260 \times D)/1000$$

Where 1 optical density unit is equivalent to 50 μg/ml double stranded DNA, and D is the dilution factor.

3.11.3 Agarose gel electrophoresis of DNA

Agarose (2 %) was dissolved in boiling 1X TAE buffer containing 1 μg/ml ethidium bromide. The gel was then cast on a gel bed with a suitable comb using a horizontal gel apparatus. Gel was placed in an electrophoresis tank containing 1X TAE buffer to a level just above the gel surface. Equal amount of sample were loaded into gel. During electrophoresis an electrical potential difference of 6 V/cm was applied to the gel. Gel was then visualized and photographed using Gel Doc (BioRad).

Tris-acetate-EDTA (TAE) (50X):

40 mM Tris-acetate

1 mM EDTA (pH 8.0)

Running buffer:

0.8 mM Trizma base

20 mM Glacial acetic acid

0.02 mM EDTA (pH 8.0)

0.1 μg/mL Ethidium bromide

Ethidium bromide is an intercalating fluorescent compound used as nucleic acid stain for both double-stranded DNA and single-stranded RNA. When excited at 260 nm wavelength it emits fluorescence at 590 nm.

3.12 RNA methodology

3.12.1 Total RNA extraction.

Total RNA was extracted from cells using RNAqueous extraction kit (Ambion).

Procedure:

1. A549 (3×10^6 cells) were plated in complete medium. The day after cells were incubeted with 100 nM ouabain for the indicated time.
2. At the end of the treatment cells were detached, centrifuged, suspended in 350 μL of Lysis/Binding Solution and pipetted up and down several times to completely lyse the cells and obtain a homogenous lysate.
3. Then 350 μL of 64 % ethanol was added to the lysate and gentle mixed
4. The lysate-ethanol mixture was applied to a filter cartridge assembled in a collection tube (supplied in the kit) and centrifuge 30 sec at 15000 rcf.
5. 700 μL of Wash Solution #1 was applied to the filter cartrige and then centrifuged 30 sec at 15000 rcf. The flow-through was discarded.
6. 500 μL of Wash Solution #2/3 was added to the filter cartrige and then centrifuged 30 sec at 15000 rcf. The flow-through was discarded. This step was repeated two times.
7. Finally the filter cartrige was putted into a fresh collection tube and 40 μL of preheated Elution Solution was added in the center of the filter. The eluate was recovered by centrifugation for 30 sec at 15000 rcf. This step was repeated two times and the second elution was collected into the same tube as the first elution.
8. The RNA was mixed with 40 μL of LiCl Precipitation Solution, incubated at -20 C for 60 minutes and centrifuged at 12,000 g for 15 min at 4°C. RNA appeared as a gel-like pellet, and the supernatant was removed.
9. RNA was washed with 75 % ethanol in RNAse-free water (1 ml ethanol) and centrifuged at 11,000 g for 15 min at 4°C. Afterwards, RNA was briefly air-dried, then dissolved in RNAse-free water and stored at -80°C.

RNase-free water:

0.01% diethylpyrocarbonate (DEPC)

Autoclaved distilled water in RNase-free glass bottles

3.12.2 Preparation of RNA sample prior to RT-PCR.

Duplicate tubes were prepared for the positive and negative reverse transcriptase (RNA) samples used in the amplification reaction. To avoid DNA contamination all samples were treated for 15 min at room temperature with Deoxyribonuclease I, Amplification Grade (Invitrogen). To a RNase-free 0.5-ml microcentrifuge tube were added the following:

7 μL RNA sample
1 μL 10X DNase I Reaction Buffer (200 mM Tris-HCl pH 8.4, 20 mM $MgCl_2$, 500 mM KCl)
0.5 μL DNase I, Amp Grade, 1U/μL
DEPC-treated water to 10 μL

After an incubation of 30 minutes at room temperature, DNase I was inactivated by the addition of 1 μL of 25 mM EDTA solution (pH 8.0) (Invitrogen) to the reaction mixture. DNase was completely denatured by heating at 70°C for 15 min.

3.12.3 Agarose gel electrophoresis of RNA for quality determination

Agarose was dissolved in boiling 1X TAE buffer. The gel was than cast on a gel bed with a suitable comb using a horizontal gel apparatus. Gel was placed in an electrophoresis tank containing 1X TAE buffer to a level just above the gel surface. For gel electrophoresis, to each RNA sample was added 0.62 mM Ficoll 400 (Sigma Aldrich), a highly branched sucrose and epichlorohydrin copolymer that acts as a stabilizer in the electrolyte, and 4 μg/mL Orange G sodium salt (Sigma Aldrich), as tracking dye for nucleic acid gel electrophoresis. During electrophoresis an electrical potential difference of 6 V/cm was applied to the gel. Gel was then placed on a 3UV transilluminator for

viewing. A single fluorescent band near the loading lane is assigned to high molecular weight RNA, while a fluorescent smear directed to the anode suggests partial or total RNA degradation.

3.12.4 RNA spectrophotometric quantification

The yield of total RNA was determined by measuring the spectrophotometric absorption at 260 nm. The absorbance of RNA samples at 260 nm and 280 nm, diluted in sterile distilled water, was used to evaluate protein contamination (A260/A280 ratio). A260 should be higher than 0.15, with an absorbance of 1 unit at 260 nm corresponding to 40 μg RNA per ml. This relation is valid only for measurements at neutral pH. The A260/A280 ratio was determined and used to assess the purity of the sample. The concentration of RNA purified was calculated by the following equation:

[RNA] in μg/μL = (A260 x D)/1000

Where 1 optical density unit is equivalent to 40 μg/mL single-stranded RNA, and D is the dilution factor.

3.12.5 First-Strand cDNA Synthesis

Retrotranscription reaction mixture was prepared in a final volume of 10 μL. The following components were added to a nuclease-free microcentrifuge tube:

1 μL 75 ng/μL Random examers (Invitrogen)
0.5 μL 10 mM dNTP Mix (Sigma Aldrich)
5 μL total RNA

The mixture was heated to 65°C for 6 min for primer annealing and incubated on ice for at least 1 min. To the tubes was then added:

2 μL 5X RT Buffer (Fermentas)
0.5 μL RNase OUT (Invitrogen)
0.5 μL SuperScriptTM III Reverse Transcriptase (Fermentas)

SuperScript™ III Reverse Transcriptase is an engineered version of M-MLV (Moloney Murine Leukemia Virus) RT, with RNase H activity and an increased thermal stability.

RT reaction was performed at 50°C for 70 min and inactivated by heating at 75°C for 15 min. cDNA was stored at -20°C until use.

3.12.6 Amplificability of cDNA samples

Many substances are known RT-PCR inhibitors and may compromise DNA amplificability: haemoglobin, urea, humic acid, citric acid, polysaccharides, bilirubin, heparin, DNA extraction reagent residues, chelants, Triton X-100, and sodium dodecyl sulfate (Wilson, 1997). Amplification of a fragment of glyceraldehyde 3-phosphate dehydrogenase (GAPDH) was used as a control for DNA quality and amplificability. Non-amplificable sample DNA was re-extracted and the amplification of the GAPDH house-keeping gene was repeated. To specifically amplify a 101 base pair (bp), the GAPDH fragment primers reported in Table 3 (see below) were used.

cDNA samples were amplified using HotStarTaq® DNA Polymerase (Invitrogen) in a MX 3000P Thermal Cycler (Stratagene). All reaction mixtures were prepared in an area separate from that used for DNA preparation, and disposable tips containing hydrophobic filters were used to minimize cross-contamination.

PCR mix composition:

1 μL 10X PCR Buffer (Invitrogen)
0.25 μL 25 mM $MgCl_2$
0.25 μL dNTP mix (Sigma)
500 nM Forward Primer
500 nM Reverse Primer
2.5 units/reaction HotStarTaq DNA Polymerase (Invitrogen)
0.5 μL cDNA
DEPC water to 10 μL

A negative control (without template DNA) was always included to evaluate accidental reagent contamination.

Each PCR program started with an initial heat activation step at 94°C for 4 min, followed by 30 cycles of 30 s at 94°C, 30 s at 60°C and 72°C for 30 s. At the end, the mix is maintained at 72°C for 7 min, and then cooled to 25°C until reaction stop. The final PCR products were detected by agarose gel electrophoresis and stained with 1.6 % GelRed (Biotium Inc., U.S.A.).

3.12.7 Real Time Quantitative PCR

Real Time PCR allows one to measure the amount of PCR product after each round of amplification, making use of a fluorescent label that binds to the accumulating DNA molecules. Fluorescence values are recorded during each cycle of the amplification process. The fluorescent signal is directly proportional to the DNA concentration. The linear correlation between PCR products and fluorescence intensity is used to calculate the amount of template present at the beginning of the reaction. Within the exponential increase phase, the point upon the amplification baseline at which the detected fluorescence is significantly higher than the background signal is called the threshold cycle or Ct Value; it is inversely correlated to the logarithm of the initial DNA copy number. At the threshold level it is assumed that all reactions contain an equal number of specific amplicons. As a qPCR detection method the fluorescent binding dye SYBR® Green I was used: it binds all double-stranded DNA (dsDNA). After excitation at 497 nm, an increase in emission fluorescence at 520 nm results during the polymerization step followed by a decrease as DNA is denatured. Fluorescent measurements are taken at the end of the elongation step of each PCR cycle. SYBR® Green I binds non-specifically to any dsDNA, which results in non specific fluorescence. Non-specific binding yields fluorescence readings in the "no template control" (NTC) due to dye molecules binding to primer dimers and misprimed products. The specificity of qRT-PCR was tested in reaction without reverse transcriptase (no-RT control) to evaluate the specificity of DNA amplification, with DNase-digested RNA. qPCR was performed in a final volume of 10 µL.

Reaction mix composition:

5 µL SYBRGreen JumpStart Taq ReadyMix (Sigma Aldrich)
0.1 µL ROX
200 nM Forward Primer (see Table 3)
200 nM Reverse Primer (see Table 3)
0.5 µL cDNA
DEPC water to 10 µL

Typical thermal profile: initial denaturation (94°C, 2 min), 50 cycle denaturation (94°C, 30 s), primer annealing (60°C, 30 s), and elongation (72°C, 40s) steps, followed by a final denaturation step (72°C, 7 min).

To test reaction efficiency, a standard curve was generated performing qPCR with a serial dilution of template containing the PCR target, and extending past both the highest and lowest levels of target expected in test samples.

Table 3. *Real Time RT-PCR primer pairs.*

Gene	**Primer sequence (5'-3')**
Homo sapiens glyceraldehyde-3-phosphate dehydrogenase (GAPDH), mRNA	Forward primer CACCATCTTCCAGGAGCGAG Reverse primer CCTTCTCCATGGTGGTGAAGAC
Homo sapiens ATG4 autophagy related 4 homolog B (S. cerevisiae) (ATG4B), mRNA	Forward primer ATCGCTGTGGGGTTTTTCTG Reverse primer GACCCCAGGATTTTCAAAGG
Homo sapiens beclin 1, autophagy related (BECN1), mRNA	Forward primer TGAATGAGGATGACAGTGAACA Reverse primer CATCTGGTTTTCAACACTCTTC
Homo sapiens ATG12 autophagy related 12 homolog (S. cerevisiae) (ATG12), mRNA	Forward primer CTTACGGATGTCTCCCCAGA Reverse primer ATGAGTCCTTGGATGGTTCG
VPS34 Homo sapiens phosphoinositide-3-kinase, class 3 (PIK3C3), mRNA	Forward primer AAGCAGTGCCTGTAGGAGGA Reverse primer TGTCGATGAGCTTTGGTGAG
Homo sapiens BCL2/adenovirus E1B 19kDa interacting protein 3 (BNIP3), mRNA	Forward primer CTCCACCAGCACCTTTTGATGA Reverse primer GAACGCAGCATTTACAGAACAA
Homo sapiens BCL2/adenovirus E1B 19kDa interacting protein 3-like (BNIP3L), mRNA	Forward primer CTACCCATGAACAGCAGCAA Reverse primer ATCTGCCCATCTTCTTGTGG

3.13 Statistical analysis

Results are presented as mean ± standard error of the mean (SE). Statistical significance of the differences between experimental groups were calculated by one-way ANOVA followed by the linear trend's, Dunnett's or Bonferroni's Multiple Comparison Test; $P<0.05$ was considered to be statistical significant. Graphs and statistical analysis were performed using GraphPad Prism version 5.0 for Windows, GraphPad Software.

Results

4.1 Effect of ouabain on cell survival and proliferation

Exponentially growing cultures of Jurkat and A549 cells were incubated with increasing doses of ouabain and the number of viable cells was evaluated after 24 h of treatment using MTT test. Ouabain elicited a decrease in cell viability in a dose- and time-dependent manner in both cell lines with a maximum effect at 100 nM, the highest dose used (figure 17).

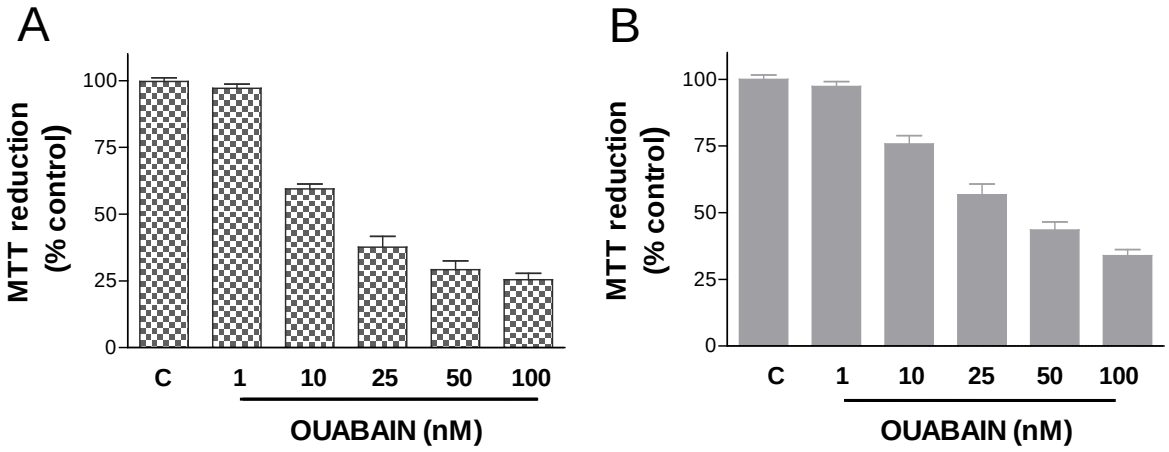

Figure 17. *Effect of ouabain on cell viability in A549 (A) and Jurkat (B) cells.* Both A549 and Jurkat cells were incubated with ouabain (1-100 nM) for 24 h, MTT assay was performed as described in Methods. Data are expressed as mean ± SE of four experiments performed in sixtuplicate. $P<0.0001$, One-way ANOVA, post-test for linear trend.

A reduction of tumor cell number determined by MTT test might depend upon the occurrence of cell death (cytotoxic effect) or antiproliferative activity (cytostatic effect). Thus, to further characterize the effects of ouabain on MTT reduction, the ability of the cardenolide to induce cell death or to affect proliferation was further investigated. Jurkat and A549 cells were exposed for 24 or 48 h to different concentrations of ouabain, then phosphatidylserine translocation at the cell surface and cell membrane permeability was measured by flow cytometric analysis of Annexin V–FITC/PI staining. Double-staining of cells with Annexin V and PI allows for the discrimination of living cells (unstained with either fluorochrome, Annexin V^-/PI^-) from early apoptotic cells (Annexin V^+/PI^-), late apoptotic cells (Annexin V^+/PI^+) or necrotic cells (stained only with PI). Figure 18 shows that ouabain caused an increase in the percentage of cells in both early and late apoptosis, without any significant increase in the percentages of necrotic cells (Annexin V^-/PI^+) at 50 and 100 nM.

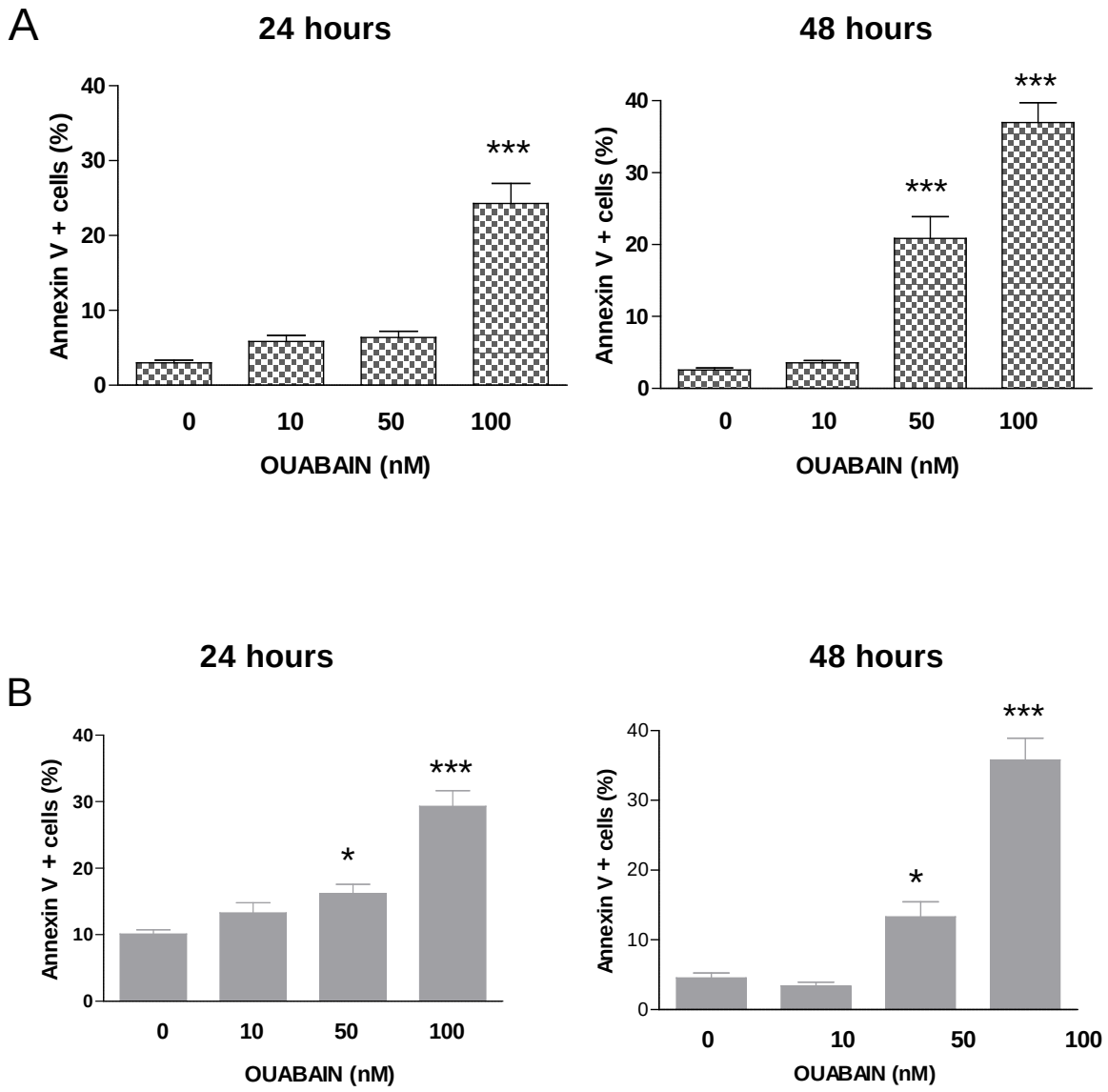

Figure 18. *Effect of ouabain on annexin V binding in A549 (A) and Jurkat (B) cells.* Cells were treated with ouabain (10-100nM) for the indicated time. Then flow cytofluorimetric analysis of Annexin V binding was performed as described in Methods. Data are expressed as mean ± SE. of four experiments performed in triplicate. ***P<0.0001, *P<0.05 One-way ANOVA, post-test Dunnet

At low concentration (1-20 nM) ouabain induced an antiproliferative effect, as seen with Trypan blue exclusion assay and clonogenic assay. Trypan blue exclusion assay showed that ouabain (20 nM) caused a decrease in the number of A549 and Jurkat cells with no increase in the fraction of Trypan blue permeable cells. The antiproliferative effect of low concentrations of ouabain was clear after 72 hours of treatment (figure 19).

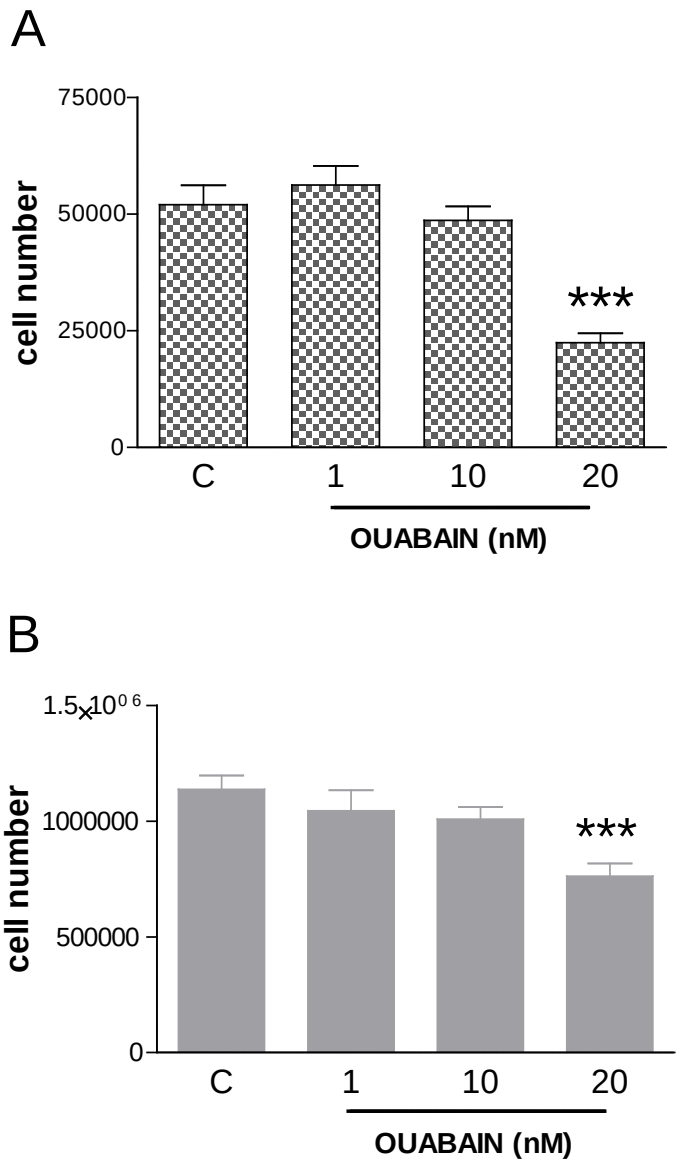

Figure 19. *Effect of ouabain on cell number measured by Trypan blue exclusion in A549 (A) and Jurkat (B).* Cells were incubated with ouabain (1-20 nM) for 72 h. Ouabain did not increase the percentege of Trypan blue permeable cells respect to the control. Data are expressed as mean ± SE of four experiments preformed in duplicate. ***P<0.0001 (vs control) One-way ANOVA, post-test Dunnet

The clonogenic assay was performed to confirm the antiproliferative action of low concentrations of ouabain in A549 cells. Clonogenic assay is a technique for studying the effectiveness of specific agents on the survival and proliferation of cells and for detecting slight effect on cell grown not detectable with other methods. Figure 20 shows that incubation of cells in a medium containing 20 nM ouabain for 8 days significantly reduced the number of A549 colonies. These results indicate that low concentrations of ouabain inhibit cell proliferation while ouabain concentrations above 50 nM induce cell death both in A549 and Jurkat cells.

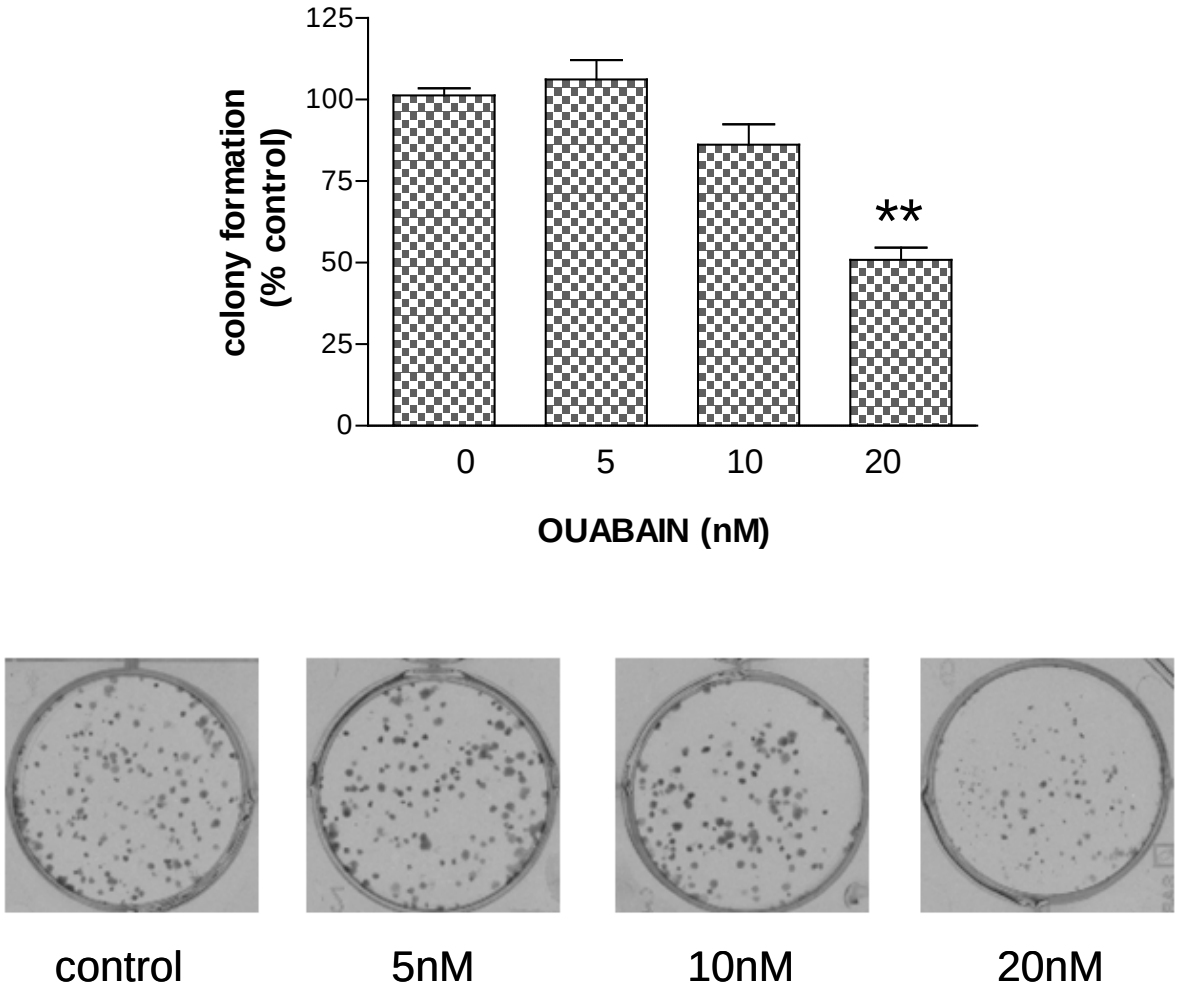

Figure 20. *Effect of ouabain on colony formation in A549 cells*. Cells were treated with ouabain (1-20nM) for eight days. At the end of the treatment colony formation was measured as described in Methods. *(A)* Data are expressed as mean ± SE of three indipendent experiments performed in duplicate. **P<0.001 (vs control) One-way ANOVA, post-test Dunnet *(B)* Images of wells treated with Crystal violet from a representative experiment are shown. Images were collected using VersaDOC (Bio-Rad) (80mm plane)

In the last years many in vitro studies have demonstrated that cardiac glysosides regulate cell survival and proliferation in a different manner depending whether the cell line is normal (inducing proliferative and antiapoptotic effects) or is a cancer cell line (inducing cell death) (see Introduction). In agreement with these reports, we have previously demonstrated that nanomolar concentrations of ouabain have an antiapoptotic effect in HUVEC (Trevisi *et a*l., 2004). In order to compare the effect of ouabain in not transformed human lymphocytes with its effect on Jurkat, a series of experiments were performed with human peripheral blood mononuclear cells (PBMC). Figure 21 shows that incubation of PBMC for 48 h with (10-100 nM) didn't increase AnnexinV/PI binding, thus demonstrating that in normal blood mononuclear cells ouabain is not cytotoxic. However, in contrast to HUVEC and other normal cell lines, ouabain did not protect PBMC from apoptosis induced by staurosporine.

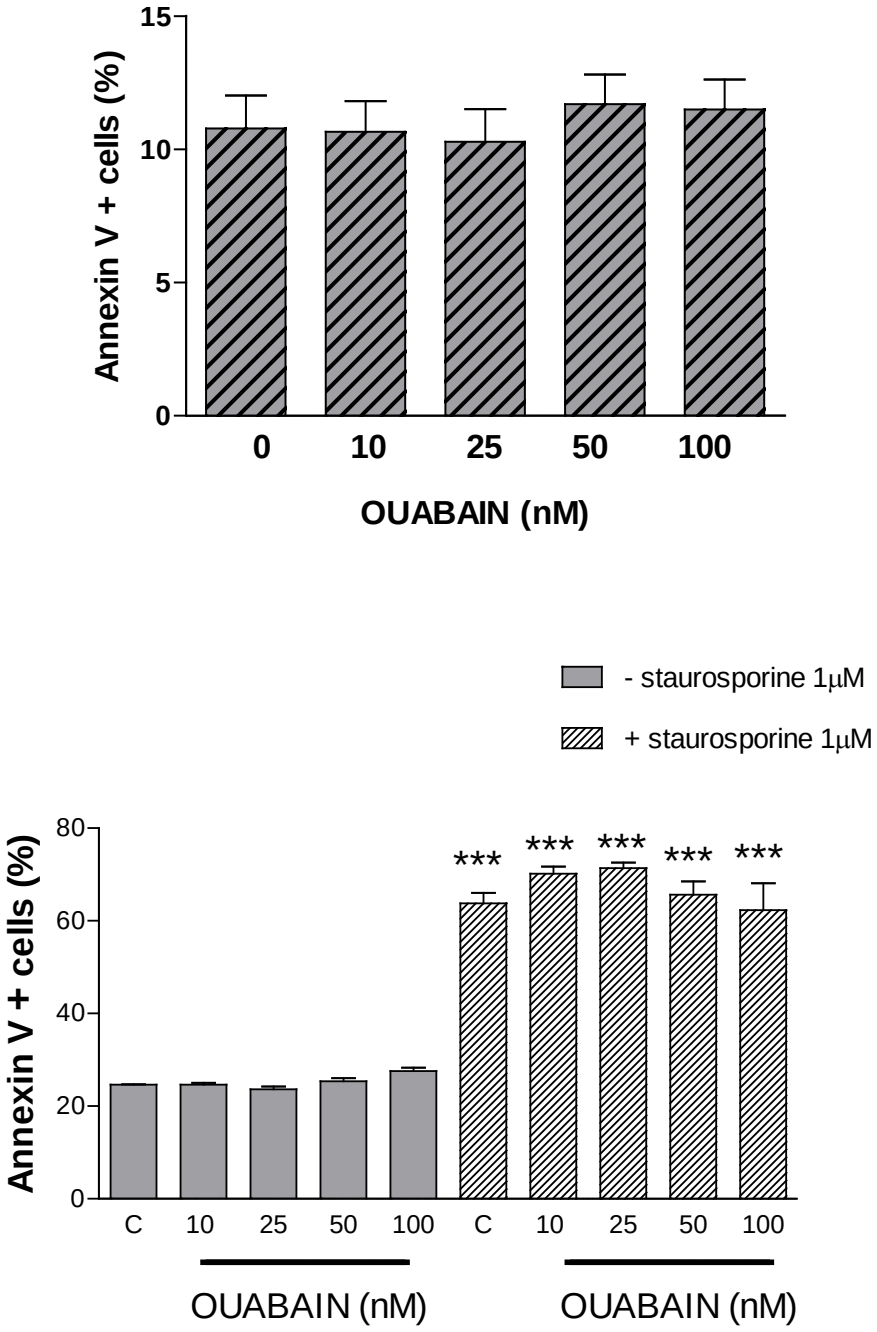

Figure 21. *Effect of ouabain on Annexin V binding in PBMC. (A)* Cells were treated with ouabain at the indicated concentration for 48 hours *(B)* Cells were incubated with ouabain at the indicated concentration and then staurosporine 1μM was added for 24 hours.

At the end of the treatment flow cytometry analysis of Annexin V binding was performed, as described in Methods. Data are expressed as mean ± SE of three indipendent experiments performed in triplicate. ***P<0.0001 (vs control) One Way ANOVA, post test Dunnet

4.2 Signaling pathways activated by ouabain

4.2.1 Src-MEK-ERK pathway

Binding of ouabain to Na/K ATPase stimulates Src kinase, which in turn phosphorylates EGFR, leading to activation of Ras-Raf-MEK-ERK pathway (see Introduction). Rapid activation of Src family kinases after ouabain binding to the Na/K ATPwas demonstrated in different cells types, including cardiac myocytes, vascular smooth muscle cells and kidney epithelial cells (Aydemir-Koksoy *et al*., 2001; Haas *et al*., 2000; Haas *et al*., 2002). Furthermore, it has been suggested that the antiproliferative and apoptotic effect of bufalin in PC-12 cells is due to a sustained ERK activation and cell cycle arrest (Subramaniam and Unsicker, 2006). For this reason, it was investigated whether ouabain induces activation of Src-ERK pathway also in Jurkat and A549 cells. Western blotting analysis showed that in both cell lines the treatment with 100 nM ouabain induced an increase in Src and ERK 1/2 phosphorylation that was detected after 30 min and persisted after 24 h (Figure 22). To investigate the role of Src and ERK activation in the cytotoxic action of ouabain two inhibitors were used: PP2, a specific inhibitor of Src family kinases (Hanke *et al*., 1996) and U0126, a specific inhibitor of MEK, the kinase that activates ERK 1/2 (Favata *et al*., 1998). As shown in figure 23A, treatment of A549 cells with PP2 (50 μM) or U0126 (10 μM) did not abolish the cytotoxic activity of 100 nM ouabain. In Jurkat both inhibitors attenuated the effect of ouabain (figure 23B).

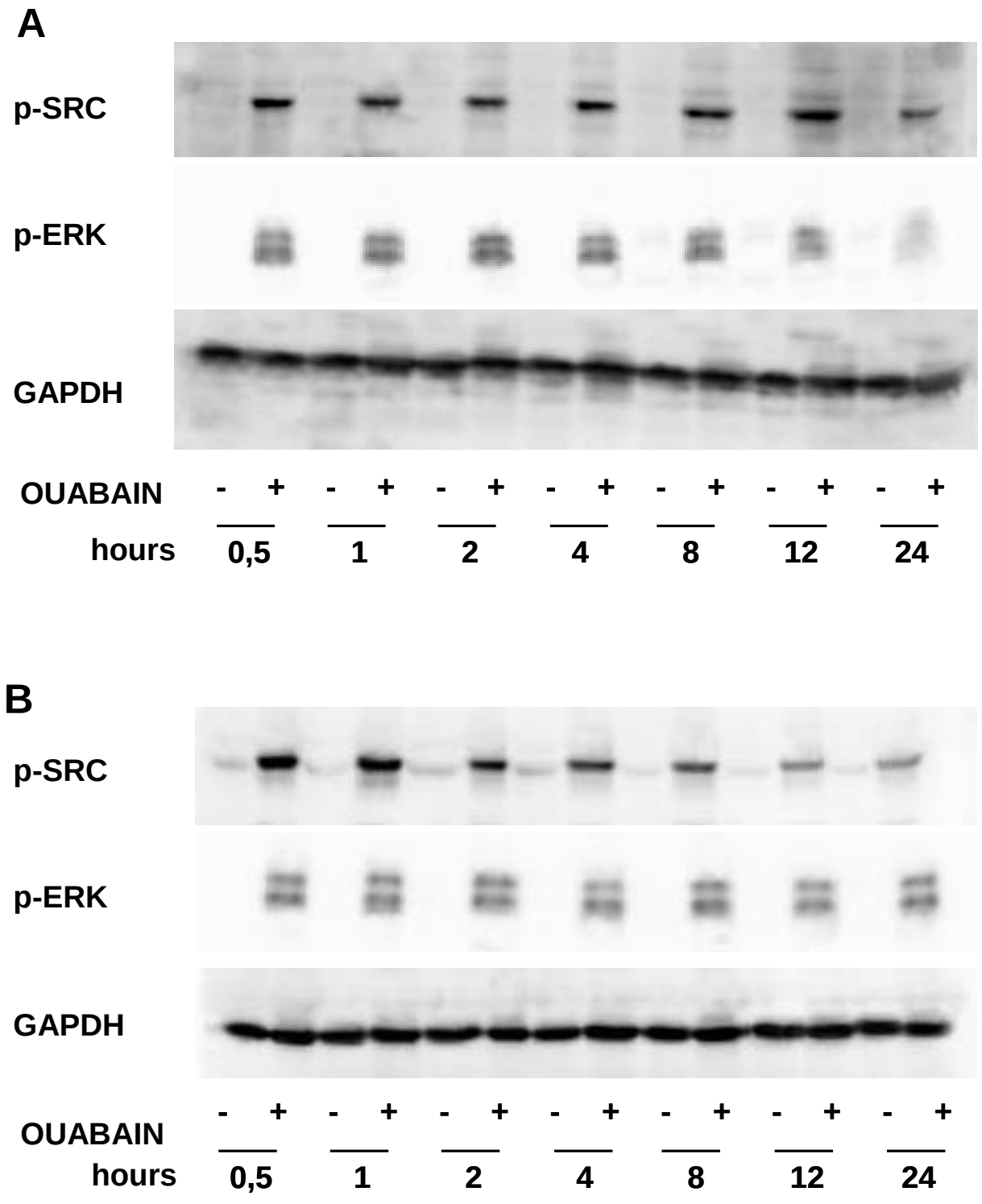

Figure 22. *Western blot analysis of Src and ERK phosphorylation in A549 (A) and Jurkat (B) cells.* Cells were treated with or without ouabain 100 nM for the indicated time. At the end of the treatment cells were lysed and Western blot analysis was performed as described in Methods. A rapresentative experiment is shown.

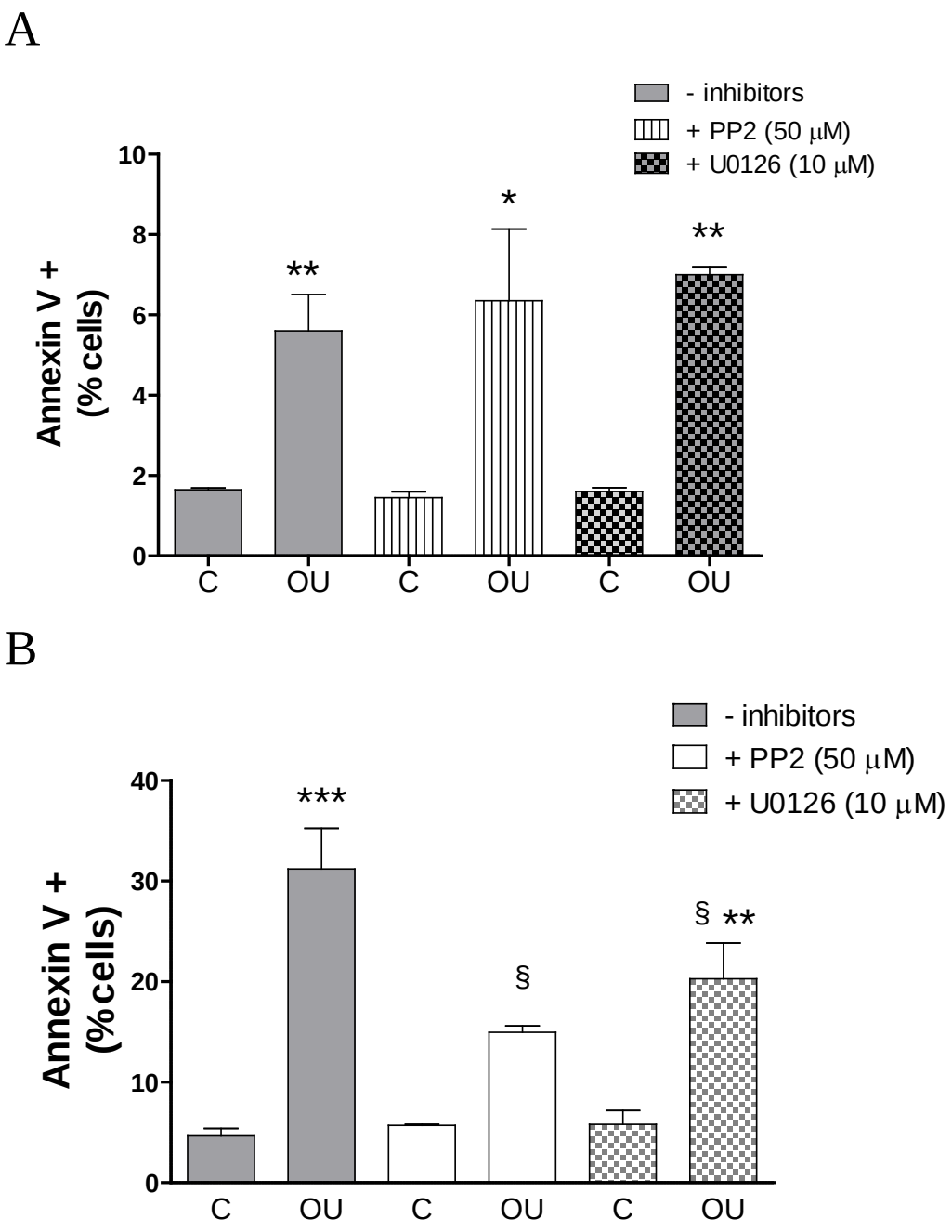

Figure 23. *Effect of Src and MEK inhibition on the cytotoxic action of ouabain in A549 (A) and Jurkat (B) cells.* Cells were pretreated with PP2 (50 μM) or U0126 (10 μM) for 30 minutes before ouabain (100 nM) addition and incubated for further 24 hours (inhibitors were present in the medium during all the treatment). Then flow cytometric analysis of Annexin V binding was performed as described in Methods. Data are expressed as mean ± SE of two indipendent experiment performed in duplicate. ***P<0.0001, **P<0.001,*P<0.05 (*vs* control); § P<0.05 (*vs* ouabain alone). One Way ANOVA post test Bonferroni

4.2.2 PI3K-Akt pathway

Akt, a serine threonine kinase, promotes cell survival and inhibits cell death by phosphorylating several downstream targets, which include effectors such as Forkhead transcription factors (FKHR) and mTOR (Benbrook and Masamha, 2011). It has been demonstrated that oleandrin decreases the amount of the active form of Akt (phospho-Akt) in several cancer cell lines U-937 (histiocytic lymphoma), HL-60 (human promyelocytic lymphoma) Hela (human cervix) and MCF-7 (human breast) (Raghavendra *et al*., 2006).

In agreement with these results, ouabain (100 nM) caused a decrease of phospho-Akt levels clearly visible after 4 h both in A549 and Jurkat cells (figure 24 and 25). Levels of total Akt were not modified by ouabain treatment indicating that ouabain reduced Akt activation without affecting total protein levels.

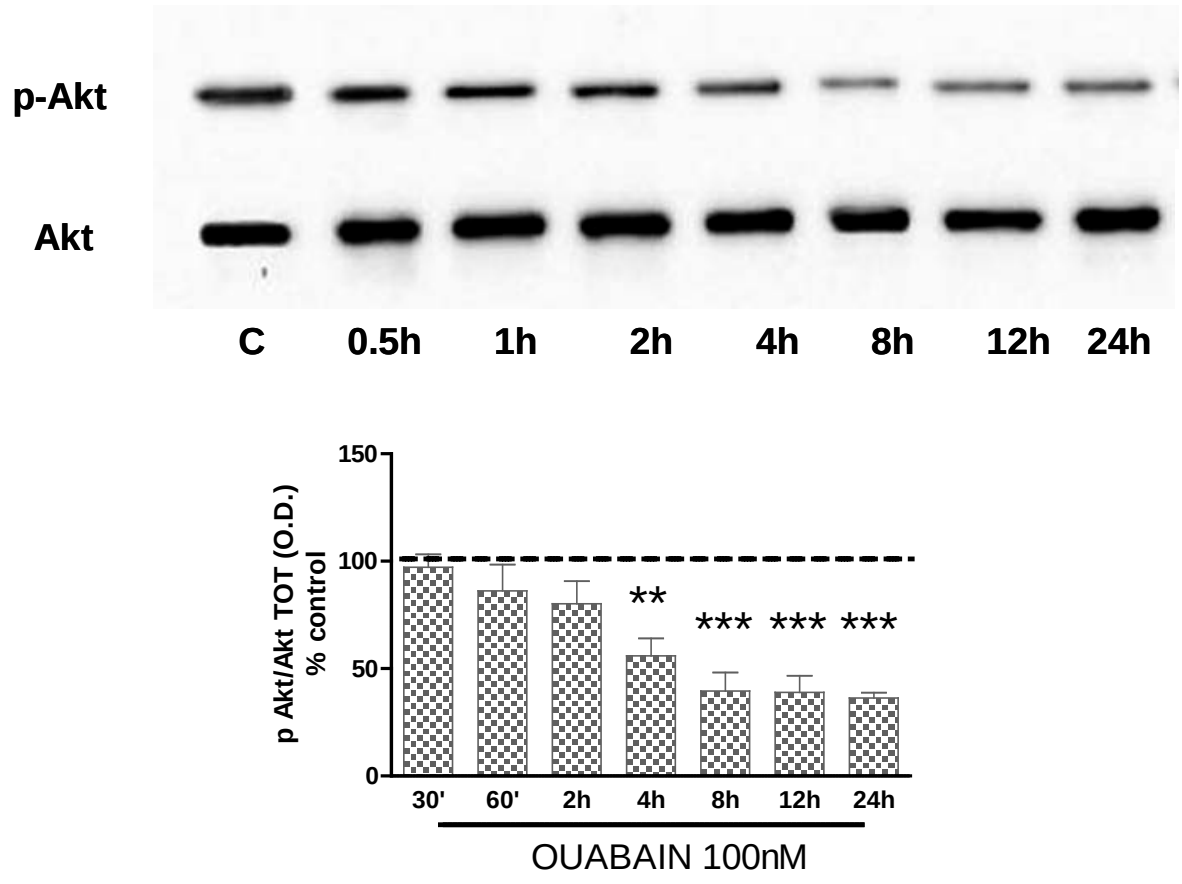

Figure 24. *Effect of ouabain on Akt phosphorylation in A549 cells.* Cells were treated with 100 nM ouabain for the indicated time. At the end of the treatment cells were lysed and subjected to Western blotting analysis as described in Methods. Data are the mean ± SE of three independent experiments, **P<0.01, ***P<0.001 One Way ANOVA post test Dunnet

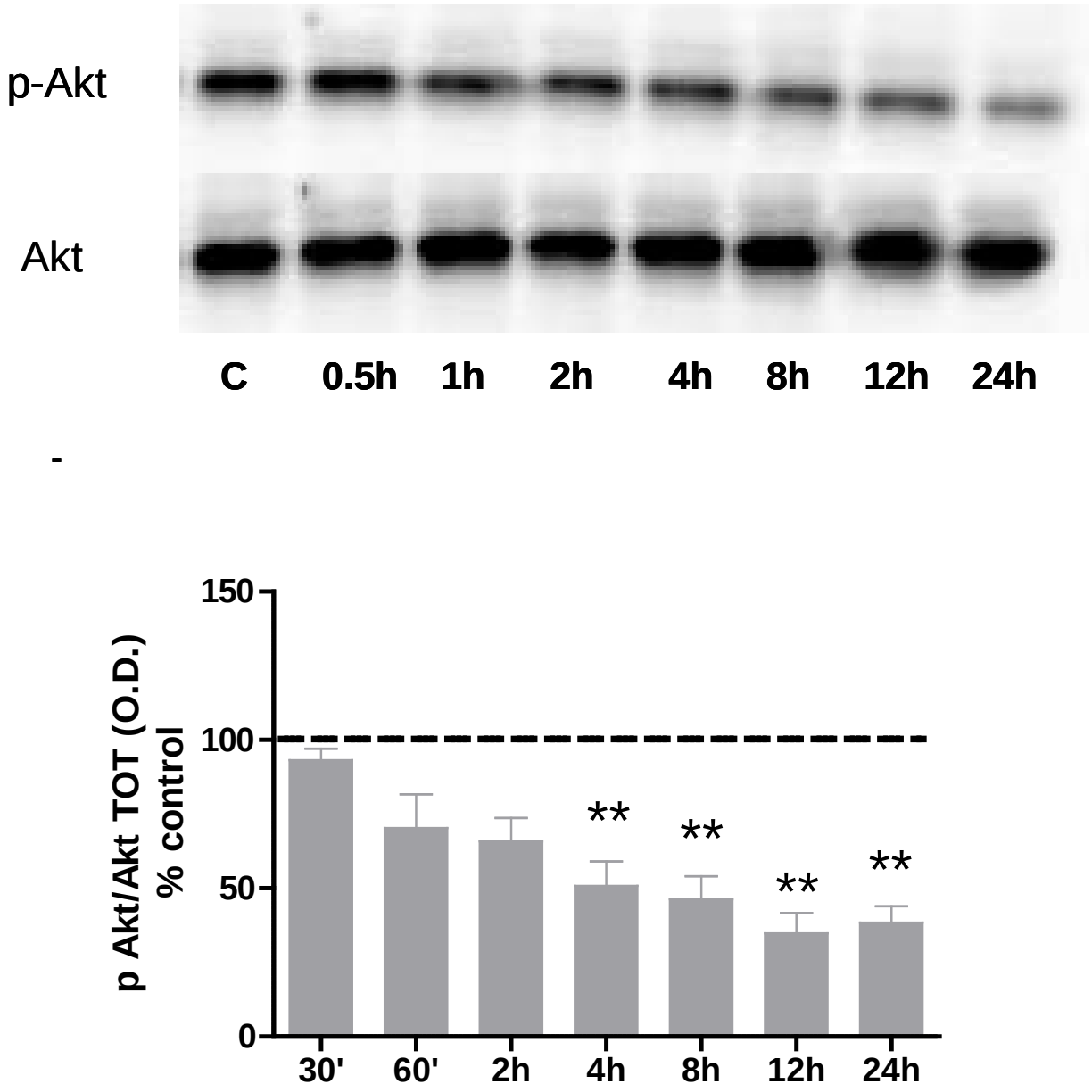

Figure 25. *Effect of ouabain on Akt phosphorylation in Jurkat cells.* Cells were treated with 100 nM ouabain for the indicated time. At the end of the treatment cells were lysed and subjected to Western blotting analysis as described in Methods. Data are the mean ± SE of three independent experiments, **P<0.01. One Way ANOVA post test Dunnet

4.2.3 ROS pathway

ROS production by mitochondria is an essential second messenger for many, but not all, of the downstream events that are linked to Na/K ATPase (Liu and Xie, 2010), thus the effect of ouabain on intracellular ROS was determined by flow cytometry in the two cell lines. As shown in Figure 26, 100 nM ouabain induced an increase in ROS levels only in A549 cells. Intracellular ROS levels were very high (+ 700 %) after 15 h of treatment.

To verify the involvement of ROS in the mechanism of cell death induced by ouabain in A549 cells, it was tested the effect of the antioxidant N-acetylcystein (NAC) on ouabain induced ROS production and cell death. NAC is a ROS scavenger acting as cystein prodrug and GSH precursor both *in vivo* and *in vitro* (Weinander *et al*., 1994). As expected, the presence of NAC in the incubation medium prevented the increase of intracellular ROS (figure 27 A). However, the treatment of cells with NAC did not block ouabain-induced cell death (figure 27 B).

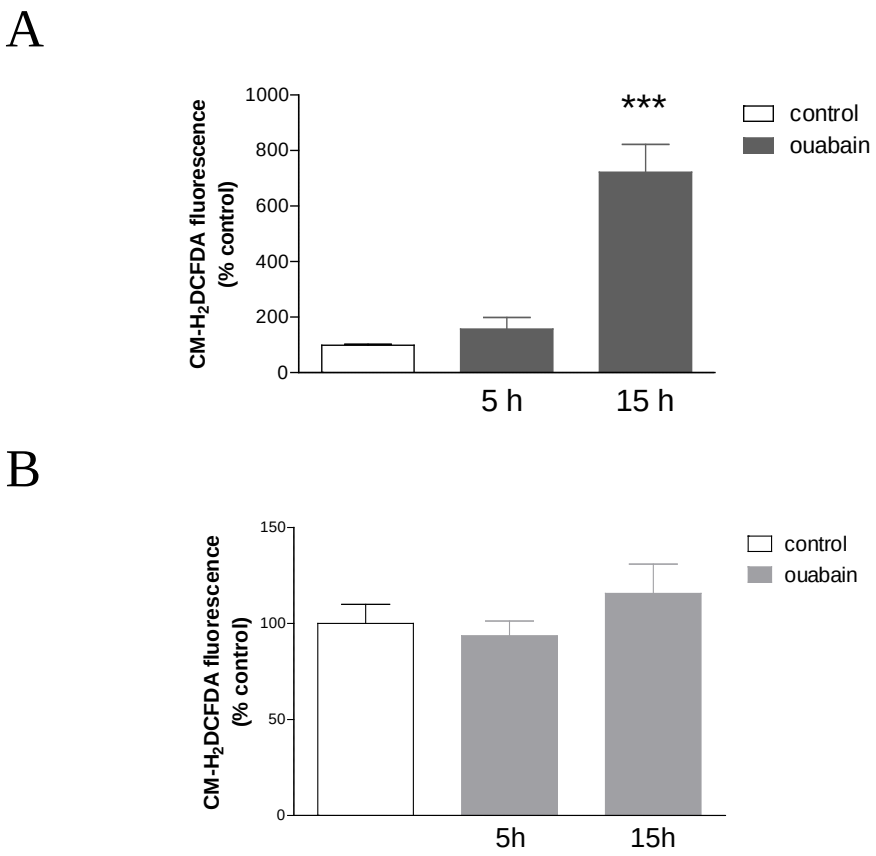

Figure 26. *Effect of ouabain on intracellular ROS in A549 (A) and Jurkat (B) cells.* Cells were treated with 100 nM ouabain for the indicated time, at the end of the treatment intracellular ROS production was determined by flow cytometric analysis of CM-H_2DCFDA fluorescence as described in Methods. Data are the mean ± SE of three independent experiments perfermed in duplicate, ***P<0.001 (*vs* control) One Way ANOVA post test Dunnet

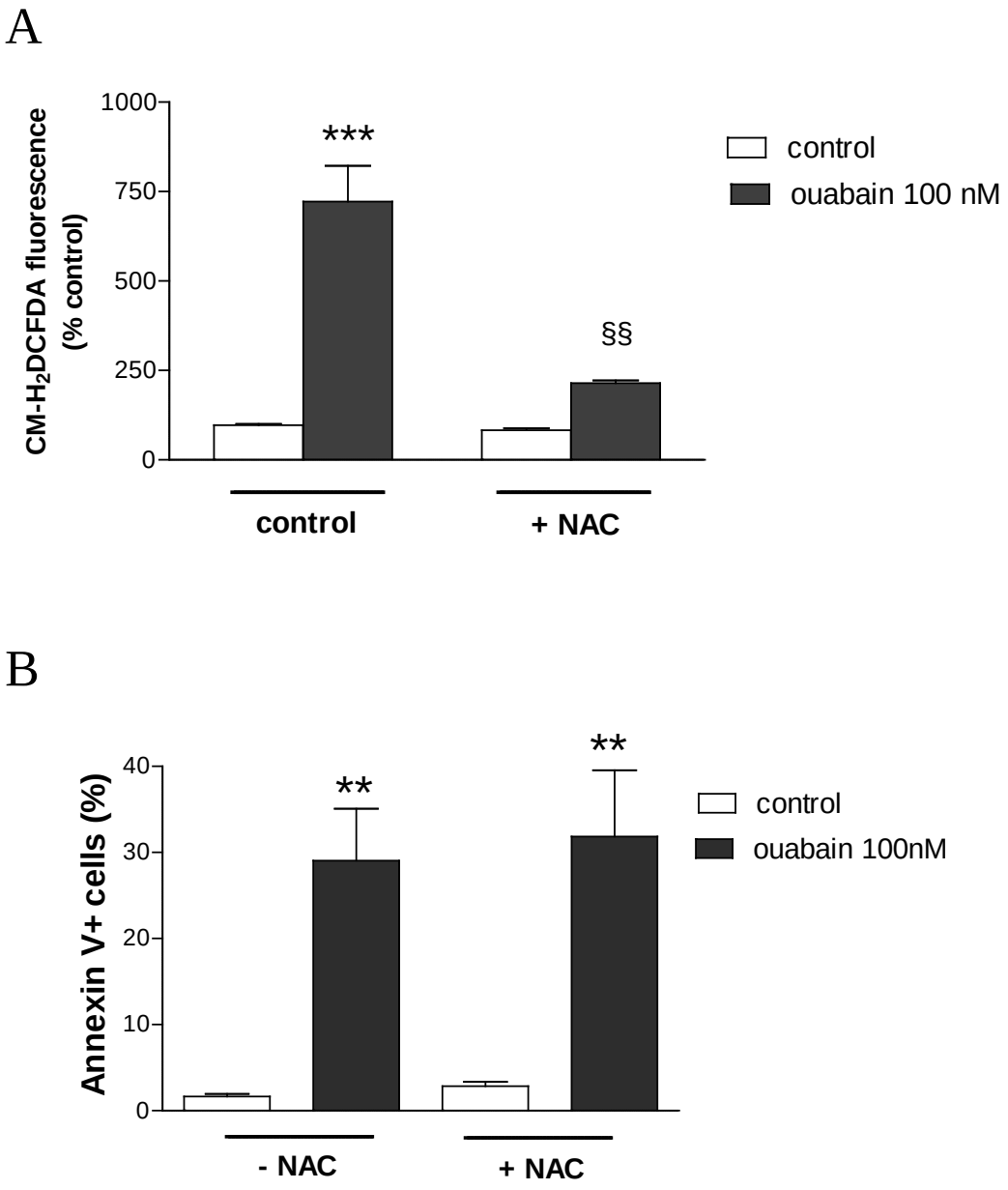

Figure 27. *Effect of NAC (10 mM) on ouabain induced ROS production and cell death in A549 cells. (A)* Cells were pretreated with NAC for 30 minutes and then 100 nM ouabain was added for 15 h (NAC was present during all the treatment), then intracellular ROS production was determined by flow cytometry as described in Methods; data are the mean ± SE of three independent experiments perfermed in duplicate, ***P<0.001 (vs control), §§ P<0.01 (vs ouabain). (*B)* Cells were pretreated with NAC for 30 minutes and then 100 nM ouabain was added for 24 h (NAC was present during all the treatment), then flow cytometric analysis of Annexin V binding was performed as described in Methods; data are expressed as mean ± SE of three indipendent experiment performed in duplicate, **P<0.01 (vs control) One Way ANOVA post test Dunnet

4.3 Biochemical analysis of ouabain induced cell death

In order to characterize the type of cell death induced by ouabain, some biochemical and morphological features were investigated.

4.3.1 Bcl-2 levels

Antiapoptotic members of the Bcl-2 family (e.g., Bcl-2, Bcl-xL, Bcl-w, Mcl-1, and A1) contain four BH domains which are absolutely required for their survival functions. The BH1–BH3 domains form a hydrophobic groove and the N-terminal BH4 domain stabilizes this structure. These domains do not have any enzymatic activity but mediate the interaction of Bcl-2 with other protein partners acting as membrane bound scavengers for BH3-containing death factors and other proapoptotic molecules (Borner, 2003).

It has been shown that Bcl-2 is cleaved in cells undergoing programmed cell death (Borner, 2003). In agreement with these results it was found that incubation with ouabain (100 nM) caused a decrease of Bcl-2 expression in both cell lines. In A549 cells this decrease occurred since 2 h of treatment while in Jurkat cells Bcl-2 reduction was evident after 4 h of treatment.

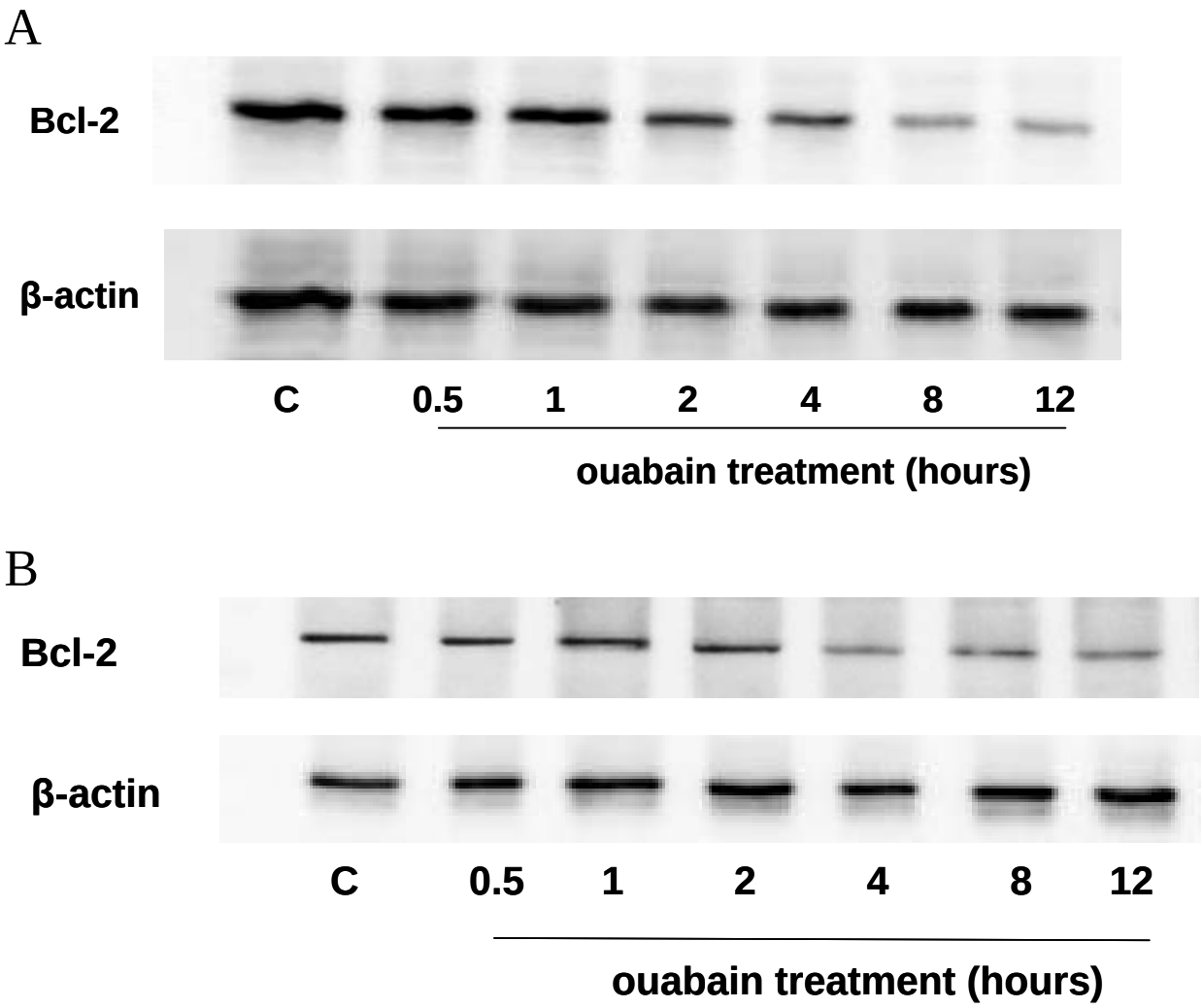

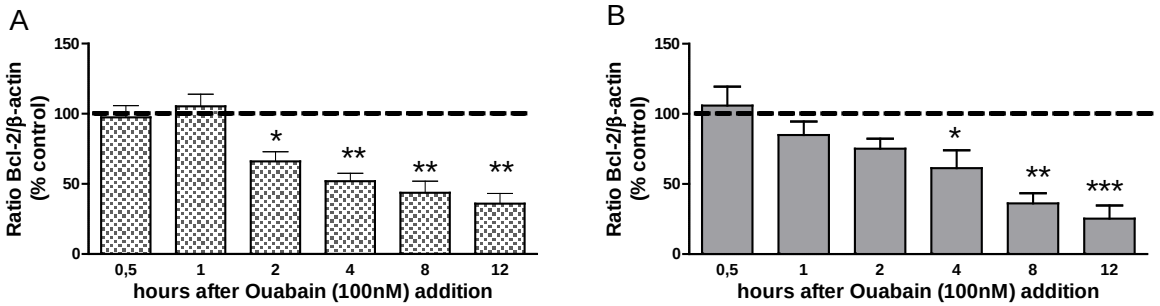

Figure 28. *Effect of ouabain on Bcl-2 expression in A549(A) and Jurkat (B) cells.* Cells were treated with 100 nM ouabain for the indicated time. At the end of the treatment cells were lysed and subjected to Western blotting analysis as described in Methods. Data are the mean ± SE of three independent experiments, *P<0.05, **P<0.01, ***P<0.001 (vs control). One Way ANOVA, post test Dunnet

4.3.2 Mitochondrial membrane potential

The Bcl-2 family of proteins are involved in regulating cell survival. In fact their scavenger action against proapoptotic molecules prevent the opening of pores on the OMM (outer mitochondrial membrane) that caused a mitochondrial membrane depolarization and a release of apoptogenic proteins (Bernardi P *et al*., 2001).

Mitochondrial membrane potential was assessed using TMRM, a cationic lipophilic dye that enters the negatively charged mitochondria where it accumulates depending on the inner-membrane potential. When the mitochondrial $\Delta\Psi m$ collapses in apoptotic cells, TMRM dyes no longer accumulate inside the mitochondria and become more evenly distributed throughout the cytosol. When dispersed in this manner, overall cellular fluorescence levels drop dramatically.

Ouabain (100 nM) induced mitochondrial membrane depolarization clearly visible after 3 h of treatment in A549 cells. Mitochondrial membrane depolarization kinetic induced by ouabain in Jurkat was slightly different, with a small increase after 3 h of treatment and a subsequent decrease that was maximal after 9 h. A transient mitochondrial hyperpolarization before reduction of MMP was observed in Jurkat. A form of mitochondrial hyperpolarization that shortly preceded the late events of swelling and rupture of the outer membrane has been attributed to the energy of the proton gradient not being dissipated by ATP synthesis, producing a hyperpolarized state (Marzo *et al*., 1998). A more recent study of p53-induced apoptosis demonstrated that the generation of reactive oxygen species led to a transient increase in MMP after induction of p53 expression, just preceding mitochondrial depolarization (Li *et al.*, 1999). However, the precise mechanism(s) involved in mitochondrial hyperpolarization is still unclear.

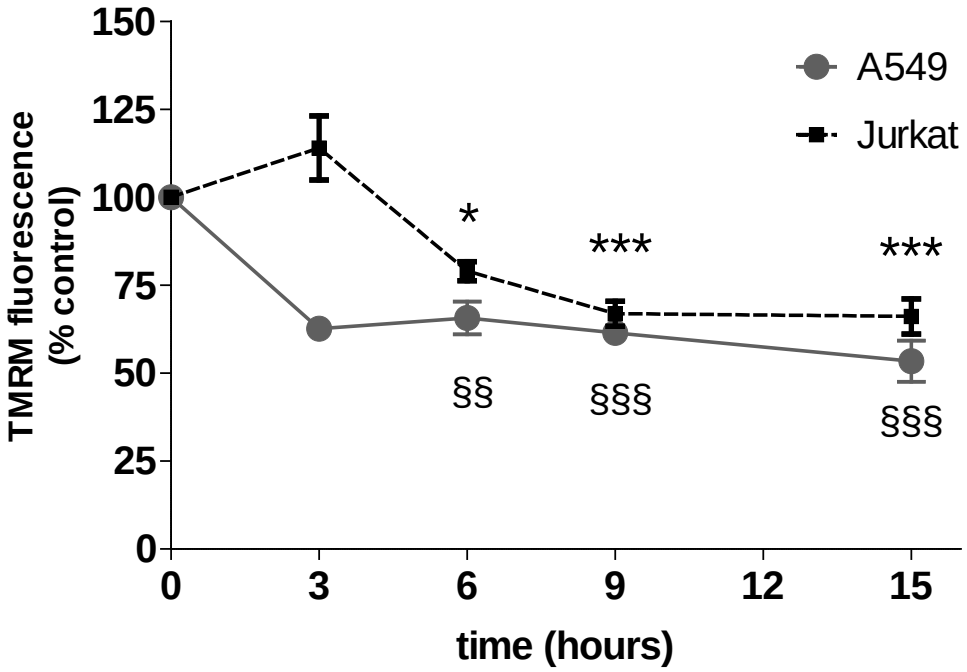

Figure 29. *Effect of ouabain on mitochondrial membrane potential*. Cells were treated with 100 nM ouabain for the indicated time. At the end of the treatment flow cytometric analysis of TMRM fluorescence was performed as described in Methods. Data are the mean ± SE of three independent experiments performed in duplicate, *P<0.05, ***P<0.001 (vs control Jurkat); §§P<0.001, §§§P<0.0001 (vs control A549). One Way ANOVA post test Dunnet

4.3.3 Caspase 3/7 activation

Caspases are a family of cysteine proteases that cleave their target proteins next to aspartate amino acids and are the central component of the apoptotic pathway. Caspase 3/7 activity was assessed in both cell lines after ouabain treatment

In Jurkat cells ouabain (50-100 nM) caused a significant activation of caspase 3/7 that was maximal after 18 h of incubation (figure 30).

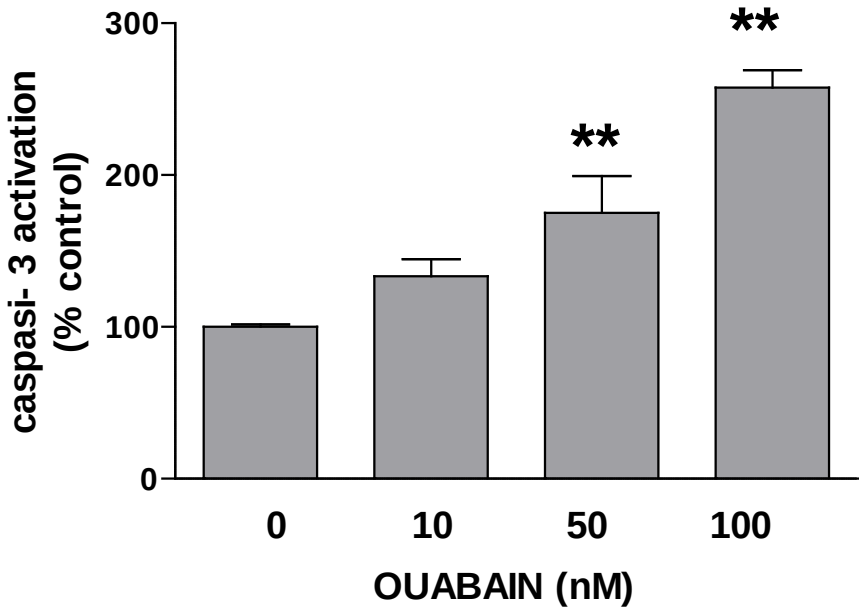

Figure 30. *Effect of ouabain on caspase 3/7 activity in Jurkat cells*. Cells were treated with the indicated concentration of ouabain for 18 hours. At the end of the treatment caspase 3/7 activity was measured as described in Methods. Data are the mean ± SE of three independent experiments performed in duplicate, **P<0.001 (vs control) One Way ANOVA post test Dunnet

On the contrary, no caspase 3/7 activation was found in A549 cells treated with ouabain for respectively 6, 12 and 24 hours (figure 31). Cells were able to respond to staurosporine, a classical stimulus that induces an increase in caspase 3/7 activity.

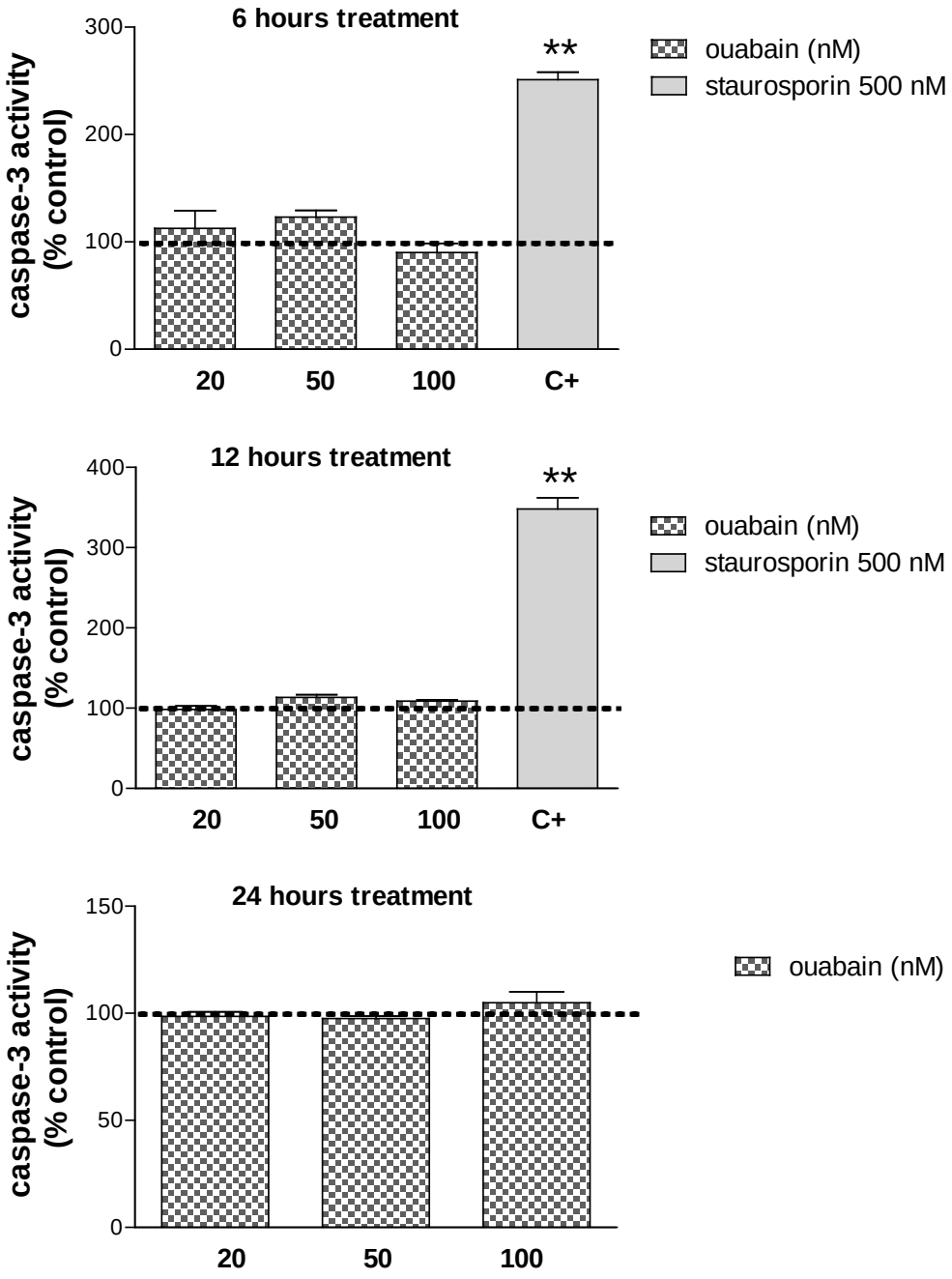

Figure 31. *Effect of ouabain on caspase 3/7 activity in A549 cells*. Cells were treated with the indicated concentration of ouabain for the indicated time. At the end of the treatment caspase 3/7 activity was assessed as described in Methods. Data are the mean ± SE of three independent experiments performed in duplicate. **P<0.001 (vs control) One Way ANOVA post test Dunnet

As expected, treatment of Jurkat cells with the pan caspase inhibitor Z-VAD-fmk, (Slee *et al*., 1996) abolished the cytotoxic effect of ouabain as evidenced by the decrease of Annexin V+ cells (figure 32). In A549 cells, the same treatment caused a decrease in Annexin V+/PI- cells (figure 33 A) with no effect on Annexin V+/PI+ cells (figure 33 B), indicating that Z-VAD-fmk did not block the increase in membrane permeability caused by the death process. This was confirmed by the analysis of morphological cell features acquired during flow cytometry (figure 34) and by microscopic evaluation (figure 35).

The inability of Z-VAD-fmk to block ouabain induced cell death in A549 was further confirmed using a cell viability test based on the measure of intracellular ATP. As shown in figure 36 there was no difference in ATP levels between cells treated with ouabain plus Z-VAD-fmk or ouabain alone (figure 36). Overall, these data indicate that decrease of Annexin V+/PI- in A549 cells treated with ouabain plus Z-VAD-fmk is not related to an inhibition of cell death and, in this case, could be considered as an artefact.

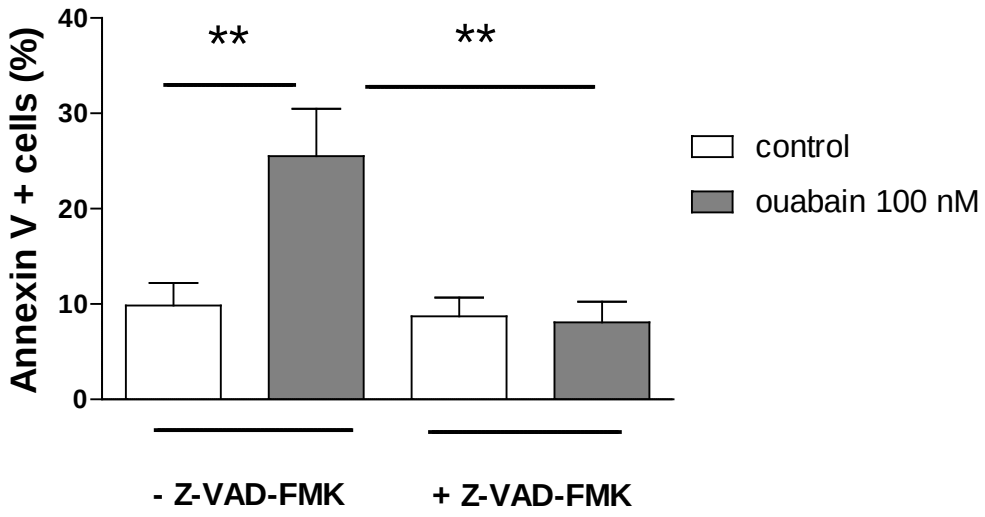

Figure 32. *Effect of Z-VAD-fmk on cytotoxic effect of ouabain in Jurkat cells*. Cells were pre treated with Z-VAD-fmk (100 μM) for 60 minutes and then ouabain 100 nM was added for 24 hours (the inhibitor was present during all the treatment). Then flow cytometric analysis of Annexin V/PI binding was performed as described in Methods. Data are the mean ± SE of three independent experiments performed in duplicate, **P<0.001. (vs control) One Way ANOVA post test Dunnet

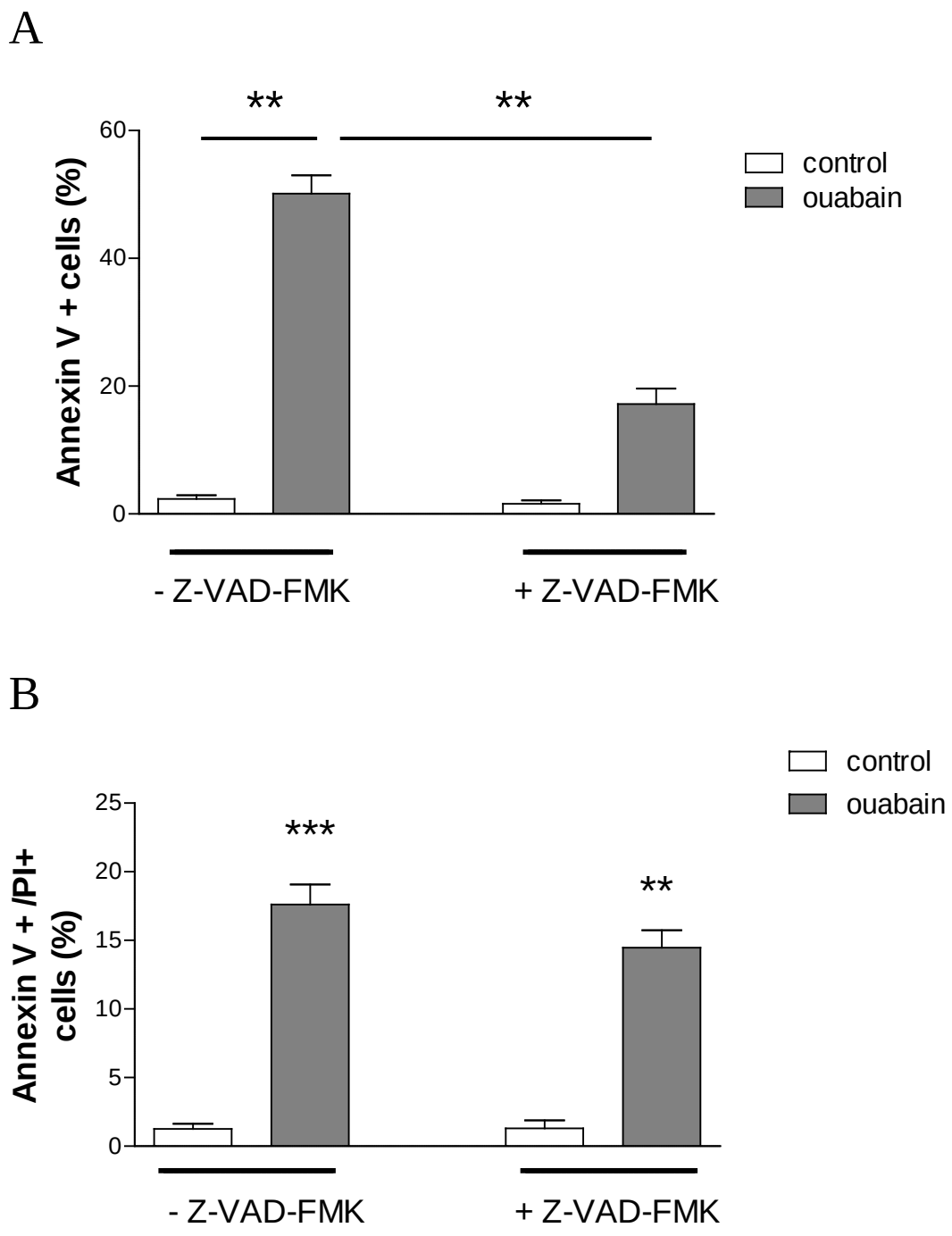

Figure 33. *Effect of Z-VAD-fmk on Annexin/PI binding in A549 cells treated with ouabain. (A.)* AnnexinV+/PI- cells. *(B)* Annexin V+/PI+ cells. Cells were pretreated with Z-VAD-fmk (100 μM) for 60 minutes and then ouabain 100 nM was added for 24 hours (the inhibitor was present during all the treatment). Then flow cytometric analysis of Annexin V/PI binding was preformed as described in Methods. Data are the mean ± SE of three independent experiments performed in duplicate, **P<0.001, ***P<0.0001 (vs control) One Way ANOVA post test Dunnet

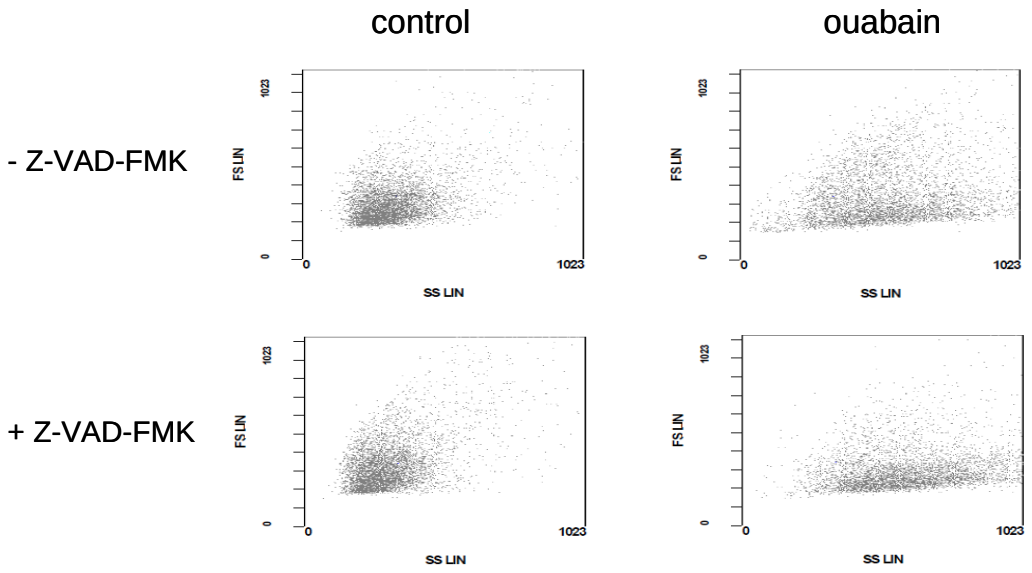

Figure 34. *Morphology of A549 cells treated with ouabain with or without Z-VAD-fmk.* Cells were pretreated with Z-VAD-fmk (100 μM) for 60 minutes and then ouabain 100 nM was added for 24 hours (the inhibitor was present during all the treatment). At the end of the treatment flow cytometric analysis of morphology was preformed as described in Methods. FS: forward scatter; SS: side scatter. A representative experiment is shown.

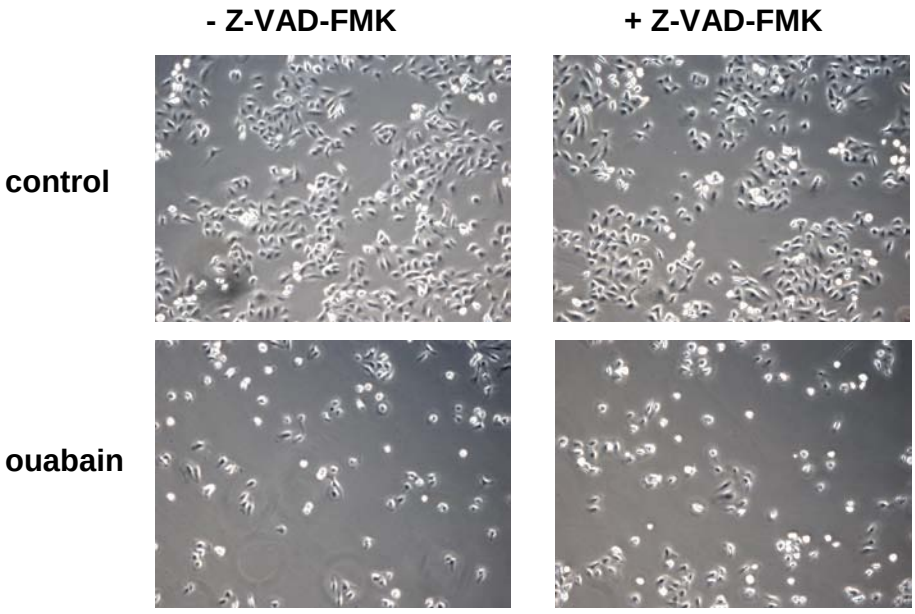

Figure 35. *Microscopical examination of A549 cells treated with ouabain with or without Z-VAD-fmk.* Cells were pre treated with Z-VAD-fmk (100 μM) for 60 minutes and then ouabain 100 nM was added for 24 hours (the inhibitor was present during all the treatment).. At the end of the treatment images were collected using a Nikon inverted microscope (20X plane) provided with a digital camera. A representative experiment is shown.

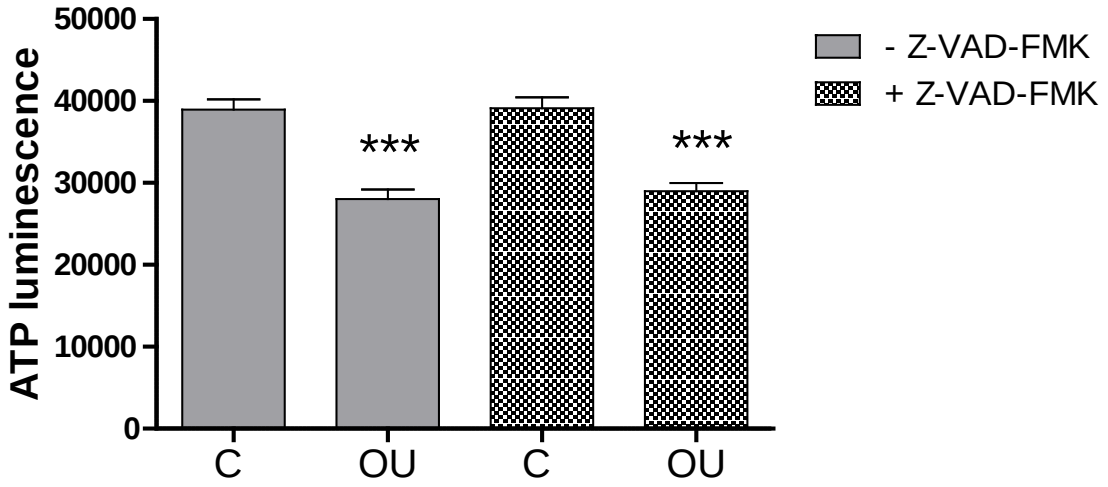

Figure 36. *Intracellular ATP content in A549 cells treated with ouabain with or without Z-VAD-fmk.* Cells were pretreated with Z-VAD-fmk (100 μM) for 30 minutes and then ouabain 100 nM was added for 24 hours (the inhibitor was present during all the experiment). At the end of the treatment intracellular ATP analysis was performed as described in Methods. Data are the mean ± SE of three independent experiments performed in triplicate, ***P<0.0001 (vs control) One Way ANOVA post test Dunnet

4.3.4 Pattern of DNA fragmentation

One hallmark of caspase-mediated apoptosis that may also propel cell differentiation is chromatin alteration and DNA damage/fragmentation. A select handful of nucleases have been implicated in apoptotic DNA fragmentation, and caspase-activated DNase (CAD) is the most characterized. CAD is held in check through association with its inhibitor, inhibitor of caspase-activated DNase (ICAD), which is cleaved by caspase 3 to release CAD. After activation, unobstructed CAD configures into a scissor-like dimer, cleaving DNA with minimal sequence specificity and creating fragments of 200 bp or multiples (Larsen *et al*., 2010). This fragments, after loading in a agarose gel, give a characteristic pattern typical of apoptosis death.

Analysis of DNA fragmentation pattern of A549 and Jurkat cells after treatment with 100 nM ouabain for 24 hours is shown in figure 37. It is observed that there is a different behaviour between the two cell lines. Jurkat cells treated with ouabain (line 4) showed the characteristic DNA ladder, typical for caspase-dependent apoptosis and similar to the fragmentation pattern obtained with Jurkat cells treated with staurosporine (positive control for caspase-dependent apoptosis, line 6). Diversely, A549 cells presented a smear of DNA that is not characteristic of caspase-dependent apoptosis and is similar to DNA obtained from Jurkat cells treated with H_2O_2 (positive control for caspase-independent cell death, line 5).

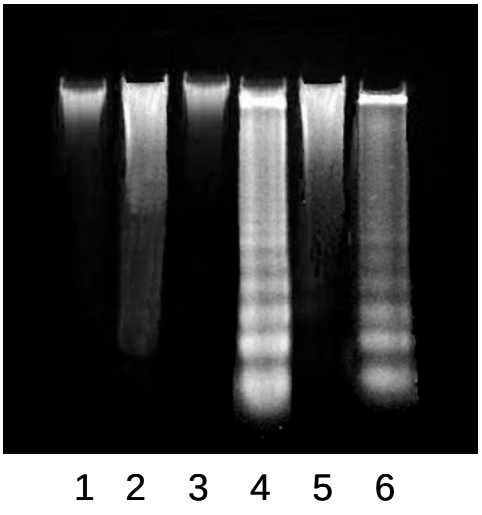

Figure 37. *DNA fragmentation pattern of A549 and Jurkat cells treated with or without ouabain 100 nM for 24 hours*. Experiment was performed as described in Methods.1) A549 control; 2) A549 ouabain 100 nM; 3) Jurkat control; 4) Jurkat ouabain 100 nM; 5)Jurkat treated with H_2O_2 200 μM 12 hours; 6) Jurkat treated with staurosporine 0.5 μM 12 hours. A representative experiment is shown

4.4 Autophagic cell death in A549 cells

Based on the above results showing that in Jurkat cells ouabain produces a decrease in antiapoptotic protein Bcl-2, an increase in mitochondrial permeabilty, caspase-dependent cell death and DNA ladder, we can affirm that ouabain induces caspase-dependent apoptosis in Jurkat cells, probably activating the mitochondrial (intrinsic) pathway.

On the other hand, ouabain-induced cell death in A549 seems to proceed via a different mechanism from classical apoptosis, although some characteristics of this type of cell death are still present (Bcl-2 decrease and increase in mitochondrial permeability). Due to the multiple interconections between apoptosis and autophagy (see Introduction), we tested the hypothesis that ouabain-induced cell death could result from autophagy (also called type II-programmed cell death).

To determine whether ouabain induces autophagy in A549 cells, we examined by immunofluorescence the intracellular distribution of the autophagy marker LC3 upon ouabain treatment. As shown in figure 37, a change in the distribution of LC3 fluorescence from a diffuse cytosolic pattern in untreated cells to a punctate pattern upon ouabain treatment was observed. Furthermore, an increased time-dependent conversion of the normal LC3-I to the autophagic LC3-II isoform was observed in cells treated with 100 nM ouabain (figure 38). Same data is obtained when cells are subjected to aminoacid starvation for 12 h (positive control for autophagy).

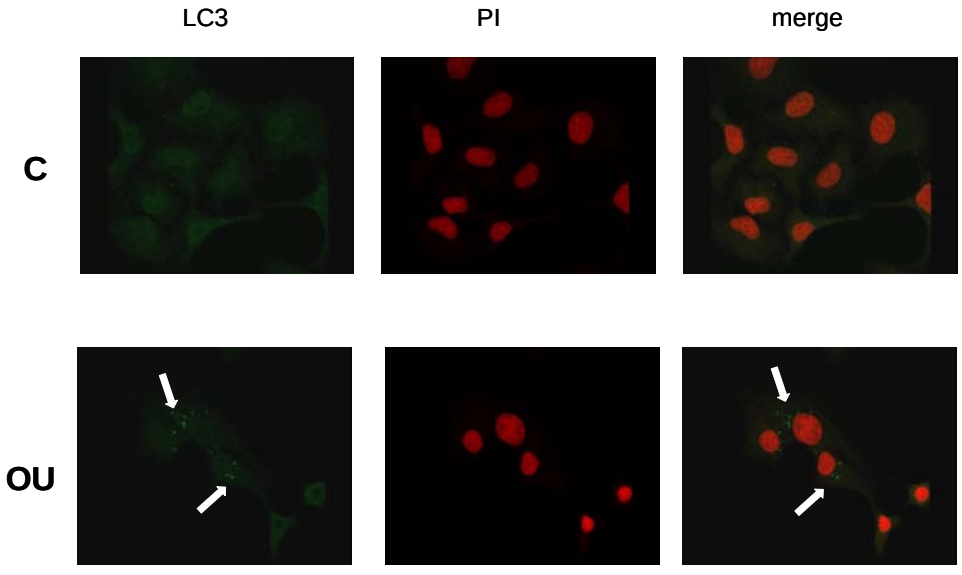

Figure 37. *Immunocytochemical analysis of LC3 localization after ouabain treatment in A549 cells.* Cells were treated with ouabain 100 nM for 12 h, then fixed with paraformaldehyde 4 % and subjected to immunocytochemistry as described in Methods. LC3 antybody was used. PI: propidium iodide, a nuclear staining. A representative experiment is shown.

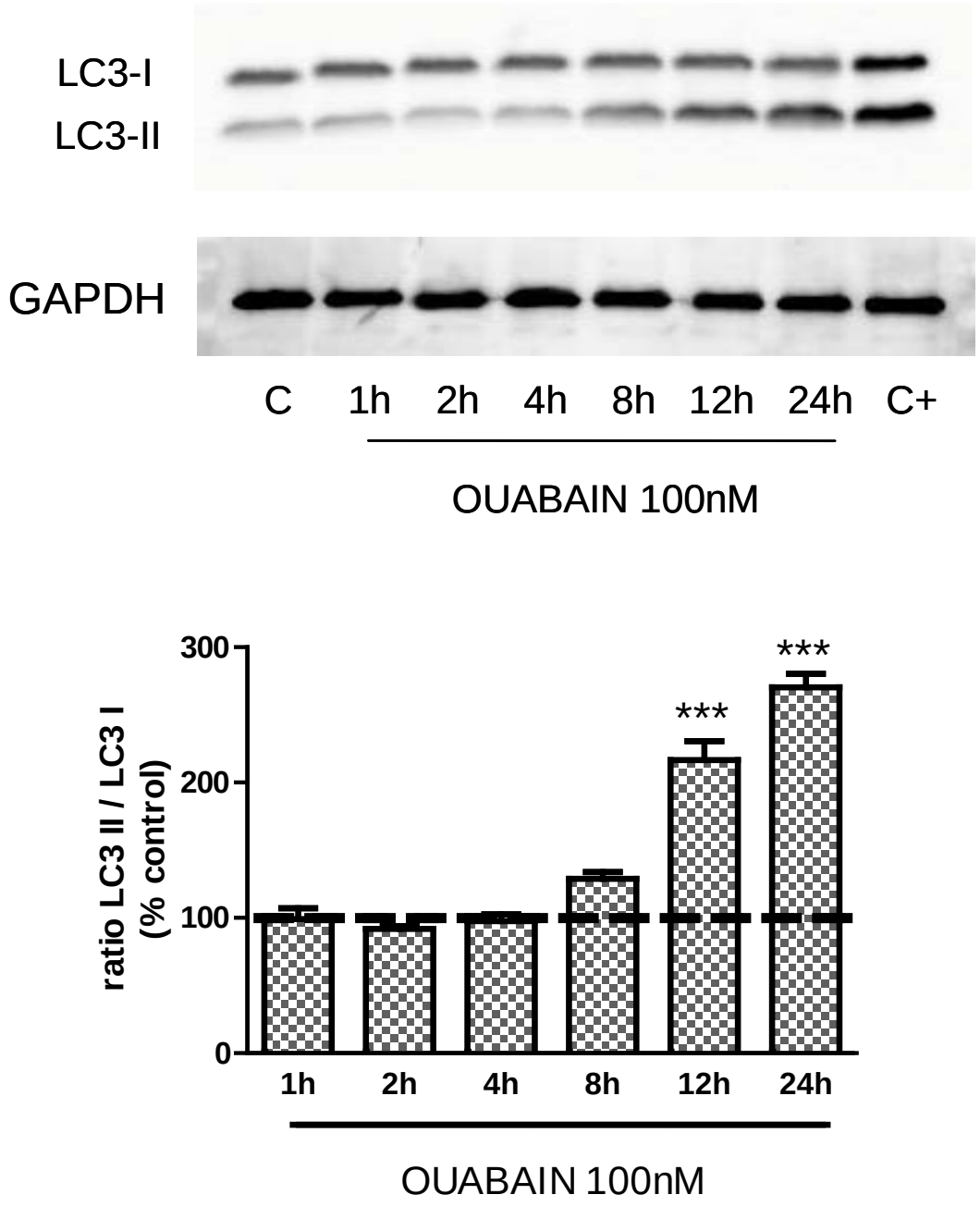

Figure 38. *Western blotting analysis of LC3 conversion in A549 cells treated with ouabain.* Cells were treated with 100 nM ouabain for the indicated time. At the end of the treatment cells were lysed and subjected to Western blotting as descrived in Methods. C+: cells were starved in a saline buffer plus glucose for 12 h. Data are the mean ± SE of three independent experiments ***P<0.0001 (vs control) One Way ANOVA post test Dunnet

We also studied the autophagic flux after ouabain treatment, which is a more accurate reflection of the autophagic activity (Klionsky *et al.*, 2008). This was achieved using chloroquine, a drug that block fusion of autophagosomes with lysosomes (Klionsky *et al.*, 2008). If the amount of LC3-II further increases in the presence of chloroquine, this would indicate enhancement of the autophagic flux during ouabain treatment. Instead, if LC3-II levels remain unchanged, the increase in LC3-II would be due to inhibition of autophagic degradation. Thus, A549 cells were treated with ouabain 100 nM for 12 hours and chloroquine (50 μM) was added two hours before the end of the treatment. Figure 39 shows that in ouabain-treated cells chloroquine induced a further increase in the accumulation of LC3-II, thus suggesting that ouabain enhanced the autophagic flux.

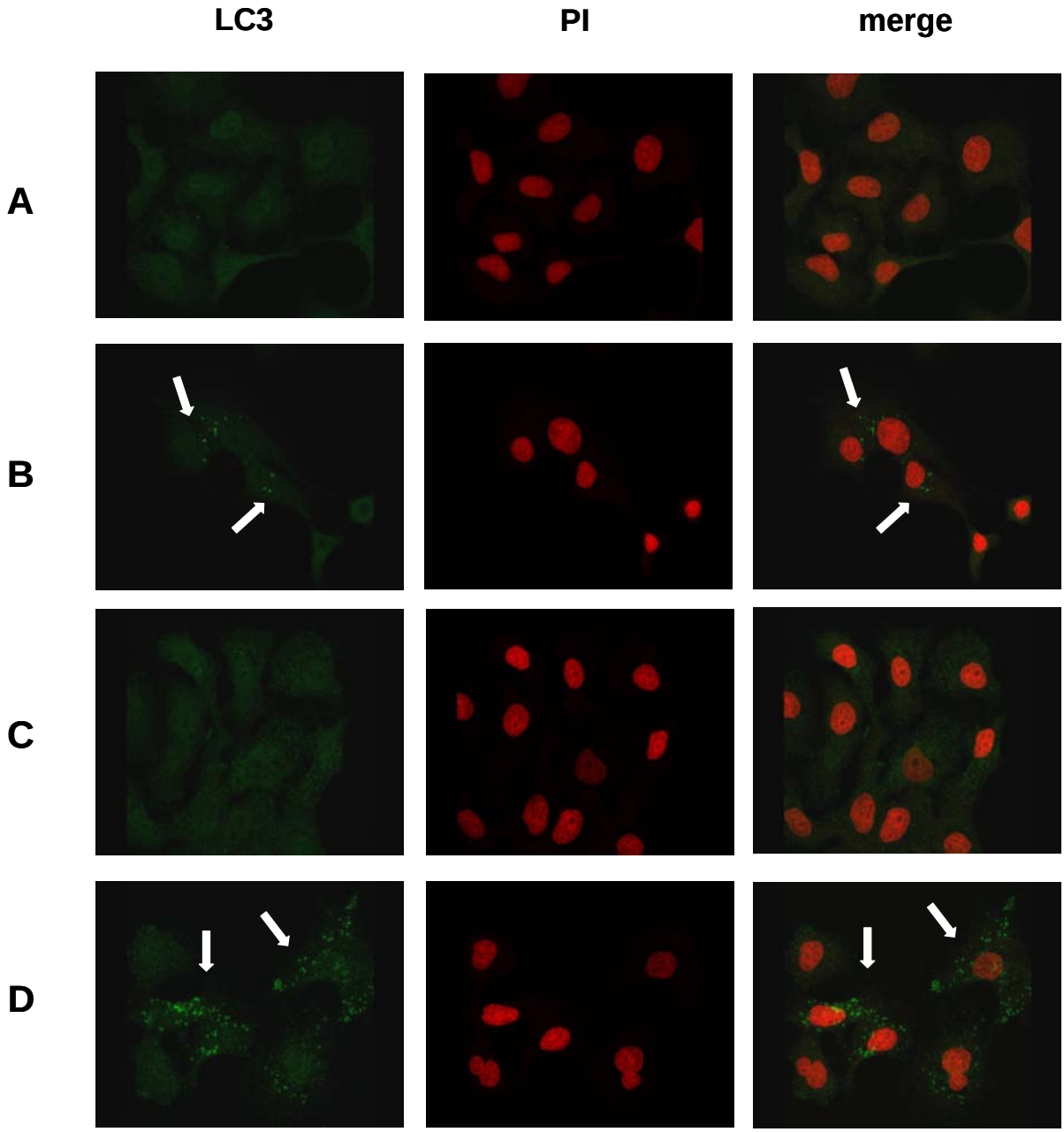

Figure 39. *Effect of chloroquine on autophagic flux in A549 cells treated with ouabain.* Cells were treated with ouabain 100 nM for 12 h. Where indicated chloroquine was added two hours before the end of the treatment. At the end of the treatment cells were fixed with paraformaldehyde 4% and then subjected to immunocytochemistry as described in Methods. LC3 antybody was used. PI: propidium iodide, a nuclear staining. A: control; B: ouabain 100 nM; C control + choloquine (50 μM); D ouabain 100nM + chloroquine. A representative experiment is shown.

Another indicator of autophagic flux is obtained monitoring the degradation of adaptor protein p62. p62 is required for the formation of ubiquitinated protein aggregates and the interaction of p62 with both ubiquitinated proteins and LC3 is thought to mediate delivery of these aggregates to the autophagic system where the complex is degradated (Klionsky DJ *et al*., 2008).

Western blotting analysis of p62 showed a decrease in p62 expression since 8 hours of incubation with ouabain 100 nM (figure 40). This data was confirmed by immunocytochemistry performed on cells after 12 hours of incubation with ouabain (figure 41A). Decrease of p62 expression induced by ouabain was enhanced if chloroquine was added 2 hours before the end of treatment (figure 41B).

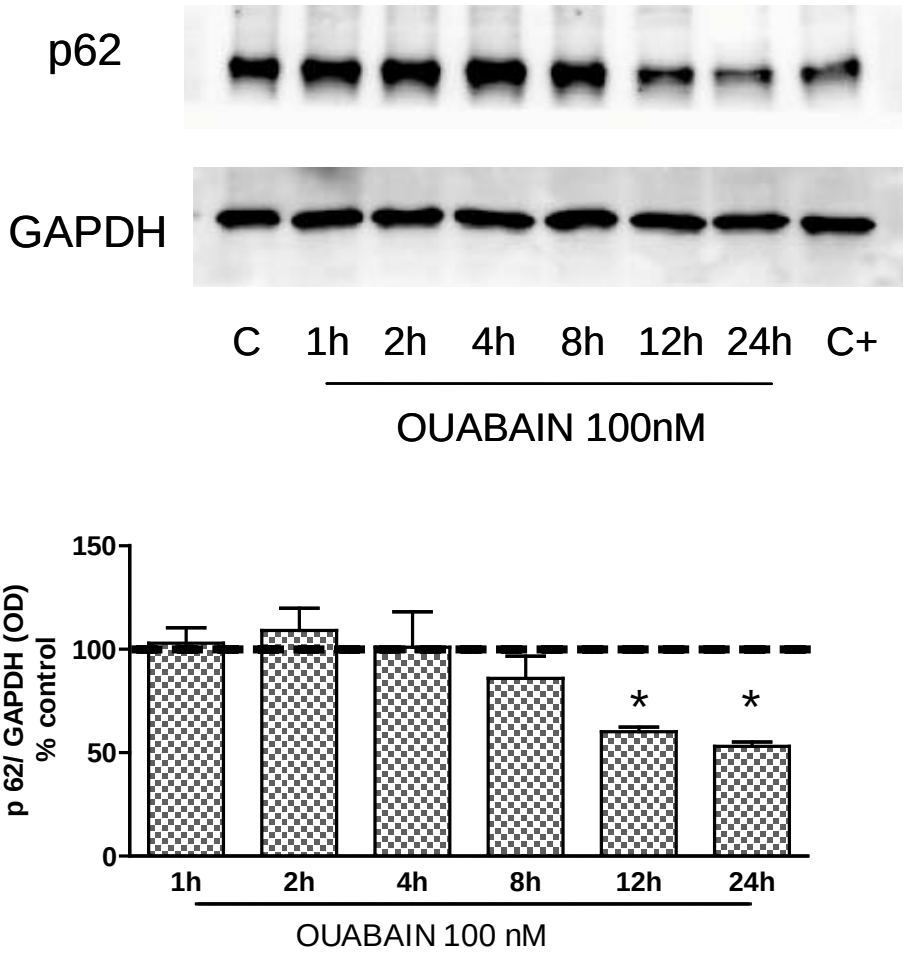

Figure 40. *Western Blotting analysis of p62 in A549 cells treated with ouabain*. Cells were treated with 100 nM ouabain for the indicated time, then cells were lysed and subjected to Western blotting as descrived in Methods. C+ cells were starved in a saline buffer plus glucose for 12 h.. Data are expressed as mean ± SE of three experiments. *P<0.05. One Way ANOVA post test Dunnet

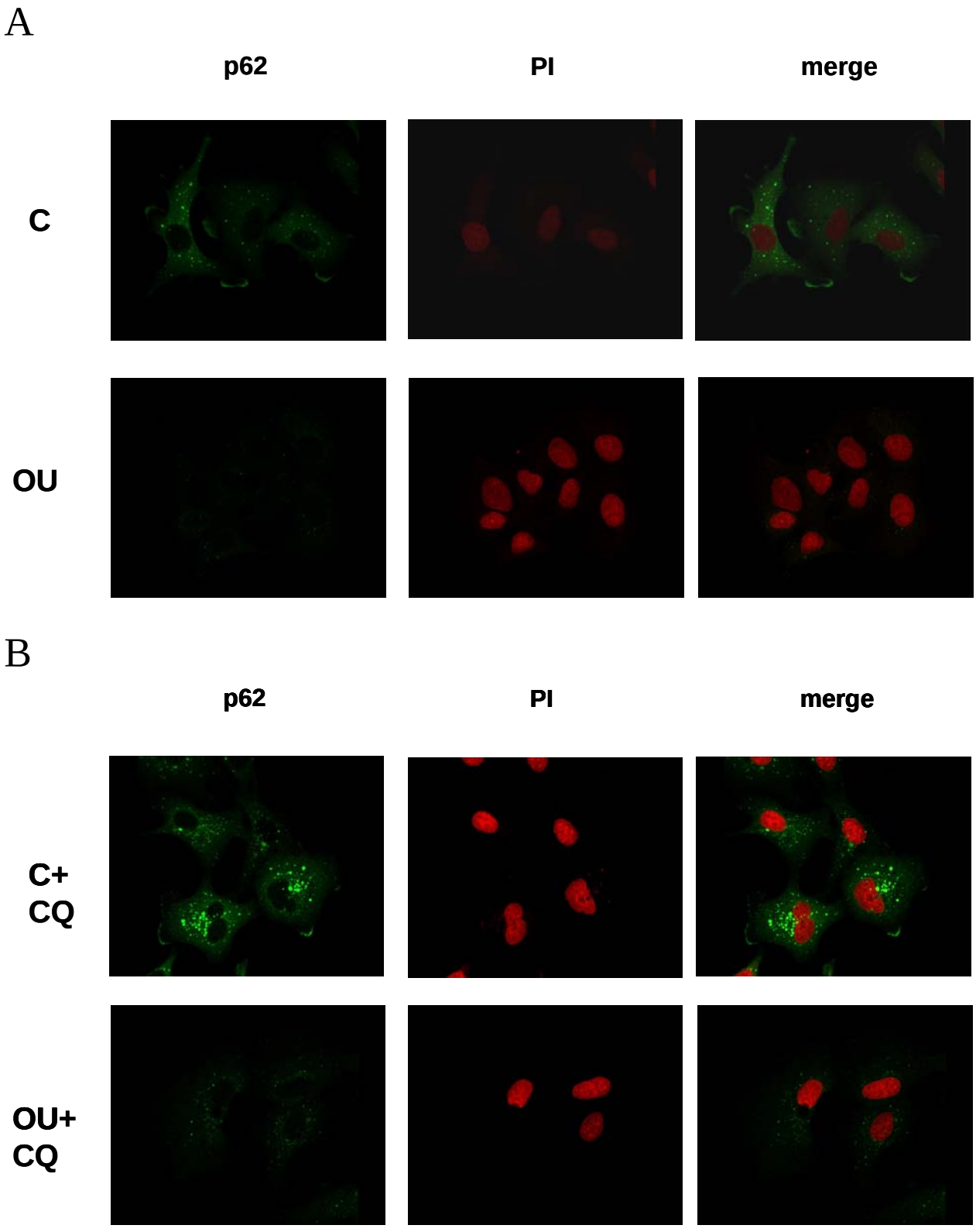

Figure 41. *Effect of ouabain on p62 degradation in A549 cells in absence (A) or presence (B) of choloquine.* Cells were treated with ouabain 100 nM for 12 hours. Where indicated 50 μM chloroquine (CQ) was added two hours before the end of the treatment. At the end of the treatment cells were fixed with paraformaldehyde 4% and then subjected to immunocytochemistry as described in Methods. LC3 antibody was used. PI: propidium iodide, a nuclear staining.. A representative experiment is shown.

It is now emerging that the positioning of lysosomes regulates the mTOR complex 1 (mTORC1) signalling pathway (Korolchuk *et al*., 2011; Pous and Codogno, 2011). In fact, lysosomes are maintained at the periphery of the cell through a microtubule-dependent mechanism involving kinesins (KIF1B-β and KIF2A) and the monomeric GTPase ARL8B. mTORC1, which is bound to the cytoplasmic surface of lysosomes, is activated by upstream signalling when is located at the cell periphery. In case of autophagy, the increase in cytoplasmic pH prevents the transfer of lysosomes to a peripheral location through the release of kinesins and ARL8B from microtubules, resulting in the accumulation of lysosomes in the perinuclear area and inactivation of mTORC1. A major consequence of mTORC1 inactivation is the stimulation of autophagosome formation and the fusion of autophagosomes with lysosomes in the perinuclear area (Pous and Codogno, 2011).

In order to follow lysosome localization during ouabain treatment, immunocytochemistry of the lysosomal protein LAMP2 was performed. Figure 42 shows that after 12 hours of ouabain treatment lysosomes are preferentially clustered in the perinuclear area. Same localization of lysosomes is observed when cells are subjected to aminoacid starvation for 12 h (positive control for autophagy).

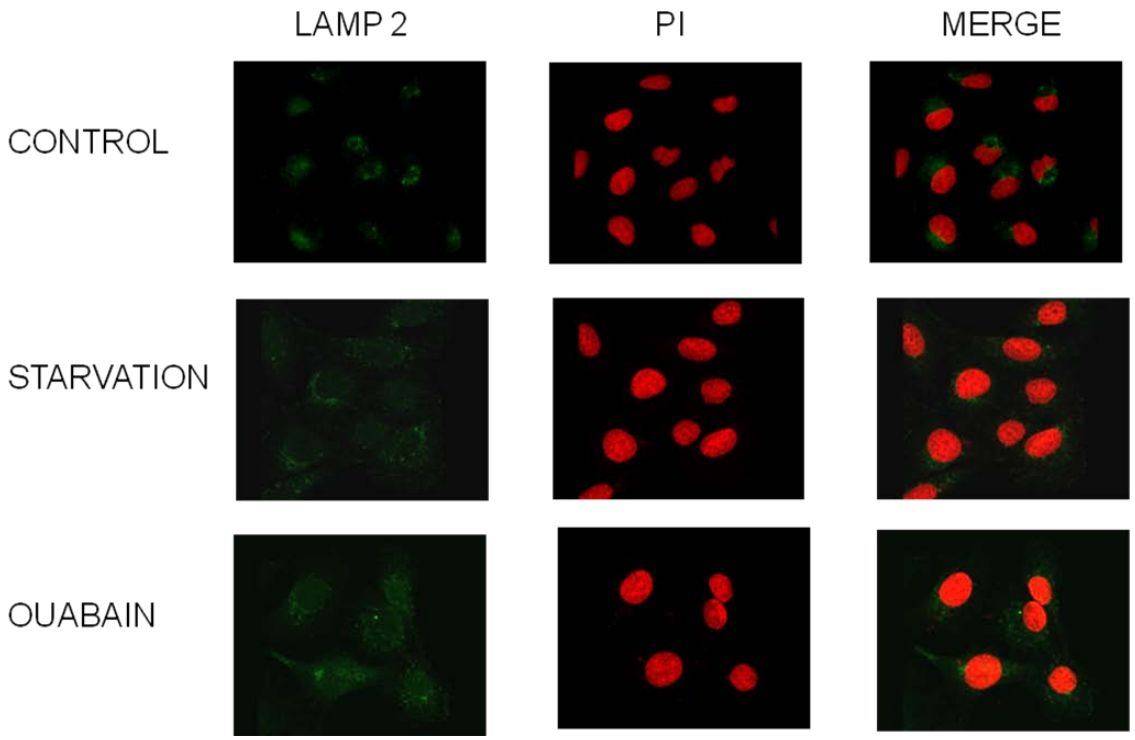

Figure 42. *Effect of ouabain on lysosome localization in A549 cells.* Cells were treated with ouabain 100 nM for 12 h or starved in a saline buffer plus glucose for 12 h. At the end of the treatment cells were fixed with paraformaldehyde 4 % and then subjected to immunocytochemistry as described in Methods. LAMP2 antybody was used. PI: propidium iodide, a nuclear staining. A representative experiment is shown.

Pharmacological inhibition of the initial stage of autophagy with 3-methyladenine (3-MA) (Seglen and Gordon, 1982) was performed to test the role of autofagy in the mechanism of cell death induced by ouabain in A549. 3-MA prevented the conversion of LC3-I to LC3-II demostrating its ability to inhibit autophagy in our experimental conditions (figure 43 A). Most importantly, 3-MA completely antagonized cell death induced by ouabain thus supporting our initial hypothesis (figure 43 B). The effect of 3-MA was confirmed by analysis of cell morphology and microscopic evaluation (fig ure 44).

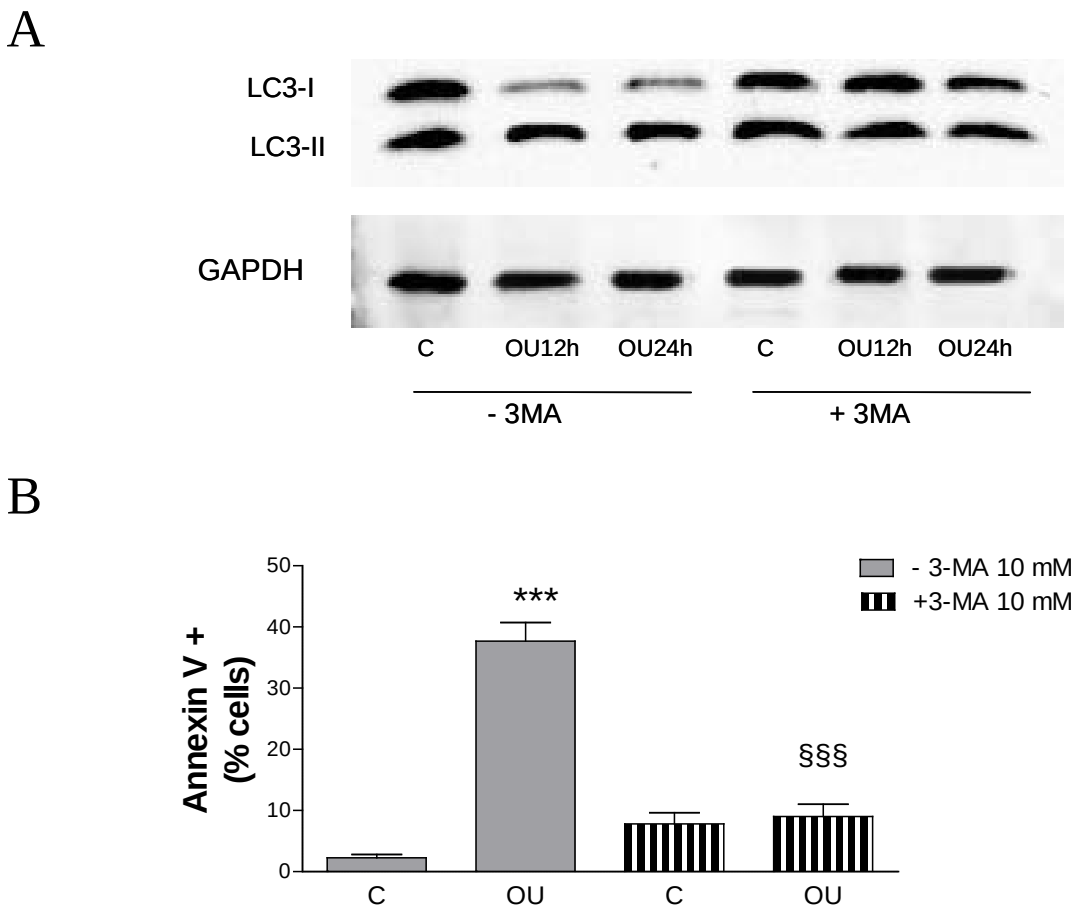

Figure 43. *Effect of 3-methyladenine (3MA) 10 mM on cytotoxic effect of ouabain in A549 cells. (A) Western blotting analysis of LC3 conversion in presence of 3MA (10 mM).* Cells were or not pretreated with 3 MA for 60 min and then 100 nM ouabain was added for the indicated time (the inhibitor was present during all the treatment). At the end of the treatment cells were lysed and subjected to Western blotting as descrived in Methods. A representative blot is shown. *(B) Flow cytometry analysis of Annexin V binding.* Cells were pretreated with 3 MA and then ouabain 100 nM was added for 24 hours (the inhibitor was present during all the treatment). At the end of the treatment flow cytometric analysis of Annexin V binding was performed as described in Methods. Data are expressed as mean ± SE of three independent experiments performed in duplicate. ***P<0,001 (vs control); §§§ P<0,001 (vs ouabain alone). One Way ANOVA post test Bonferroni

A

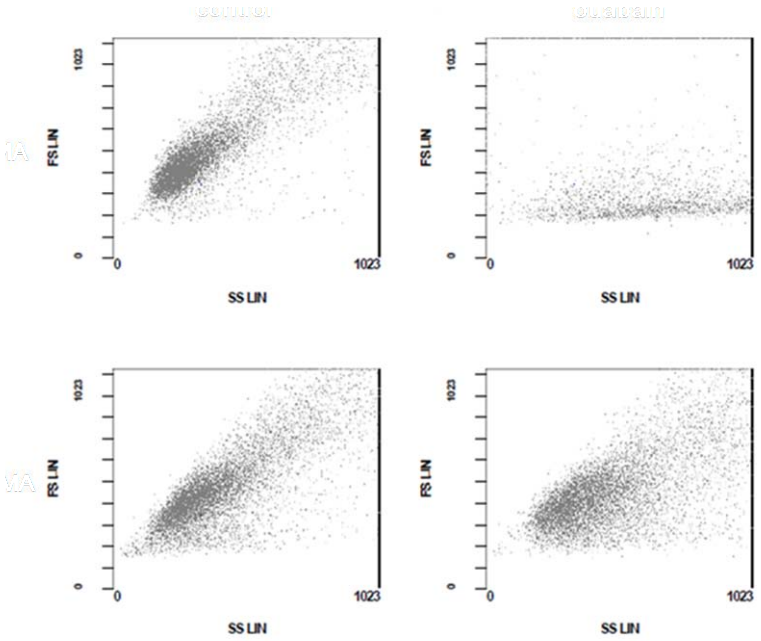

B

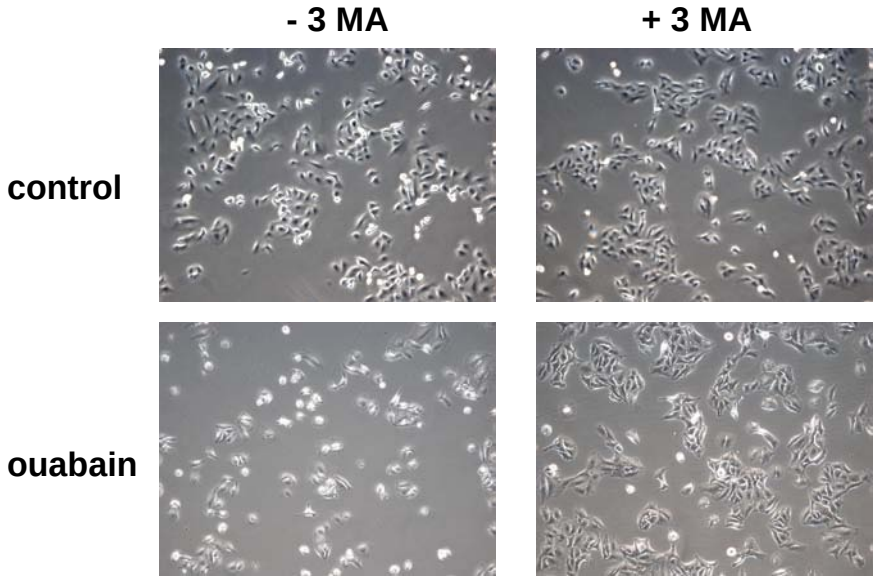

Figure 44. *(A)Morphology of A549 cells treated with ouabain with or without 3-MA.* Cells were pretreated with 3-MA (10 mM) for 60 minutes and then ouabain 100 nM was added for 24 hours (the inhibitor was present during all the treatment). At the end of the treatment flow cytometric analysis of morphology was preformed as described in Methods. FS: forward scatter; SS: side scatter. A representative experiment is shown *(B) Microscopical examination of A549 cells treated with ouabainin presence or not of 3-MA.* Cells were pre treated with 3-MA (10 mM) for 60 minutes and then ouabain 100 nM was added for 24 hours (the inhibitor was present during all the treatment). At the end of the treatment images were collected using a Nikon inverted microscope (20X plane) provided with a digital camera. A representative experiment is shown.

As expected, 3-MA was unable to block ouabain-induced apoptosis in Jurkat cells (figure 45). In addition, no LC3 conversion was detected in Jurkat cells treated with ouabain (figure 46).

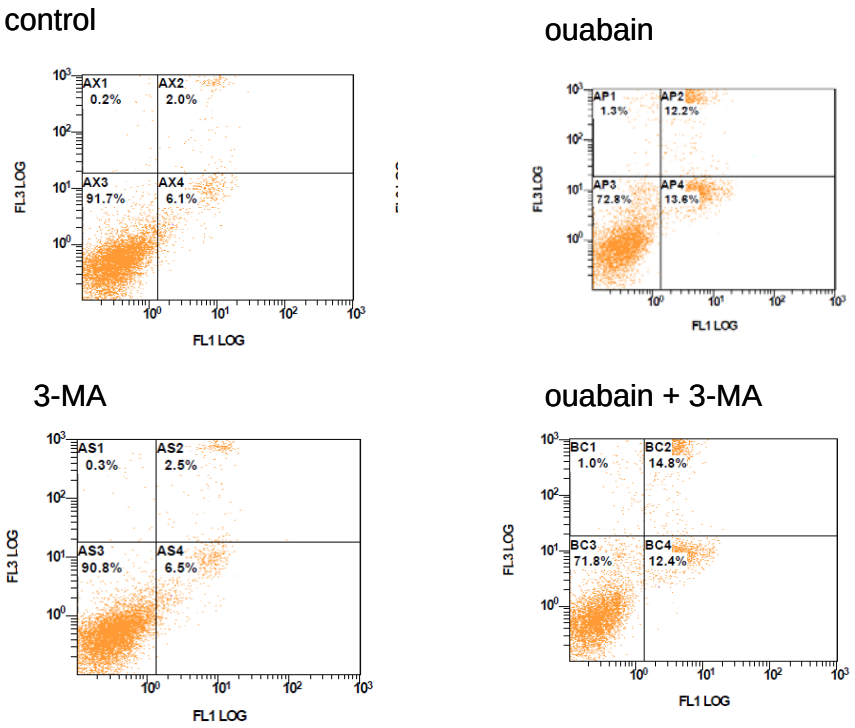

Figure 45. . *Effect of 3-MA on ouabain induced apoptosis in Jurkat cells.* Cells were pretreated with 3-MA (10 mM) and then ouabain 100 nM was added for 24 hours (the inhibitor was present during all the treatment). At the end, flow cytometric analysis of Annexin V binding was performed as described in Methods. A representative experiment is shown.

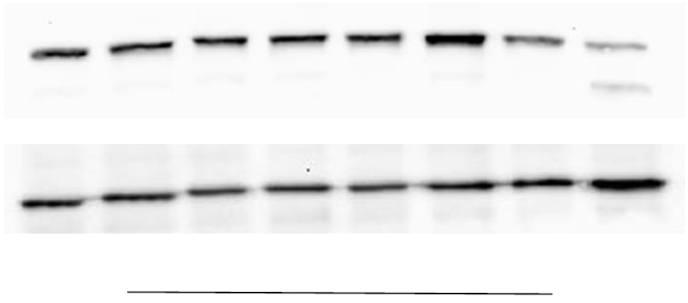

Figure 46 *Western blotting analysis of LC3 conversion in Jurkat treated with ouabain.* Cells were treated with 100 nM ouabain for the indicated time, C+ cells were treated with PBS for 3 h (positive control for autophagy). At the end of the treatment cells were lysed and subjected to Western blotting as descrived in Methods. A representative experiment is shown.

Furthermore, 3-MA abolished the increase in intracellular ROS level, suggesting the idea that sustained elevation of intracellular ROS are a consequence rather than a cause of cell death (figure 47).

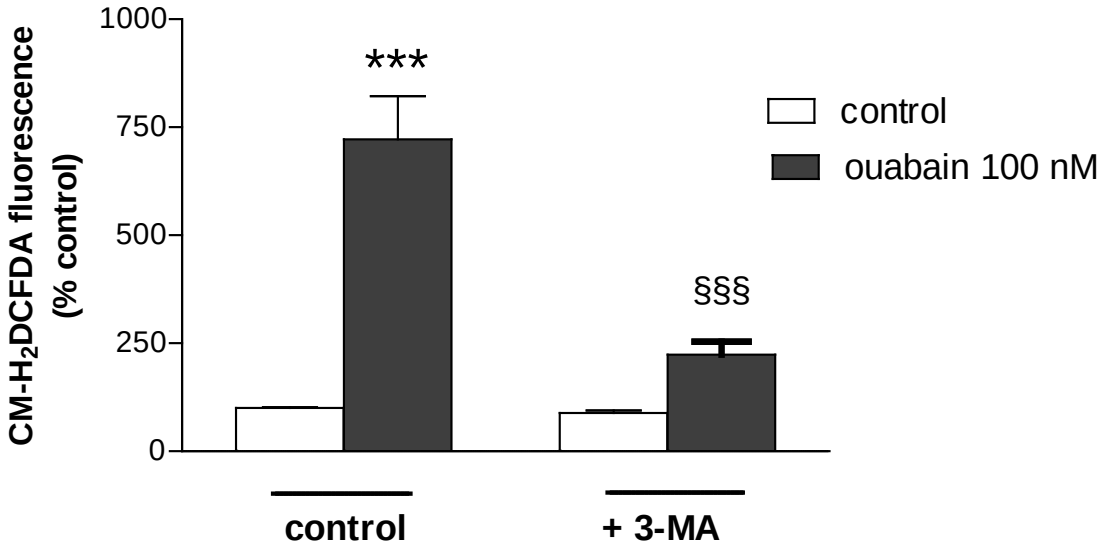

Figure 47. *Effect of 3-MA on intracellular ROS production in A549 cells*. Cells were pretreated with 3MA (10 mM) for 60 min and then ouabain 100 nM was added for 15 hours (the inhibitor was present during all the treatment). At the end flow cytometric analysis of CM-H_2DCFDA was performed as described in Methods. Data are expressed as mean ± SE of three experiments ***P<0.0001 (vs control) §§§ P<0.0001 (vs ouabain alone) One Way ANOVA, post test Bonferroni

The process of autophagy starts with the activation of ULK in a complex that includes ATG13 and FIP200 (see Introduction). This complex is regulated by mTOR which senses nutrient levels in the environment and under high-nutrient conditions inhibits autophagy. mTOR is in turn controlled directly by the level of intracellular aminoacids and indirectly by two different kinases: Akt/PKB (that transmits signals from growth factors) and AMPK (a sensor of the cell energy status). Thus it is important to investigate whether these two kinases are involved in ouabain-induced autophagy.

Akt leads to the activation of mTOR complex I via tuberous sclerosis complex (TSC) and Ras homolog enriched in brain (Rheb). Autophagy is negatively regulated by mTOR which senses nutrient levels in the environment: under high-nutrient conditions inhibits autophagy by phosphorylation of ULK1/2; during periods of nutrient deprivation mTOR dissociates from the ULK1/2 complex and this allows dephosphorylation of ULK1/2 which, in turn, phosporylates and activates ATG13 and FIP200 promoting autophagy initiation (Xie and Klionsky, 2007, Rosenfeldt and Ryan, 2009, Roy and Debnath, 2010). As shown in figure 24, ouabain decreased Akt phosphorylation in A549.

AMPK is activated by ATP depletion or glucose starvation and activates autophagy entirely through its ability to inactivate mTOR complex-1 or phosphorylating ULK1 (Hardie DG, 2011). Figure 48 shows that ouabain treatment induced only a slight increase in pAMPK, statistically significant only at 24 h of treatment.

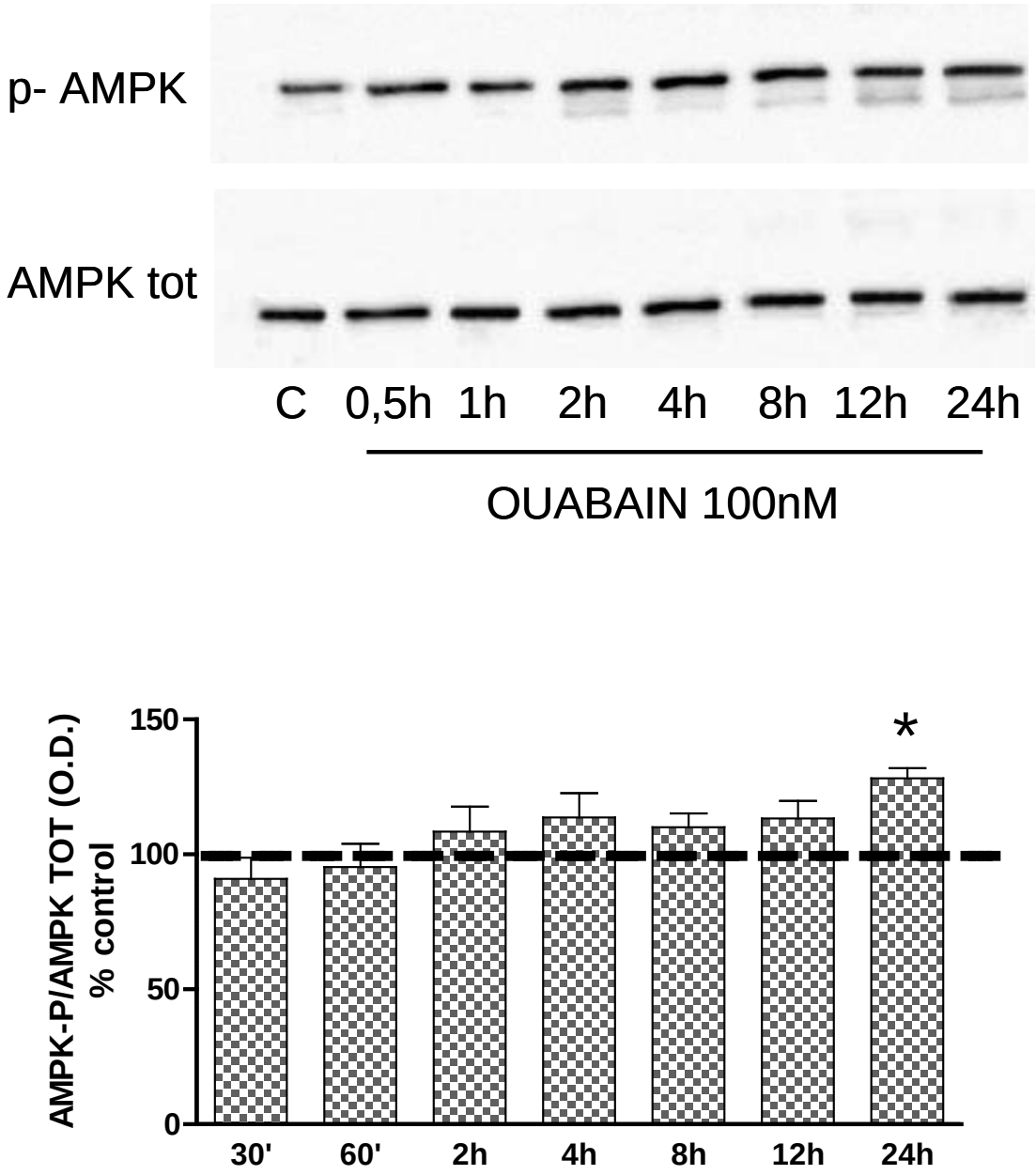

Figure 48. *Effect of ouabain on AMPK phosphorilation in A549 cells*. Cells were treated with 100 nM ouabain for the indicated time. At the end of the treatment cells were lysed and subjected to Western blotting as descrived in Methods. Data are expressed as mean ± SE of three experiment. *P<0.05 (vs control) One Way ANOVA, post test Dunnet

Inactivation of mTOR leads to the activation of FoxO, a transcription factor that controls the expression of many proteins involved in the autophagic process (Mammuccari *et al*., 2007). Quantitative RT-PCR analysis of VPS34, BNIP3, BNIP3L, ATG12, ATG4B and Beclin 1 (BECN1) showed that after 12 hours of treatment with ouabain there was a decrease in mRNA levels of VPS34, BECN1, ATG12 and ATG4B (figure 49 A). At shorter times of incubation (1, 3 and 6 hours) no changes in mRNA expression were detectable respect to control (figure 49 B). These data suggest that ouabain induced autophagy proceeds through the activation of an already existing complex of proteins.

A

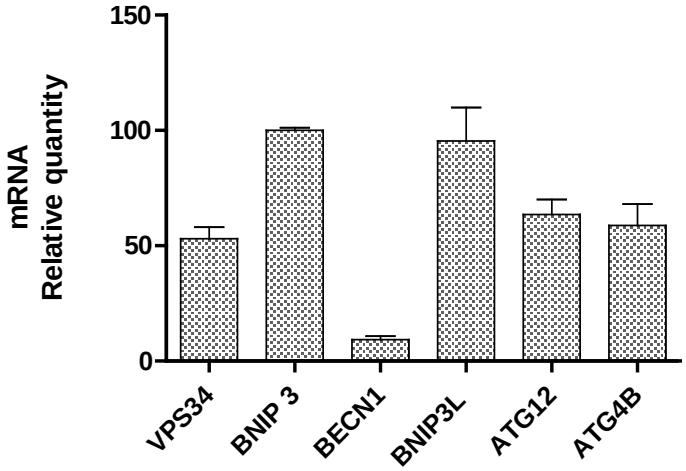

B

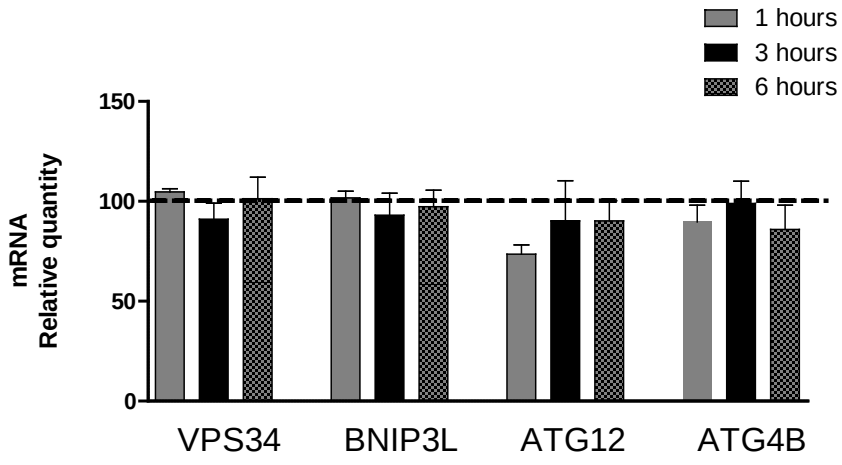

Figure 49. *Effect of ouabain on autophagy-related genes expression.* Cells were treated with ouabain 100 nM for 12 h *(A)* or 1-3-6 h *(B).* At the end of the treatment RNA was extracted and quantitative RT-PCR was performed as described in Methods. Data are expressed as mean ± SE of two independent experiment performed in duplicate.

Finally we investigated if the decrease of Bcl-2 levels induced by ouabain in A549 cells (showed in figure 28 A) could be associated to autophagy. In fact Bcl-2, by interacting with the autophagic protein Beclin 1, inhibits Beclin 1-dependent autophagy both in yeast and mammalian cells. Beclin 1 possesses a so-called BH3 domain (amino acids 114–123) that mediates the interaction with Bcl-2 and other close Bcl-2 homologs, such as Bcl-xL and Mcl-1 (Pattingre *et al.*, 2005).

Western blotting analysis (figure 50) revealed that no change in Beclin 1 expression occurred during ouabain treatment. This finding is in agreement with the data on mRNA expression. Thus it is possible that the decrease of Bcl-2 expression is sufficient to increase free Beclin 1 and trigger autophagy. It has been demonstrated that C Jun N-terminal Kinase (JNK) regulates the interaction between Bcl-2 and Beclin 1 and that JNK-dependent phosphorylation of Bcl-2 causes degradation of Bcl-2 and disruption of Bcl-2/Beclin1 complex thus allowing Beclin 1 to promote formation of the autophagy initiation complex (Zhou *et al*, 2011).

To test this hypothesis, we used a selective JNK inhibitor, SP600125 (Bennet *et al.*, 2001). Figure 51 shows that the presence of this inhibitor in the incubation medium abolished cell death induced by ouabain only in A549 cells.

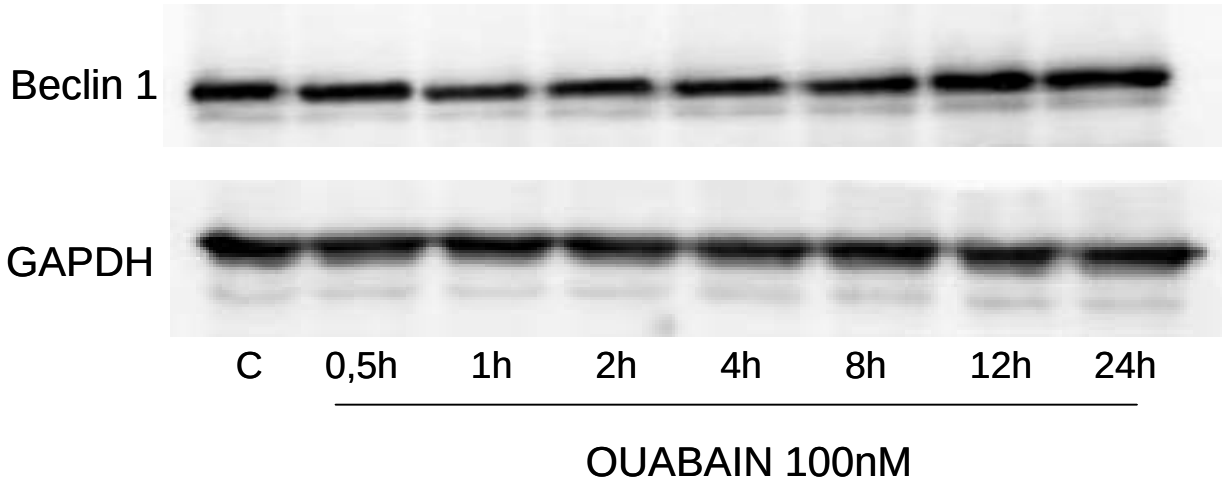

Figure 50 *Western blotting analysis of Beclin 1 expression in the presence of ouabain.* Cells were treated with 100 nM ouabain for the indicated time. At the end of the treatment cells were lysed and subjected to Western blotting as descrived in Methods. A representative experiment is shown.

A

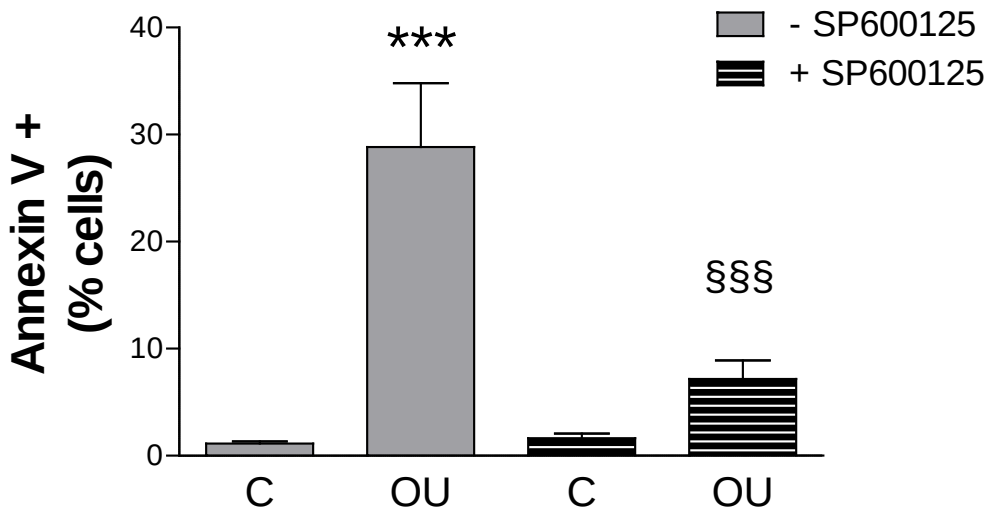

B

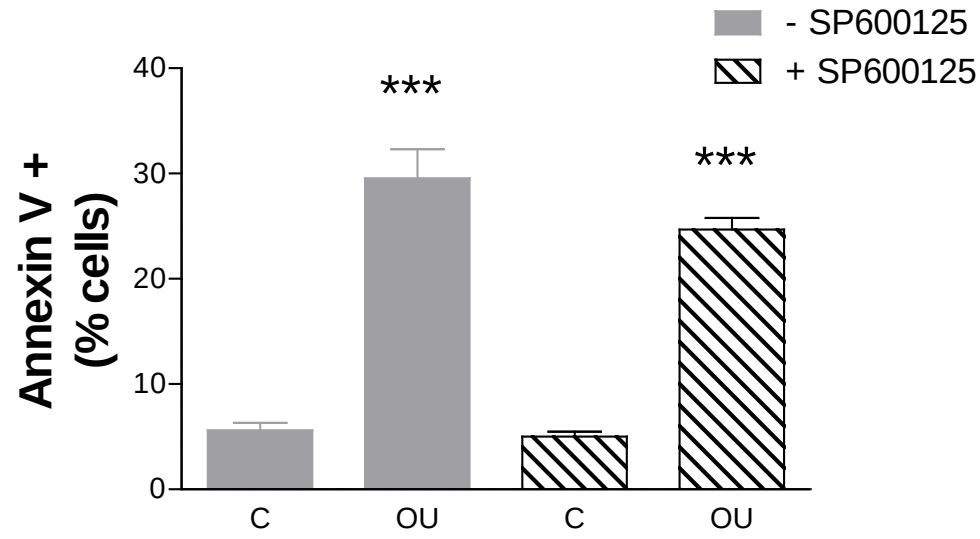

Figure 51. . *Effect of SP600125 on Annexin V binding in A549 (A) and Jurkat (B) cells treated with ouabain.* Cells were pretreated with (30 μM) SP600125 for 30 min and then ouabain 100 nM was added for 24 hours (the inhibitor was present during all the experiment). At the end of the treatment flow cytometric analysis of Annexin V binding was performed as described in Methods. Data are expressed as mean ± SE of three experiment performed in duplicate. ***P<0,001 (vs control); §§§ P<0,001 (vs ouabain alone) One Way ANOVA, post test Dunnet

4.5 Analysis of Na/K ATPase subunit expression

Structurally, Na/K ATPase exists as a heterodimer that contains a catalytic α-subunit and a glycosylated β-subunit plus a third regulatory subunit (γ). The α-subunit has binding sites for ATP, Na^+, K^+, and cardiac glycosides. Four different α isoforms (α1, α2, α3, and α4) and three different β isoforms (β1, β2, and β3) have been identified in mammalian cells. The expression of α isoforms is tissue type–specific (Schoner and Scheiner-Bobis, 2007). Variation in the expression of these isoforms occurs also in human cancers (e.g., renal, lung, hepatocellular, and colon) compared to the corresponding normal tissues (Schoner and Scheiner-Bobis, 2007). The binding affinity of cardiac glycosides to α isoforms of Na/K ATPase are very similar in humans (Schoner and Scheiner-Bobis, 2007). Thus, differences among normal and tumoral cells in sensitivity to ouabain and other cardiac glycosides seems to relate to the Na/K ATPase α isoform expression pattern.

To verify this hypothesis, analysis of Na/K ATPase α isoforms expression was performed in Jurkat and A549 cells (cancer cell lines) and compared to the expression in HUVEC and PBMC (normal cell lines). As shown in figure 52, α1 isoform is ubiquitous expressed while α2 isoform is expressed in A549, Jurkat and HUVEC. Interestingly, α3 isoform is exclusively expressed in the two cancer cell lines (figure 52).

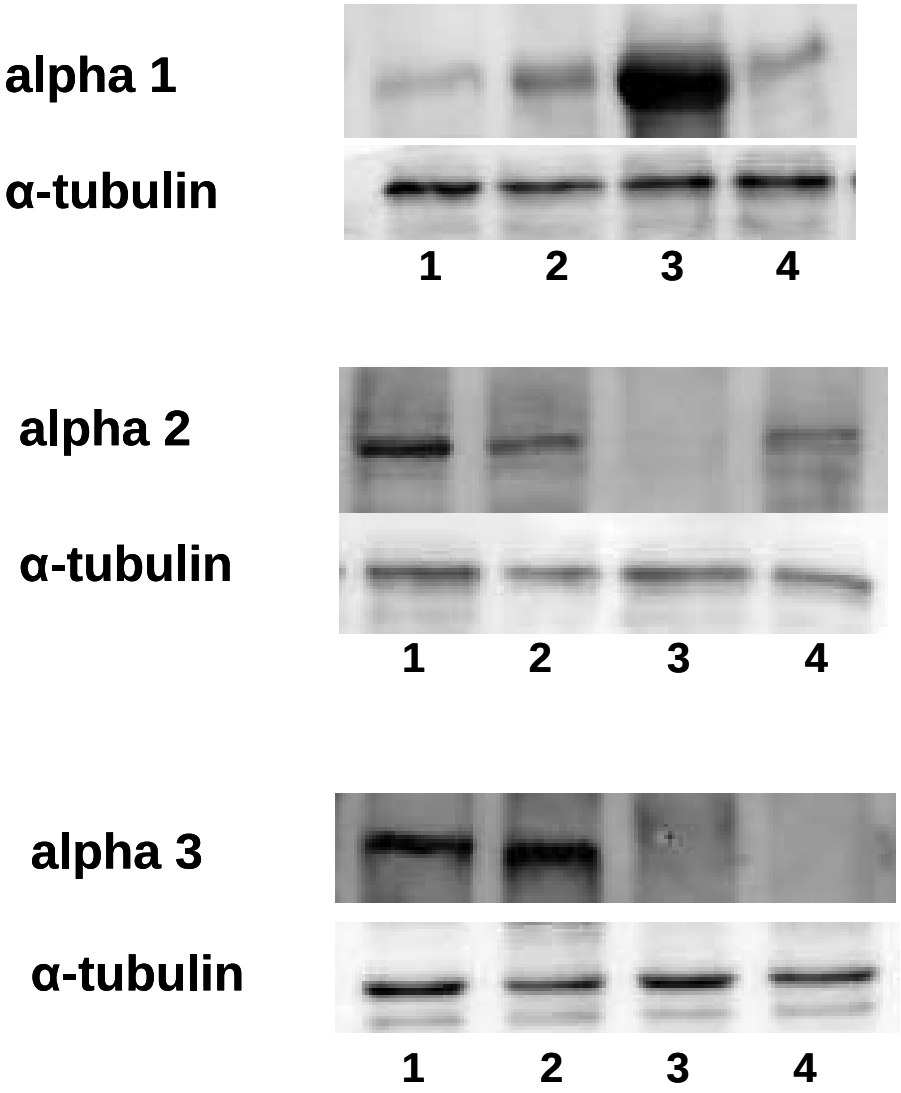

Figure 52. *Western blotting analysis of Na/K ATPase α subunits expression in (1) A549; (2) Jurkat; (3) PBMC; (4) HUVEC*

Xie and coworkers (Tian J *et al.*, 2009) found that the effect of ouabain on cell proliferation depends on whether ouabain can activate the Akt/mTOR pathway and replete cellular Na/K-ATPase against ouabain-induced endocytosis and subsequent degradation of the enzyme: in those cells where ouabain stimulated Akt/mTOR pathway, there was a translational up-regulation of Na/K-ATPase and stimulation of cell proliferation; instead in some cancer cells, where ouabain failed to activate the Akt/mTOR pathway and replete Na/K-ATPase, ouabain induced cell death.

Considering these data, we investigated if ouabain caused endocytosis of Na/K ATPase in A549 and Jurkat cells. Immunocytochemistry with antibodies against α1 and α3 isoforms showed that internalization of Na/K ATPase occurred after 6 hours of treatment in both cell lines (Figure 53). Unfortunately we don't have any data about internalization of isoenzymes containing α2 isoform because the antibody was unsuitable for immunocytochemistry.

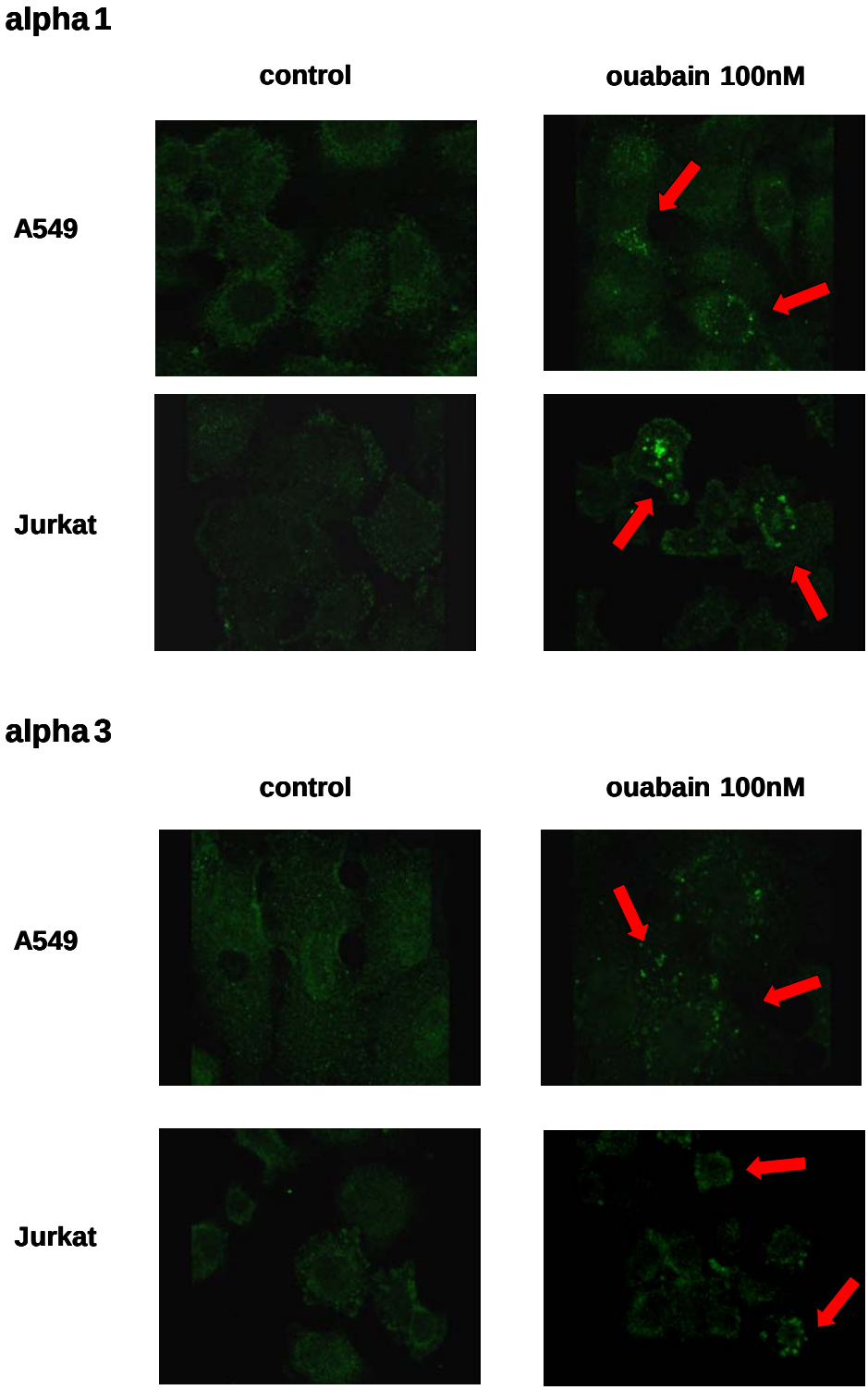

Figure 53. *Effect of ouabain on Na/K ATPase endocytosis in A549 and Jurkat cells.* Cells were treated with ouabain 100 nM for 6 h. At the end of the treatment cells were fixed with paraformaldehyde 4 % and then subjected to immunocytochemistry as described in Methods. Antibodies for α1 or α3 isoforms were used. A representative experiment is shown.

After 24 hours of treatment with ouabain no difference in protein levels of all α isoforms was found both in A549 and Jurkat cells (figures 54 and 55). Ouabain-induced endocytosis did not lead to a significant reduction of Na/K-ATPase over time probably because it was compensated by up-regulation of α expression.

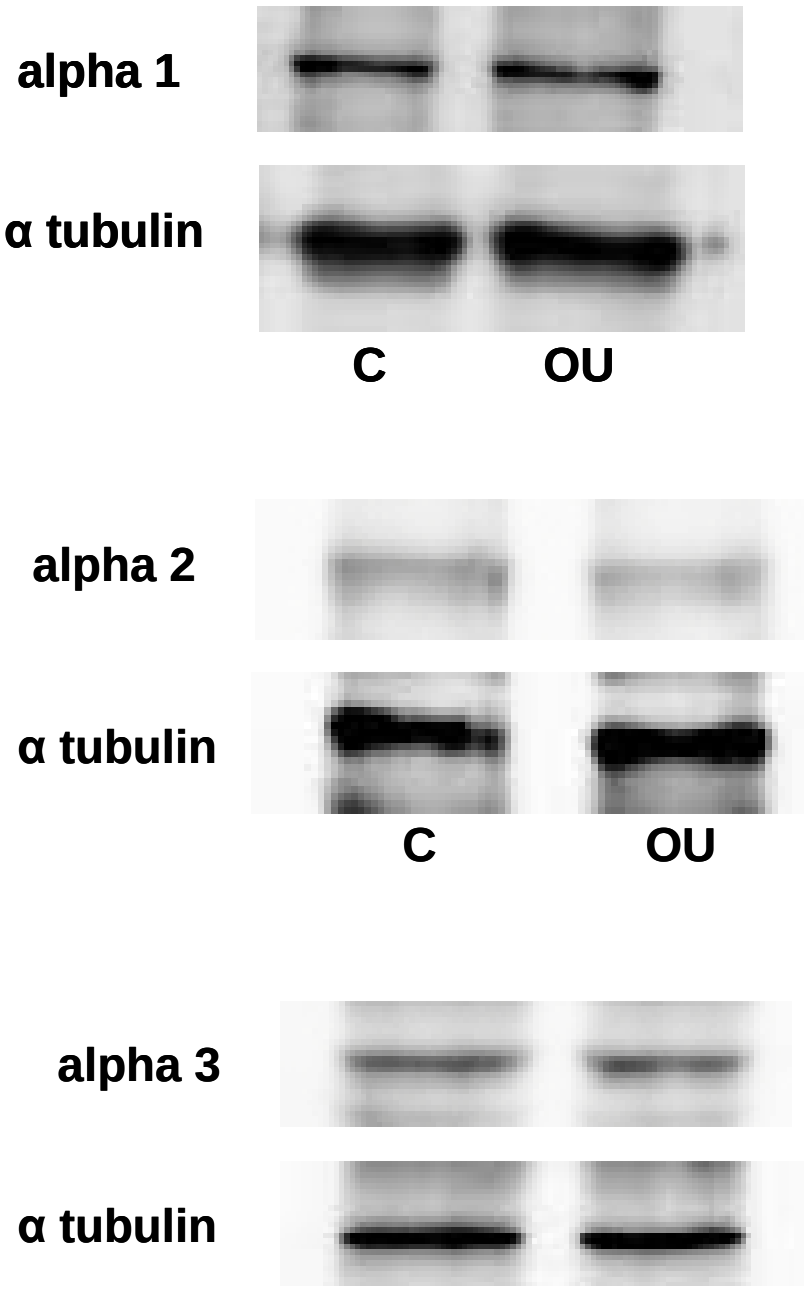

Figure 54. *Western blotting analysis of Na/K ATPase α subunits expression in A549 cells.* Cells were treated with 100 nM ouabain for 24 h. At the end of the treatment cells were lysed and Western blotting was performed as described in Methods. A representative experiment is shown.

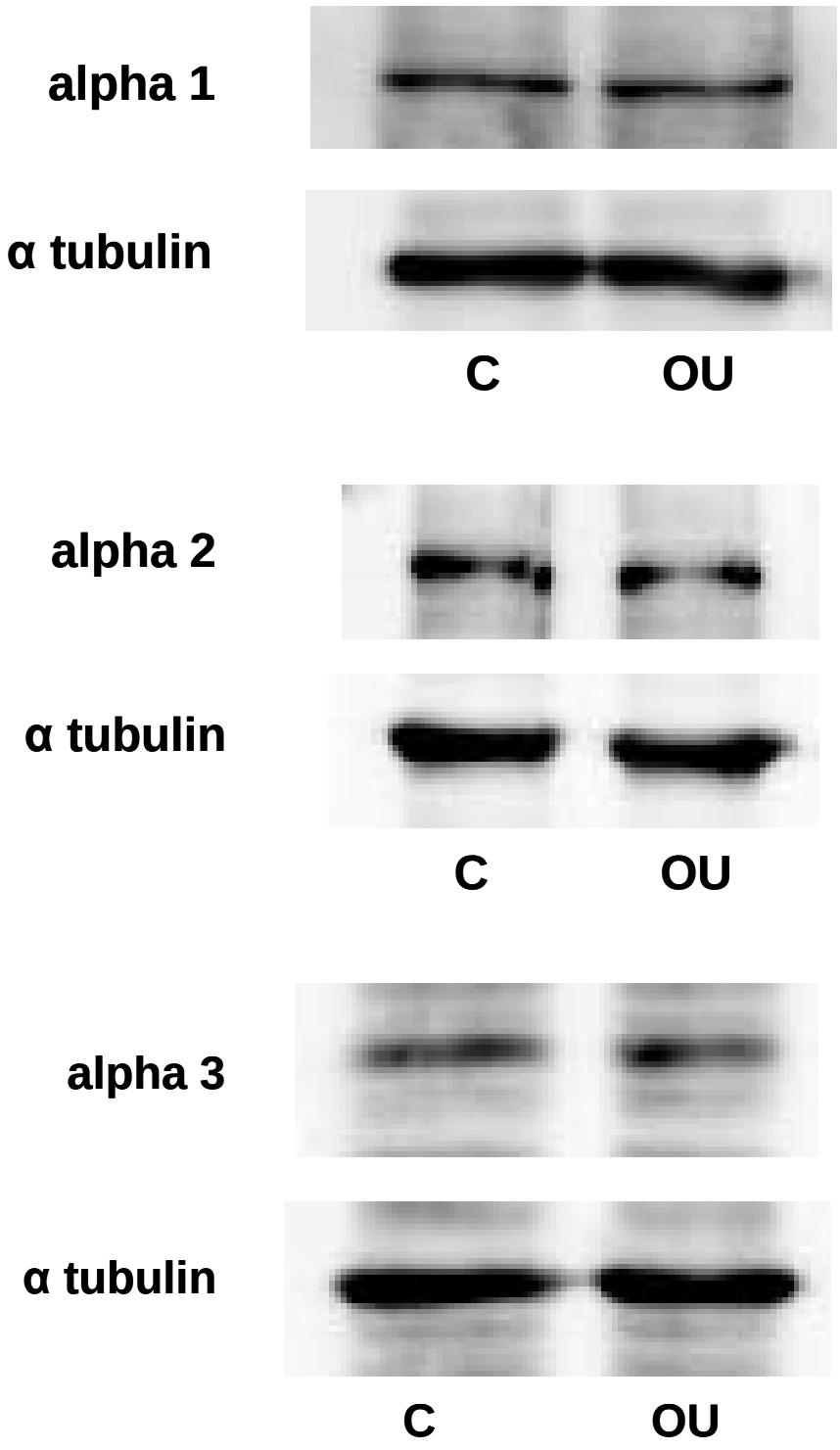

Figure 55. *Western blotting analysis of Na/K ATPase α subunits expression in Jurkat cells.* Cells were treated with 100 nM ouabain for 24 h. At the end of the treatment cells were lysed and Western blotting was performed as described in Methods. A representative experiment is shown.

Discussion

Ouabain and other cardiac glycosides such as digoxin and digitoxin are a class of natural products that are traditionally used to increase cardiac contractile force in patients with congestive heart failure and cardiac arrhythmias. The therapeutic effect of cardiac glycosides is mostly explained by the hypothesis that inhibition of Na/K ATPase activity causes accumulation of sodium in cardiac cells which are enforced to promote the Na/Ca exchange system in the cell membrane, thus leading to a higher level of intracellular and myocardial calcium concentration (Horisberger, 2004). The elevated intracellular calcium concentration results in increased inotropism, accentuating the force of myocardial contraction by increasing the velocity and extent of sarcomere shortening, thus translating into increased stroke work for a given filling volume of pressure.

In recent years evidence has emerged that Na/K ATPase functions as a signal transducer. Na/K ATPase has been shown to associate directly with other proteins in signaling complexes that regulate cell proliferation and survival in several cell types (Liu and Xie, 2010). This function is regulated by the binding of ouabain (or other cardiac glycosides) at concentrations that do not inhibit the pumping function. Interestingly, the effect of cardiac glycosides on cell proliferation and growth appears to be different depending whether the cells are normal or tumorous. In fact, recent studies have shown that in normal cells cardiac glycosides induce cell proliferation or protect from apoptosis while in several cancer cell lines these compounds inhibit cell proliferation and/or induce apoptosis (Newman *et al*., 2008 and Schoner and Scheiner-Bobis, 2007).

We used two cancer cell lines, Jurkat (a human T cell lymphoblast-like cell line lymphoblast) and and A549 (human lung adenocarcinoma epithelial cell line) as models for testing the effect of nanomolar concentration of ouabain against cancer cell lines. The objectives of the study were: to characterize the effect of ouabain on proliferation and survival in these cell lines; to identify the signal transduction pathways activated by ouabain and comparing them with those activated in normal cells; to ascertain whether

differences in sensitivity to ouabain between normal and cancer cells are related to a specific pattern of Na/K ATPase α isoform expression.

Our results indicate that ouabain at nanomolar concentrations (1-100 nM) has an antiproliferative and cytotoxic effect on both cancer cell lines. It should be noted that these range of concentrations protect HUVEC from apoptosis induced by serum deprivation and staurosporine treatment, as previously shown in our laboratory (Trevisi L *et al.*, 2004). Furthermore, as demonstrated in this study, ouabain did not affect cell viability of not transformed human PBMC, thus confirming its selective cytotoxic action against cancer cells.

Lower concentrations of ouabain (10-20 nM) were cytostatic in both cell lines. This effect was detectable by cell counting only after long time of incubation (72 hours) or by clonogenic assay (8 days incubation). These results indicate that in early experiments using MTT assay to measure cell viability, the significant decrease of MTT reduction after 24 hours of treatment with 10-20 nM ouabain was predominantly due to ouabain's ability to interfere with MTT assay (Trevisi *et al*., 2006) and in minor part due to the cytostatic effect of ouabain.

Ouabain induced cell death at higher concentrations, with a maximal effect observed at 100 nM, both in Jurkat and A549. Interestingly, early events activated by ouabain are common for both cell lines but the execution of programmed cell death is different. We found that ouabain induces caspase-dependent apoptosis in Jurkat cells while it induces autophagic cell death in A549.

In both cell lines ouabain decreased levels of the antiapoptotic protein Bcl-2 and increased mitochondrial membrane permeability. These two events are usually associated to caspase-dependent apoptosis. In fact, Bcl-2 acts as membrane bound scavenger for BH3-containing death factors and other proapoptotic molecules, which increase the permeability of the outer mitochondrial membrane and promote the release of the proapoptotic factors such as cytochrome c (Hengartner, 2000). In the cytosol, cytochrome c activates the apoptosome, a complex essential for the recruitment and subsequent activation of caspase-9. Caspase-9 then activates caspase-3 and caspase-7, thus promoting the execution of apoptosis (Hengartner, 2000). In Jurkat cells treated with ouabain we observed caspase 3/7 activation and DNA ladder fragmentation, two hallmarks of caspase-dependent apoptosis. Caspase activation represents the unique mechanism of

execution of cell death in Jurkat since pan caspase inhibitor Z-VAD-fmk, completely blocked ouabain-induced cell death. Our results are in agreement with previous findings reporting the cytotoxic effect of ouabain and other cardiac glycosides (such as digoxin) in Jurkat cells (Daniel *et al*., 2003), however our study examines more completely the initial events associated to ouabain induced apoptosis. In a study that analizes the effect of six bufadienolides on Jurkat cells, it is shown that these compounds induced mitochondrial membrane depolarization and activation of caspase-8, -9 and -3. Interstingly, they showed that overexpression of Bcl-2 protected Jurkat cells from apoptosis, thus indicating the central role of Bcl-2 in apoptosis induced by cardiac glycosides (Ihenetu *et a*l., 2007).

In A549 no signs of caspase-dependent apoptosis were observed. This is in agreement with the studies coming from Mijatovic's laboratory demonstrating that the cardenolide-related compound UNBS1450 causes cell death in A549 through a caspase-independent mechanism involving NF-κB inactivation, decrease of Hsp70 expression and lysosomal membrane permeabilization (Mijatovic *et al*., 2006a; Mijatovic *et al*., 2006b).

Our results show that ouabain induces autophagic cell death in A549. To our knowledge this is the first evidence of induction of this tipe of programmed cell death by ouabain. This is demonstrated by the presence of numerous markers of autophagosome formation in cells treated with ouabain: the conversion of LC3-I to its lipidated form LC3-II; the change in the distribution of LC3 fluorescence from a diffuse cytosolic pattern to a punctate pattern; the lysosomal localization in the perinuclear area (Klionsky *et al*., 2008; Korolchuk *et al*., 2011; Pous and Codogno, 2011). Most importantly cell death induced by ouabain was completely blocked by treatment with an inhibitor of autophagy such as 3-MA. No markers of autophagy were observed in Jurkat cells treated with ouabain and 3-MA was ineffective in preventing cell death.

Autophagy is a dynamic, multi-step process that can be modulated at several steps, both positively and negatively. An accumulation of autophagosomes could, for example, reflect either increased autophagosome formation due to increases in autophagic activity, or to reduced turnover of autophagosomes. Therefore, the use of autophagy markers such as LC3-II needs to be complemented by knowledge of overall autophagic flux to permit a correct interpretation of the results and to affirm whether or not a stimulus induces cell death by autophagy (Klionsky *et al*., 2008). We used two strategies to misure autophagic flux: we treated the cells in the presence of chloroquine, a lysosomotropic reagent, which

inhibits autophagosome-lysosome fusion so the degradation of LC3-II is blocked, resulting in the accumulation of LC3-II (Fujita *et al.*, 2008); we analyze the expression of the protein p62 (also known as SQSTM1/sequestome 1) that is selectively incorporated into autophagosomes through direct binding to LC3 and is efficiently degraded by autophagy, thus, the total cellular expression levels of p62 inversely correlate with autophagic activity (Mizushima *et al*, 2010). The results obtained in this study clearly show that ouabain increases autophagic flux in A549 and this process causes cell death.

An important point is to understand how autophagy is activated in A549 cells. As mentioned before, Bcl-2 decrease precedes ouabain-induced cell death in both cell lines. Bcl-2 family of proteins were formerly recognized as central regulators of apoptosis but most recently it has been demonstrated that antiapoptotic proteins, in particular Bcl-2, are also involved in the regulation of autophagy. Bcl-2, by interacting with the autophagic protein Beclin 1, inhibits Beclin 1-dependent autophagy. In fact, Beclin 1 possesses a BH3 domain that mediates the interaction with Bcl-2 and other close Bcl-2 homologs, such as Bcl-xL and Mcl-1 (Pattingre *et al*., 2005). In ouabain-treated A549 cells Beclin 1 expression remained constant therefore we hypothezise that the decrease of Bcl-2 levels permits the release of Beclin 1 and the subsequent autophagic vesicle nucleation. Further studies will be required to clarify this point, first of all analysis Bcl-2/Beclin-1 complexes by immunoprecipitation. Furthermore, it could be interesting to study the effect of Bcl-2 overexpression or Beclin 1 silencing on ouabain-induced cell death.

One of the main objectives of this study was to identify the signal transduction pathways activated by ouabain and comparing them with those activated in normal cells. Since Na/K-ATPase has no intrinsic tyrosine kinase activity, activation of non-receptor tyrosine kinase Src is an essential step to trigger further protein kinases cascades and generate second messengers (Liu and Xie, 2010). One of these pathways is the Ras/Raf/MEK/ERK cascade, which is involved in the increase of proliferation and growth, as well as in protection from apoptosis, induced by ouabain and other cardiac glycosides in normal cells (Trevisi *et al.*, 2004, Aydemir-Koksoy *et al.* 2001, Kometiani *et al*., 1998; Saunders and Scheiner-Bobis, 2004; Dmitrieva and Doris, 2003). On the contrary, evidence for ERK-dependent induction of cell death by cardiac glycosides is scanty. It has been reported that sustained ERK activation is involved in bufalin-induced apoptosis of human leukemia U937 cells (Watabe *et al*., 1996). The results presented in this study show that

ouabain induces a rapid increase in Src and ERK1/2 phosphorylation, thus demonstrating that also in A549 and Jurkat cells ouabain activates the known signaling cascades of the Na/K ATPase signalosome. However, we observed that these pathways are not involved in the mechanism of ouabain cytotoxicity, as confirmed by the lack of inhibition of cell death when a selective inhibitor of Src (PP2) or MEK (U0126) is used in combination with ouabain. Based on these results we suggest that in A549 and Jurkat ouabain simultaneously triggers survival and death signals, with a prevalence of cell death pathways.

Decrease of Akt activation is another common feature of ouabain action in Jurkat and A549 cells. It should be noted that in normal cells ouabain activates PI3K/Akt pathway stimulating cell proliferation and growth and protecting cells from apoptosis (Schoner and Scheiner-Bobis, 2007; Trevisi *et al* 2004). Activated Akt is a well established survival factor that inhibits the function of proapoptotic proteins such as BAD and caspase-9 (Cardone *et al.,* 1998; Datta *et al.,* 1997). It can also activate the cAMP-response element-binding protein (CREB) both in vitro and in vivo inducing Bcl-2 expression in a myriad of cell types (Wilson *et al.,* 1996; Riccio *et al.,* 1999; Bonni *et al.,* 1999; Pugazhenthi *et al.,* 1999). Therefore the decrease of Akt activation could be directly linked to the decrease of Bcl-2 expression in both cell lines.

Furthermore, Akt activates mTOR, a central checkpoint that negatively regulates autophagy, indeed, inibition of PI3K/Akt/mTOR pathway induces autophagy (Chen *et al.*, 2010). mTOR senses nutrient levels in the environment: under high-nutrient conditions it inhibits autophagy by phosphorylation of ULK1/2 while during periods of nutrient deprivation it dissociates from the ULK1/2 complex, thus allowing dephosphorylation of ULK1/2 which in turns promote autophagy initiation (Xie and Klionsky, 2007; Rosenfeldt and Ryan, 2009; Roy and Debnath, 2010). Therefore decrease of Akt activation induced by ouabain in A549 could be one of the initial signals triggering autophagy, both through the reduction of Bcl-2 levels and inhibition of mTOR. Several experimental evidences demonstrate that inhibition of Akt/mTOR signaling induces autophagic cell death in A549 (Viola *et al*., 2012; Hung *et al.,* 2009; Ling *et al.*, 2011).

A different interpretation of ouabain regulation of PI3K/Akt/mTOR pathway is given by Xie and coworkers since they have shown that ouabain effects on cell growth are intrinsically coupled to changes in the cellular amount of Na/K-ATPase via the

PI3K/Akt/mTOR pathway (Tian *et al*., 2009). In fact, they reported that ouabain induced Na/K ATPase endocytosis both in normal and cancer cell lines, but in normal cells (in which ouabain induced cell proliferation) ouabain activated PI3K/Akt/mTOR pathway and increased Na/K ATPase synthesis. On the other hand, ouabain did not activate PI3K/Akt/mTOR pathway, there was no increase of Na/K ATPase synthesis and inhibited cell proliferation in cancer cells. Diversely from Xie's work, in our study we found that ouabain induced Na/K ATPase endocytosis (measured after 6 hours of treatment) in both cancer cell lines, however we didn't detect any effect of ouabain on α subunits levels after 24 hours of treatment. It is possible that differences between our results and those obtained by Xie et al. are due to differences in experimental conditions or to the use of different cancer cell lines.

Overall these data indicate that decrease of Akt activation could be one of the initial death signals activated by ouabain that lead to apoptosis in Jurkat and autophagy in A549 cells. However further studies will be necessary to elucidate the role of Akt in ouabain-induced cell death and the mechanism of ouabain-induced dephosphorylation of Akt. A possible mechanism could be activation of phosphatase and tensin homolog (PTEN), a tumor-suppressor gene often mutated in cancer cells. PTEN specifically cleaves the D3 phosphate of phosphatidylinositol (3,4,5)-triphosphate (PIP-3), the second messenger produced by the activity of PI3K. Keeping PIP-3 levels low, PTEN inhibits PI3K/Akt pathway (Di Cristofano and Pandolfi, 2000). Loss of PTEN function results in an increased concentration of PIP-3 and Akt hyperactivation, leading to cell proliferation and protection from various apoptotic stimuli (Di Cristofano and Pandolfi, 2000). It has been shown that loss of PTEN in cancer cells leads to up-regulation of the Bcl-2 gene and that transient transfection of cells with PTEN gene induces Akt inhibition and decrease of Bcl-2 protein levels (Huang *et al*., 2001). Furthermore, PTEN can activate autophagy through inhibition of Akt activity (Degtyarev *et al*., 2008).

The last signaling pathway we analyzed in our study was JNK pathway. JNKs belong to the mitogen-activated protein kinase family and are involved in the regulation of cell proliferation, differentiation and apoptosis. JNKs are responsive to stress stimuli, such as cytokines, ultraviolet irradiation, heat shock, osmotic shock and oxidative stress (Dhanasekaran and Reddy, 2008). There are few studies demonstrating the involvement of JNK activation in the mechanism of action of cardiac glycosides. In particular, it has

been reported that cytotoxic action against cancer cells of some cardiac glycosides such as bufalin and oleandrin is dependent on JNK pathway activation (Schoner and Scheiner-Bobis, 2007). Furthermore, it has been shown that nanomolar concentrations of ouabain induced JNK activation and inhibition of cell proliferation (but not cell death) in a human breast cancer cell line (Kometiani *et al.,* 2005). It should be noted that JNK might be involved in autophagy because it regulates the interaction between Bcl-2 and Beclin 1. In fact, JNK-dependent phosphorylation of Bcl-2 causes degradation of Bcl-2 and disruption of Bcl-2/Beclin1 complex thus allowing Beclin 1 to promote formation of the autophagy initiation complex (Pattingre *et al.,* 2005). In our study we observed that JNK inibition with SP600125 was effective in preventing cell death only in A549 cells treated with ouabain, thus suggesting that activation of JNK pathway by ouabain is specific for ouabain-induced autophagy. Interestingly, similar results were obtained in a recent paper from Xie and coworkers (Xie *et al*., 2011). They reported that in colon cancer cells bufalin induces autophagic cell death via a JNK-dependent pathway that causes increase ATG5 and Beclin 1. They found that JNK activation by bufalin is dependent on ROS production and treatment with the antioxidant N-acetylcysteine partially inhibited bufalin-induced autophagy. We instead observed that sustained increase of ROS levels (observed only in A549 cells) is the consequence and not the cause of autophagy since treatment with N-acetylcysteine did not affect ouabain-induced cell death and inihibition of autophagy by 3-MA prevented ROS production. Further studies will be performed to determine the levels of JNK phosphorylation in A549 and Jurkat cells during ouabain treatment, and to measure the expression of phophorylated Bcl-2 and total Bcl-2 in the presence of JNK inhibitors.

An unusual attribute of compounds such as ouabain, oleandrin, bufalin, and digitoxin is that they are, on the one hand, almost completely nontoxic to normal cell lines but posses anticancer activity at nanomolar concentrations. The differential effects of cardiac glycosides on human tumor vs normal cells are essential for their possible use in anticancer therapy.

The receptor for cardiac glycosides is the α isoform of Na/K ATPase, thus many laboratories have explored the possibility that the different effect of cardiac glycosides in malignant versus normal cells might be related to differences in the Na/K ATPase α subunit expression patterns. Support for this hypothesis is based on the observation that

malignant cells often exhibit altered expression patterns of Na/K ATPase isoforms and that expression of Na/K ATPase isoforms are subject to developmental and hormonal cues that become altered during the development of disease (Schoner and Scheiner-Bobis, 2007). In consideration to this fact we have analyze the expression of α isoforms in the two cancer cell lines and compared to normal cells. We found that cells expressing α3 isoform (A549 and Jurkat) are sensitive to cytotoxic effects of ouabain, whereas in cells that completely lack of α3 expression (HUVEC and PBMC) ouabain is ineffective or even protective. These results might indicate the importance of α3 relative to α1 on the sensitivity of human cancer cells to ouabain treatment and are in agreement with the findings of Newman and co-workers using a variety of human cancer cells lines (Newman *et al*., 2008; Yang P *et al*., 2009). In fact, they showed that cells expressing α3 isoform were more sensitive to oleandrine than cells (either from rodent or human origin) not expressing this isoform. They also found a higher sensitivity to oleandrin in those human cancer tissues where the relative expression of α3 was higher than α1. By genetic manipulation in which α3 isoform was knocked down (by α3 siRNA) or α1 protein was restored (by transfection of α1 cDNA), they obtained cells that lost their sensitivity to oleandrin. Another study reports that decrease of α1 and increase of α3 isoforms occurs in colon tissue when a normal phenotype changes to a malignant one (Sakai *et al*., 2004). On the other hand, Mijatovic *et al.* (Mijatovic *et al*., 2007) suggest that, rather than α3 subunit, α1 is the isoform that represents a novel anticancer target. They have shown that human lung cancer cell lines overexpressing the α1 subunit were sensitive to a few selected cardenolides.

It remains to be determined whether the altered expression of α1 or α3 (as suggested by our own work) or perhaps the specific ratio of α3:α1 is the most important predictor of cell sensitivity to cardiac glycosides. More research, using human tissues and not just cell lines will shed light on the potential importance and perhaps even the prognostic value of Na/K ATPase subunit composition within individual types of tumors. Moreover it will be interesting to test the cytotoxic effect cardiac glycosides on excitable tissues such as central and peripheral nervous tissues mainly expressing α3 isoform (Urayama *et al*., 1989). This type of studies might be useful for the screening of cardiac glycoside derivatives with a selective activity against cancer cells with no effect on normal tissues, in particular cardiovascular, thus resulting in a more targeted therapy.

In conclusion, the results presented in this study demonstrate the antineoplastic activity of ouabain and its selective cytotoxic effect against cancer cell lines. This selectivity is explained by the activation of precise death signals, such as inactivation of PI3K/Akt cascade and activation of JNK, that promote apoptosis or autophagy depending on the cancer cell type. Whether the activation of death pathways is due to a specific expression pattern of Na/K ATPase α isoforms needs to be further investigated, however α3 subunit appears important in determining the ability of cardiac glycosides to cause antiproliferative and cytotoxic effects. Our findings contribute to the elucidation of the signal pathways and molecular mechanisms of the anticancer effect of ouabain. Research studies on cardiac glycosides derivatives as anticancer agents represent a promising form of targeted cancer chemotherapy.

References

Abarquez RF (2001) **The old but reliable digitalis: persistent concerns and expanded indications.** *Int. J. Clin. Pract.* 55: 108-114

Abramowitz J, Dai C, Hirschi KK,. Dmitrieva RI, Doris PA, Liu L, Allen JC. (2003) **Ouabain- and marinobufagenin-induced proliferation of human umbilical vein smooth muscle cells and a rat vascular smooth muscle cell line, A7r5.** *Circulation.* 108: 1049-1054.

Afaq F, Saleem M, Aziz MH, Mukhtar H. (2004) **Inhibition of 12-O-tetradecanoylphorbol-13-acetate-induced tumor promotion markers in CD-1 mouse skin by oleandrin.** *Toxicol. Appl. Pharmacol.* 195: 361–369

Akiyama M, Ogura M, Iwai M, Iijima M, Numazawa S, Yoshida T. (1999) **Effect of bufalin on growth and differentiation of human skin carcinoma cells in vitro.** *Hum. Cell.* 12, 205–209.

Akopyanz NS, Broude NE, Bekman EP, Marzen EO, Sverdlov ED. (1991) **Tissue-specific expression of Na,K-ATPase beta-subunit. Does beta 2 expression correlate with tumorigenesis?** *FEBS Lett*. 289: 8–10.

Allen JC, Abramowitz J, Koksoy A. (2003) **Low concentrations of ouabain activate vascular smooth muscle proliferation.** *Ann. N.Y. Acad. Sci.* 986, 504–508.

Alnemri ES, Livingston DJ, Nicholson DW, Salvesen G, Thornberry NA, Wong WW, Yuan J. (1996**). Human ICE/CED-3 protease nomenclature.** *Cell* 87: 171-178

Altairac S, Zeggai S, Perani P, Courtois Y, Torriglia A (2003) **Apoptosis induced by Na+/H+ antiport inhibition activates the LEI/L-DNase II pathway.** *Cell Death Differ* 10:548–557

Altamirano J, Li Y, DeSantiago J, Piacentino V, Houser SR, BersDM. (2006) **The inotropic effect of cardioactive glycosides in ventricular myocytes requires Na^+/Ca^{2+} exchanger function**. *J Physiol* 575: 845–454

Altieri DC (2010) **Survivin and IAP proteins in cell-death mechanisms.** *Biochem J* 430: 199–205

Amenta JS, Hlivko TJ, McBee AG, Shinozuka H, Brocher S. (1978) **Specific inhibition by NH4CL of autophagy-associated proteloysis in cultured fibroblasts.** *Exp Cell Res.* 115: 357-366.

Aperia A, Holtbäck U, Syren ML, Svensson L, Fryckstedt J, Greengard P (1994) **Activation/deactivation of renal Na+,K(+)-ATPase: a final common pathway for regulation of natriuresis.** *FASEB J.* 8: 436–439 .

Arnoult D, Gaume B, Karbowski M, Sharpe JC, Cecconi F, Youle RJ. (2003) **Mitochondrial release of AIF and EndoG requires caspase activation downstream of Bax/Bak-mediated permeabilization.** *EMBO J.* 22: 4385-4399.

Arystarkhova E, Sweadner KJ. (1997) **Hormonal and neurogenic control of Na-K-ATPase and myosin isoforms in neonatal rat cardiac myocytes.** *Am. J. Physiol*. 273: C489–C499. |

Aydemir-Koksoy A, Abramowitz J, Allen JC. (2001**) Ouabain induced signaling and vascular smooth muscle cell proliferation.** *J. Biol. Chem.* 276: 46605–46611.

Aydemir-Koksoy A, Allen AJ. (2001) **Regulation of Na(+) pump expression by vascular smooth muscle cells.** *Am. J. Physiol., Heart Circ. Physiol*. 280: H1869–H1874.

Aydemir-Koksoy A. (2002) **Na+,K+-ATPase: a review.** *J. Ank. Med. Sch*. 24: 73–82.

Bagrov AY, Shapiro JI, Fedorova OV. (2009) **Endogenous Cardiotonic Steroids: Physiology, Pharmacology, and Novel Therapeutic Targets** *Pharmacol Rev* 61:9–38

Barnard ML, Ridge KM, Saldias F, Friedman E, Gare M, Guerrero C, Lecuona E, Bertorello AM, Katz AI, Sznajder AJ. (1999) **Stimulation of the dopamine 1 receptor increases lung edema clearance.** *Am. J. Respir*. *Crit. Care Med*. 160: 982–986. |

Bauvy C, Gane P, Arico S, Codogno P, Ogier-Denis E. (2001) **Autophagy delays sulindac sulfide-induced apoptosis in the human intestinal colon cancer cell line HT-29**. *Exp. Cell Res.* 268: 139–149.

Beguin P, Crambert G, Monnet-Tschudi F, Uldry M, Horisberger JD, Garty H, Geering K. (2002) **FXYD7 is a brain-specific regulator of Na,K-ATPase alpha 1-beta isozymes.** *EMBO J*. 21: 3264–3273.

Beltz GG, Breithaupt-Grögler K, Osowski U. (2001) **Treatment of congestive heart failure--current status of use of digitoxin.** *Eur J Clin Invest*. 2:10-7.

Benbrook DM, Masamha CP. (2011) **The pro-survival function of Akt kinase can be overridden or altered to contribute to induction of apoptosis.** *Curr Cancer Drug Targets*. 11: 586-599.

Bennet BL, Sadaki DT, Murray BW, o'Leary EC, Sakata ST, Xu W, Leisten JC, Motiwala A, Pierce S, Satoh Y, Bhagwat SS, Manning AM, Anderson DW. (2001) **SP600125, an anthrapyrazolone inhibitor of Jun N-terminal kinase.** *PNAS* 98: 13681-13686

Bernardi P, Petronilli V, Di Lisa F, Forte M. (2001) **A mitochondrial perspective on cell death.** *Trends Biochem Sci.* 26: 112-117.

Bertorello AM, Aperia A, Walaas SI, Nairn AC, Greengard P. (1991) **Phosphorylation of the catalytic subunit of Na+,K(+)-ATPase inhibits the activity of the enzyme.** *Proc. Natl. Acad. Sci.* 88: 11359–11362.

Bertorello AM, Katz A. (1995) **Regulation of Na:K pump activity: pathways between receptors and effectors.** *News Physiol. Sci*. 10: 253–259.

Bhutia SK, Dash R, Das SK, Azab B, Su ZZ, Lee SG, Grant S, Yacoub A, Dent P, Curiel DT, Sarkar D, Fisher PB. (2010) **Mechanism of autophagy to apoptosis switch triggered in prostate cancer cells by antitumor cytokine melanoma differentiation-associated gene 7/interleukin-24.** *Cancer Res* 70: 3667–3676

Blanco G, Koster JC, Sanchez G, Mercer RW. (1995) **Kinetic properties of the α2β1 and α2β2 isozymes of the Na,K-ATPase.** *Biochemistry* 34: 319–325.

Blanco G, Melton RJ, Sanchez G, Mercer RW. (1999) **Functional characterization of a**

testes-specific α subunit isoform of the Na,K-ATPase. *Biochemistry* 38: 13661–13669.

Blanco G, Mercer RW (1998) **Isozymes of the Na/K-ATPase: heterogeneity in structure, diversity in function.** *Am J Physiol* 275: F633–F650.

Blanco G, Sanchez G, Mercer RW. (1995) **Comparison of the enzymatic properties of the Na,K-ATPase α3β1 and α3β2 isozymes.** *Biochemistry* 34: 9897–9903.

Blanco G. (2005a) **Na,K-ATPase subunit heterogeneity as a mechanism for tissue-specific ion regulation.** *Semin. Nephrol*. 25: 292–303.

Blanco G. (2005b) **The Na/K-ATPase and its isozymes: what we have learned using the baculovirus expression system.** *Front. Biosci*. 10: 2397–2411.

Blaustein MP, Lederer WJ. (1999) **Sodium/calcium exchange: its physiological implications.** *Physiol Rev* 79: 763–854

Blaustein MP, Zhang J, Chen L, Hamilton BC. (2006) **How does salt retention raise blood pressure?** *Am J Physiol Regul Integr Comp Physiol* 290: R514–R523

Blok LJ, Chang GT, Steenbeek-Slotboom M, van Weerden WM, Swarts HG, De Pont JJ, van Steenbrugge GJ, Brinkmann AO. (1999) **Regulation of expression of Na^+,K^+-ATPase in androgen-dependent and androgen-independent prostate cancer**. *Br. J. Cancer* 8: 28–36.

Bonni A, Brunet A, West AE, Datta SR, Takasu MA, Greenberg ME. (1999) **Cell survival promoted by the Ras-MAPK signaling pathway by transcription-dependent and -independent mechanisms.** *Science* 286: 1358–1362

Borner C, Martinou I, Mattmann C, Irmler M, Schaerer E, Martinou JC, Tschopp J. (1994). **The protein bcl-2 alpha does not require membrane attachment, but two conserved domains to suppress apoptosis**. *J Cell Biol*. 126: 1059-1068.

Borner C. (2003**) The Bcl-2 protein family: sensors and checkpoints for life-or-death decisions.** *Mol Immunol.* 39:615-647

Boukerche H, Su ZZ, Kang DC, Fisher PB. (2004) **Identification and cloning of genes displaying elevated expression as a consequence of metastatic progression in human**

melanoma cells by rapid subtraction hybridisation. *Gene* 343: 191–201.

Bovellan M, Fritzsche M, Stevens C, Charras G (2010) **Death-associated protein kinase (DAPK) and signal transduction: blebbing in programmed cell death.** *FEBS J* 277: 58–65

Boya P, González-Polo RA, Casares N, Perfettini JL, Dessen P, Larochette N, Métivier D, Meley D, Souquere S, Yoshimori T, Pierron G, Codogno P, Kroemer G. (2005**) Inhibition of macroautophagy triggers apoptosis.** *Mol. Cell. Biol.* 25: 1025–1040.

Bras M., Queenan B, Susin SA. (2005) **Programmed Cell Death via Mitochondria: Different Modes of Dying.** *Biochemistry* 70: 231-239.

Brossas JY, Tanguy R, Brignole-Baudouin F, Courtois Y, Torriglia A, Treton J (2004) **L-DNase II associated with active process during ethanol induced cell death in ARPE-19.** *Mol Vis* 10:65–73

Budihardjo I, Oliver H, Lutter M, Luo X, Wang X. (1999) **Biochemical pathways of caspase activation during apoptosis.** *Annu Rev Cell Dev Biol*. 15: 269-290.

Bursch W, Hochegger K, Torok L, Marian B, Ellinger A, Hermann RS. (2000) **Autophagic and apoptotic types of programmed cell death exhibit different fates of cytoskeletal filaments.** *J Cell Sci*. 113: 1189-1198.

Bursch W. (2001) **The autophagosomal-lysosomal compartment in programmed cell death.** *Cell Death Differ*. 8: 569–581.

Cardone MH, Roy N, Stennicke HR, Salvesen GS, Franke TF, Stanbridge E, Frisch S, Reed JC. (1998) **Regulation of cell death protease caspase-9 by phosphorylation.** *Science* 282: 1318–1321

Cargnelli G, Trevisi L, Debetto P, Luciani S, Bova S. (2000) **Effect of long-term ouabain treatment on contractile responses of rat aortae.** *J. Cardiovasc. Pharmacol.* 35: 538-542.

Ceolotto G, Sartori M, Papparella I, Candiotto M, Baritono E, Filippelli A, Cargnelli G, Luciani S, Semplicini A, Bova S. (2003) **Different effect of ouabain on endothelin-induced extracellular signal-regulated kinase stimulation in rat heart and tail artery**,

J. Cardiovasc. Pharmacol. 41, 553-561.

Chaigne-Delalande B, Moreau JF, Legembre P (2008) **Rewinding the DISC**. *Arch Immunol Ther Exp* 56:9–14

Chen JQ, Contreras RG, Wang R, Fernandez SV, Shoshani L, Russo IH, Cereijido M, Russo J. (2006) **Sodium/potassium ATPase (Na(+), K(+)-ATPase) and ouabain/related cardiac glycosides: a new paradigm for development of anti-breast cancer drugs?.** *Breast Cancer Res. Treat.* 96: 1–15.

Chen S, Rehman SK, Zhang W, Wen A, Yao L, Zhang J.(2010) **Autophagy is a therapeutic target in anticancer drug resistance.** *Biochim Biophys Acta.* 1806: 220-229.

Cho DH, Jo YK, Hwang JJ, Lee YM, Roh SA, Kim JC (2009) **Caspase-mediated cleavage of ATG6/Beclin-1 links apoptosis to autophagy in HeLa cells.** *Cancer Lett* 274: 95–100

Chowdhury I, Tharakan B, Bhat GK (2008) **Caspases—an update**. *Comp Biochem Physiol B Biochem Mol Biol* 151:10–27

Chueh SC, Guh JH, Chen J, Lai MK, Teng CM. (2001) **Dual effects of ouabain on the regulation of proliferation and apoptosis in human prostatic smooth muscle cells.** *J. Urol.* 166, 347-353.

Crambert G, Hasler U, Beggah AT, Yu C, Modyanov NN, Horisberger JD, Lelievre L, Geering G. (2000) **Transport and pharmacological properties of nine different human Na, K-ATPase isozymes.** *J. Biol. Chem*. 275: 1976–1986.

Crighton D, Wilkinson S, O'Prey J, Syed N, Smith P, Harrison PR, Gasco M, Garrone O, Crook T, Ryan KM. (2006) **DRAM, a p53-induced modulator of autophagy, is critical for apoptosis.** *Cell* 126: 121–134

Cryns V, Yuan J. (1999) **Proteases to die for.** *Genes Dev* 13: 371-376.

Daniel D, Süsal C, Kopp B, Opelz G, Terness P. (2003) **Apoptosis-mediated selective killing of malignant cells by cardiac steroids: maintenance of cytotoxicity and loss of cardiac activity of chemically modified derivatives.** *Int Immunopharmacol*. 3: 1791-

801

Datta SR, Dudek H, Tao X, Masters S, Fu H, Gotoh Y, Greenberg ME. (1997) **Akt phosphorylation of BAD couples survival signals to the cell-intrinsic death machinery.** *Cell* 91: 231–241

Davies RJ, Sandle GI, Thompson SM. (1991) **Inhibition of the Na+,K(+)-ATPase pump during induction of experimental colon cancer.** *Cancer Biochem. Biophys*. 12: 81–94.

Degenhardt K, Mathew R, Beaudoin B, Bray K, Anderson D, Chen G, Mukherjee C, Shi Y, Gélinas C, Fan Y, Nelson DA, Jin S, White E. (2006) **Autophagy promotes tumor cell survival and restricts necrosis, inflammation, and tumorigenesis.** *Cancer Cell* 10: 51–64

Degtyarev M, De Maziere A, Orr C, Lin J, Lee BB, Tien JY, Prior WW, van Dijk S, Wu H, Gray DC, Davis DP, Stern HM, Murray MJ, Hoeflich KP, Klumperman J, Friedman LS, Lin K (2008) **Akt inhibition promotes autophagy and sensitizes PTEN-null tumors to lysosomotropic agents.** *J. Cell Biol*., 183: 101–116

Devarajan P, Gilmore-Hebert M, Benz EJ. (1992) **Differential translation of the Na,K-ATPase subunit mRNAs.** *J. Biol. Chem*. 267: 22435–22439.

Dhanasekaran DN, Reddy EP. (2008) **JNK signaling in apoptosis.** *Oncogene* 27: 6245-6251.

Di Cristofano A, Pandolfi PP. (2000) **The multiple roles of PTEN in tumor suppression.** *Cell* 100: 387-390

Djavaheri-Mergny M, Maiuri MC, Kroemer G (2010) **Cross talk between apoptosis and autophagy by caspase-mediated cleavage of Beclin 1.** *Oncogene* 29:1717–1719

Dmitrieva RI, Doris PA. (2003) **Ouabain is a potent promoter of growth and activator of ERK1/2 in ouabain-resistant rat renal epithelial cells.** *J. Biol. Chem.* 278**:** 28160–28166.

Dostanic-Larson I, Lorenz JN, Van Huysse JW, Neumann JC, Moseley AE, Lingrel JB. (2006) **Physiological role of the α1- and α2-isoforms of the Na/K-ATPase and biological significance of their cardiac glycoside binding site.** *Am J Physiol Regul*

Integr Comp Physiol 290: R524–R528

Egan DF, Shackelford DB, Mihaylova MM, Gelino S, Kohnz RA, Mair W *et al.* (2011) **Phosphorylation of ULK1 (hATG1) by AMP-activated protein kinase connects energy sensing to mitophagy.** *Science 3*31: 456–461

Ernst SA, Mills JW (1980) **Autoradiographic localization of tritiated ouabain-sensitive sodium pump sites in ion transporting epithelia.** *J. Histochem. Cytochem*. 28: 72–77.

Espineda C, Chang JH, Twis J, Rajasekaran SA, Rajasekaran AK. (2004) **Repression of Na,K-ATPase β1-subunit by the transcription factor Snail in carcinoma.** *Mol. Biol. Cell* 15: 1364–1373.

Espineda C, Seligson DB, Ball JW., Rao J, Palotie A, Horva S, Huang Y, Shi T, Rajasekaran AK. (2003), **Analysis of the Na/K-ATPase alpha- and beta-subunit expression profiles of bladder cancer using tissue microarrays**. Cancer 97: 1859–1868.

Evans W. (1986) **Ch.: Trease and Evanís Pharmacognosy**. *WB Saunders Company* p. 309-316,

Ewart H, Klip A. (1995) **Hormonal regulation of the Na-K-ATPase: mechanisms underlying rapid and sustained changes in pump activity**. *Am. J. Physiol., Cell Physiol*. 269: C295–C311. |

Fadeel B, Ottosson A, Pervaiz S (2008) **Big wheel keeps on turning: apoptosome regulation and its role in chemoresistance.** *Cell Death Differ* 15:443–452

Favata MF, Horiuchi KY, Manos EJ, *et al*. (1998) **Identification of a novel inhibitor of mitogen-activated protein kinase kinase.** *J Biol Chem* 273: 18623-18632.

Feraille E, Beguin P, Carranza ML, Gonin S, Rousselot M, Martin PY, Favre H, Geering K. (2000) **Is phosphorylation of the alpha1 subunit at Ser-16 involved in the control of Na,K-ATPase activity by phorbol ester-activated protein kinase C?.** *Mol. Biol. Cell* 11: 39–50.

Ferrari P, Ferrandi M, Valentini G, Bianchi G. (2006). **Rostafuroxin: an ouabain**

antagonist that corrects renal and vascular Na+-K+-ATPase alterations in ouabain and adducin-dependent hypertension. *Am. J. Physiol. Regul. Integr.* 290: R529-535.

Fimia GM, Stoykova A, Romagnoli A, Giunta L, Di Bartolomeo S, Nardacci R *et al.* (2007) **Ambra1 regulates autophagy and development of the nervous system.** *Nature* 447: 1121–1125

Fu YF, Fan TJ. (2002) **Bcl-2 family proteins and apoptosis.** *Sheng Wu Hua Xue Yu Sheng Wu Wu Li Xue Bao (Shanghai).* 34: 389-394.

Fujita N, Itoh T, Omori H, Fukuda M, Noda T, Yoshimori T (2008) **The Atg16L complex specifies the site of LC3 lipidation for membrane biogenesis in autophagy.** *Mol Biol Cell.* 19: 2092–2100

Galluzzi L, Morselli E, Kepp O, Vitale I, Pinti M, Kroemer G (2011) **Mitochondrial liaisons of p53.** *Antioxid Redox Signal* 15: 1691-1714.

Galluzzi L, Morselli E, Kepp O, Vitale I, Younes AB, Maiuri MC, Kroemer G. (2012) **Evaluation of rapamycin-induced cell death.** *Methods Mol Biol.* 821:125-169.

Galluzzi L, Vitale I, Abrams JM, Alnemri ES, Baehrecke EH, Blagosklonny MV, Dawson TM, Dawson VL, El-Deiry WS, Fulda S, Gottlieb E, Green DR, Hengartner MO, Kepp O, Knight RA, Kumar S, Lipton SA, Lu X, Madeo F, Malorni W, Mehlen P, Nuñez G, Peter ME, Piacentini M, Rubinsztein DC, Shi Y, Simon HU, Vandenabeele P, White E, Yuan J, Zhivotovsky B, Melino G, Kroemer G.(2012) **Molecular definitions of cell death subroutines: recommendations of the Nomenclature Committee on Cell Death 2012.** *Cell Death Differ.* 19: 107-120.

Gao Z, Gammoh N, Wong PM, Erdjument-Bromage H, Tempst P, Jiang X (2010) **Processing of autophagic protein LC3 by the 20S proteasome.** *Autophagy* 6: 126–137

Geering K. (2005) **Function of FXYD proteins, regulators of Na, K-ATPase.** *J. Bioenerg. Biomembr.* 37: 387–392.

Geering K. (2006) **FXYD proteins: new regulators of Na-K-ATPase.** *Am. J. Physiol. Renal. Physiol*. 290: F241–F250.

Geng J, Klionsky DJ (2008) **The Atg8 and Atg12 ubiquitin-like conjugation systems in**

macroautophagy. 'Protein modifications: Beyond the usual suspects' review series. *EMBO Rep*. 9:. 859–864

Gick G, Hatala M, Chon D, Ismail-Beigi F. (1993) **Na,K-ATPase in several tissues of the rat: tissue specific expression of subunit mRNAs and enzyme activity.** *Membr. Biol*. 131: 229–236.

Goldin AG, Safa AR. (1984) **Digitalis and cancer.** *Lancet* 1. 1134.

Gonta-Gabriec K, Rossowski W, Szumiel I. (1986) **Properties of Na/K-ATPase and alkaline phosphatase alter during spontaneous and radiation-induced leukemogenesis in mice.** *Neoplasma* 33: 141–155.

Goto A, Yamada K, Hazama H, Uehara Y, Atarashi K, Hirata Y, Kimura K, Otama M. (1996). **Ouabainlike compound in hypertension associated with ectopic corticotropin syndrome.** *Hypertension* 28: 421-425.

Goto A, Yamada K. (2000). **Putative roles of ouabainlike compound in hypertension.** *Hypertens Res* 23: S7-S13.

Gotoh H, Kamiyama A, Shibayarna R, Sawada M, Kashimoto T. (1993) **Involvement of phosphoinositide turnover in ouabain inotropism.** *Biochem Biophys Res Commun* 194: 72–78

Gozuacik D, Kimchi A. (2004) **Autophagy as a cell death and tumor suppressor mechanism.** *Oncogene* 23: 2891–2906.

Grahame Hardie D (2011) **AMPK and autophagy get connected.** *The EMBO Journal* 30: 634–635

Green DR, Reed JC (1998) **Mitochondria and apoptosis.** *Science* 281:1309–1312.

Gross A, McDonnell JM, Korsmeyer SJ. (1999) **BCL-2 family members and the mitochondria in apoptosis.** *Genes Dev*. 13:1899-1911.

Haensel R., Sticher O., Steinegger E. (1999) **Pharmakognosie-Phytopharmazie**. *Springer, Berlin, Heidelberg* p. 578-593

Hamlyn J.M., Blaustein M.P., Bova S., DuCharme D.W., Mandel F., Mathews W.R.,

Ludens J.H. (1991). **Identification and characterization of a ouabain-like compound from human plasma.** *Proc. Natl. Acad. Sci.* 88, 6259-6263.

Hamlyn JM, Lu ZR, Manunta P, Ludens JH, Kimura K, Shah JR, Laredo J, Hamilton JP, Hamilton MJ, Hamilton BP. (1998) **Observations on the nature, biosynthesis, secretion and significance of endogenous ouabain.** *Clin Exp Hypertens*. 20: 523-33.

Hamlyn JM, Ringel R, Schaeffer J, Levinson PD, Hamilton BP, Kowarski AA, Blaustein MP. (1982) **A circulating inhibitor of (Na+/K+)ATPase associated with essential hypertension.** *Nature*. 300: 650-652.

Han KQ, Huang G, Gu W, Su YH, Huang XQ, Ling CQ. (2007) **Anti-tumor activities and apoptosis-regulated mechanisms of bufalin on the orthotopic transplantation tumor model of human hepatocellular carcinoma in nude mice.** *World J. Gastroenterol.* 13: 3374–3379 (2007).

Hanke JH, Gardner JP, Dow RL, Changelian PS, Brissette WH, Weringer EJ, Pollok BA, Connelly PA. (1996) **Discovery of a novel, potent, and Src family-selective tyrosine kinase inhibitor. Study of Lck- and FynT-dependent T cell activation**. *The Journal of biological chemistry* 271: 695–701

Haux J, Klepp O, Spigset O, Tretli S. (2001) **Digitoxin medication and cancer; case control and internal dose–response studies.** *BMC Cancer* 1: 11

Haux J, Solheim O, Isaksen T, Angelsen A. (2000) **Digitoxin, in non-toxic concentrations, inhibits proliferation and induces cell death in prostate cancer cell lines.** *Z Onkol* 32: 11–16

Haux J. (1999) **Digitoxin is a potential anticancer agent for several types of cancer.** *Med. Hypotheses* 153: 543–548.

Hengartner MO (2000) **The biochemistry of apoptosis.** *Nature* 407: 770-776.

Hieber V, Siegel GJ, Fink DJ, Beaty MW, Mata M. (1991) **Differential distribution of (Na,K)-ATPase α isoforms in the central nervous system.** *Cell Mol Neurobiol* 11:253–262.

Horisberger JD. (2004) **Recent insights into the structure and mechanism of the**

sodium pump. *Physiology* 19: 377–387.

Huang H, Cheville JC, Pan Y, Roche PC, Schmidt LJ, Tindall DJ. (2001) **PTEN induces chemosensitivity in PTEN-mutated prostate cancer cells by suppression of Bcl-2 expression.** *J Biol Chem*. 276: 38830-38836.

Hundal HS, Marette A, Mitsumoto Y, Ramlal T, Blostein R, Klip A. (1992) **Insulin induces translocation of the α2 and α1 subunits of the Na/K-ATPase from intracellular compartments to the plasma membrane in mammalian skeletal muscle.** *J Biol Chem* 267:5040–5043.

Hung JY, Hsu YL, Li CT, Ko YC, Ni WC, Huang MS, Kuo PL. (2009**) 6-Shogaol, an active constituent of dietary ginger, induces autophagy by inhibiting the AKT/mTOR pathway in human non-small cell lung cancer A549 cells.** *J Agric Food Chem.* 57: 9809-9816.

Ihenetu K, Qazzaz HM, Crespo F, Fernandez-Botran R, Valdes R Jr. (2007) **Digoxin-like immunoreactive factors induce apoptosis in human acute T-cell lymphoblastic leukemia.** *Clin Chem.* 53: 1315-22

Inada A, Nakanishi T, Konoshima T, Kozuka M, Tokuda H, Nishino H, Iwashima A. (1993) **Anti-tumor promoting activities of natural products. II. Inhibitory effects of digitoxin on two-stage carcinogenesis of mouse skin tumors and mouse pulmonary tumors.** *Biol. Pharm. Bull.* 16: 930–931.

Ingbar DH. (1998) **Lung Na,K-ATPase in pulmonary edema**, *Pulmonary Edema, Dekker, New York*

Itakura E, Kishi C, Inoue K, Mizushima N. (2008) **Beclin 1 forms two distinct phosphatidylinositol 3-kinase complexes with mammalian Atg14 and UVRAG.** *Mol Biol Cell.* 19: 5360–5372

Jaitovich AA, Bertorello AM. (2006) **NaK-ATPase: an indispensable ion pumping-signaling mechanism across mammalian cell membranes.** *Semin. Nephrol.* 26: 386–392.

James PF, Grupp IL, Grupp G, Woo AL, Askew GR, Croyle ML, Walsh RA, Lingrel JB.

(1999) **Identification of a specific role for the Na,K-ATPase alpha 2 isoform as a regulator of calcium in the heart.** Mol. Cell 3: 55–63.

Jin Z, Li Y, Pitti R, Lawrence D, Pham VC, Lill JR, Ashkenazi A. (2009) **Cullin3-based polyubiquitination and p62-dependent aggregation of caspase-8 mediate extrinsic apoptosis signalling.** *Cell* 137: 721–735

Johansson S, Lindholm P, Gullbo J, Larsson R, Bohlim L, Claeson P.(2001) **Cytotoxicity of digitoxin and related cardiac glycosides in human tumor cells.** *Anticancer Drugs* 12: 475–483

Johnson PH, Walker RP, Jones SW, Stephens K, Meurer J, Zajchowski DA, Luke MM, Eeckman F, Tan Y, Wong L, Parry G, Morgan TK, McCarrick MA, Monforte J. (2002) **Multiplex gene expression analysis for high-throughput drug discovery: screening and analysis of compounds affecting genes overexpressed in cancer cells.** *Mol. Cancer Ther.* 14: 1293–1304.

Jung CH, Jun CB, Ro SH, Kim YM, Otto NM, Cao *et al.* (2009) **ULK-Atg13-FIP200 complexes mediate mTOR signaling to the autophagy machinery.** *Mol Biol Cell.* 20: 1992–2003

Kang R, Zeh HJ, Lotze MT, Tang D (2011) **The Beclin 1 network regulates autophagy and apoptosis.** *Cell Death Differ.* 18: 571-580.

Kanzawa T, Germano IM, Komata T, Ito H, Kondo Y, Kondo S. (2004) **Role of autophagy in temozolomide-induced cytotoxicity for malignant glioma cells.** *Cell Death Differ.* 11: 448-57.

Kanzawa T, Kondo Y, Ito H, Kondo S, Germano I. (2003) **Induction of autophagic cell death in malignant glioma cells by arsenic trioxide.** *Cancer Res.* 63: 2103–2108.

Kaplan JG. (1978) **Membrane cation transport and the control of proliferation of mammalian cells.** *Annu. Rev. Physiol.* 40: 19–41.

Karin M, Gallagher E. (2005) **From JNK to Pay Dirt: Jun Kinases, their Biochemistry, Physiology and Clinical Importance.** *IUBMB Life* 57: 283–295.

Katzmarzyk PT, Rankinen T, Perusse L, Deriaz O, Tremblay A, Borecki I, Rao DC,

Bouchard C. (1999) **Linkage and association of the sodium potassium-adenosine triphosphatase alpha2 and beta1 genes with respiratory quotient and resting metabolic rate in the Quebec Family Study.** *J. Clin. Endocrinol. Metab*. 84: 2093–2097. |

Kawazoe N, Watabe M, Masuda Y, Nakajo S, Nakaya, K. (1999) **Tiam1 is involved in the regulation of bufalin-induced apoptosis in human leukemia cells.** *Oncogene* 18, 2413–2421.

Khundmiri SJ, Metzler MA, Ameen M, Amin V, Rane MJ, Delamere NA. (2006) **Ouabain induces cell proliferation through calcium-dependent phosphorylation of Akt (protein kinase B) in opossum kidney proximal tubule cells.** *Am J Physiol Cell Physiol* 291: C1247–C1257

Kim CH, Fan TH, Kelly PF, Himura Y, Delehanty JM, Hang CL, Liang L. (1994) **Isoform-specific regulation of myocardial Na,K-ATPase α-subunit in congestive heart failure. Role of norepinephrine.** *Circulation* 89: 313–320.

Kim J, Kundu M, Viollet B, GuanKL. (2011) **AMPK and mTOR regulate autophagy through direct phosphorylation of Ulk1.** *Nat Cell Biol.* 13: 132–141

Kinne-Saffran E, Kinne RK. (2002) **Herbal diuretics revisited: from "wise women" to William Withering.** *Am. J. Nephrol.* 22, 112-118

Kirkin V, Lamark T, Sou YS, Bjørkøy G, Nunn JL, Bruun JA, Shvets E, McEwan DG, Clausen TH, Wild P, Bilusic I, Theurillat JP, Øvervatn A, Ishii T, Elazar Z, Komatsu M, Dikic I, Johansen T. (2009**) A role for NBR1 in autophagosomal degradation of ubiquitinated substrates.** *Mol Cell* 33: 505–516

Kjeldsen K, Bjerregaard P, Richter EA, Thomsen PE, Norgaard A. (1988) **NaK-ATPase concentration in rodent and human heart and skeletal muscle: apparent relation to muscle performance.** *Cardiovasc. Res.* 22: 95–100. |

Klionsky DJ, Abeliovich H, Agostinis P, Agrawal DK, Aliev G, Askew DS, Baba M, Baehrecke EH, Bahr BA, Ballabio A, Bamber BA, Bassham DC, Bergamini E, *et al*. (2008). **Guidelines for the use and interpretation of assays for monitoring autophagy in higher eukaryotes.** *Autophagy* 4: 151-175.

Kometiani P, Li J, Gnudi L, Kahn B, Askari A, Xie Z. (1998) **Multiple signal transduction pathways link Na/K-ATPase to growth-related genes in cardiac myocytes. The roles of Ras and mitogen-activated protein kinases.** *J Biol Chem* 273: 15249–15256

Kometiani P, Li J, Gnudi L, Kahn B, Askari A, Xie Z.(1998) **Multiple signal transduction pathways link Na/K-ATPase to growth-related genes in cardiac myocytes. The roles of Ras and mitogen-activated protein kinases.** *J Biol Chem* 273:15249–15256.

Kometiani P, Liu L, Askari A. (2005) **Digitalis-induced signaling by Na/K- ATPase in human breast cancer cells.** *Mol Pharmacol* 67: 929–936

Koren I, Reem E, Kimchi A. (2010a) **Autophagy gets a brake: DAP1, a novel mTOR substrate, is activated to suppress the autophagic process.** *Autophagy* 6: 1179–1180

Koren I, Reem E, Kimchi A. (2010b) **DAP1, a novel substrate of mTOR, negatively regulates autophagy.** *Curr Biol.* 20: 1093-1098.

Korolchuk VI, Saiki S, Lichtenberg M, Siddiqi FH, Roberts EA, Imarisio S, Jahreiss L, Sarkar S, Futter M, Menzies FM, O'Kane CJ, Deretic V, Rubinsztein DC. (2011) **Lysosomal positioning coordinates cellular nutrient responses.** *Nat Cell Biol.* 13: 453-460.

Kotova O, Al-Khalili L, Talia S, Hooke C, Fedorova OV, Bagrov AY, Chibalin AV.(2006) **Cardiotonic steroids stimulate glycogen synthesis in human skeletal muscle cells via a Src- and ERK1/2-dependent mechanism.** *J Biol Chem* 281: 20085

Kulikov A, Eva A, Kirch U, Boldyrev A, Scheiner-Bobis G. (2007) **Ouabain activates signaling pathways associated with cell death in human neuroblastoma.** *Biochim. Biophys. Acta* 1768: 1691–1702

Kuma A, Hatano M, Matsui M, Yamamoto A, Nakaya H, Yoshimori T, Ohsumi Y, Tokuhisa T, Mizushima N. (2004) **The role of autophagy during the early neonatal starvation period.** *Nature* 432:1032-1036.

Kvansakul M, Yang H, Fairlie WD, Czabotar PE, Fischer SF, Perugini MA, Huang DC

Colman PM. (2008) **Vaccinia virus anti-apoptotic F1L is a novel Bcl-2-like domain-swapped dimer that binds a highly selective subset of BH3-containing death ligands**. *Cell Death Differ***.** 15: 1564–1571.

Lahm A, Paradisi A, Green DR, Melino G (2003) **Death fold domain interaction in apoptosis.** *Cell Death Differ* 10:10–12

Larsen BD, Rampalli S, Burns LE, Brunette S, Dilworth FS, Megeney LA (2010). **Caspase 3/caspase activated DNase promote cell differentiation by inducing DNA strand breaks.** *Proc. Natl. Acad. Sci USA* 107: 4230.4235.

Lecuona E, Garcia A, Sznajder JI. (2000) **A novel role for protein phosphatase 2A in the dopaminergic regulation of Na,K-ATPase.** *FEBS Lett.* 481: 217–220.

Lee JS, Li Q, Lee JY, Lee SH, Jeong JH, Lee HR, Chang H, Zhou FC, Gao SJ, Liang C, Jung JU. (2009) **FLIP-mediated autophagy regulation in cell death control.** *Nat Cell Biol* 11: 1355–1362

Li C, Grosdidier A, Crambert G, Horisberger JD, Michielin O, Geering K. (2004) **Structural and functional interaction sites between Na,K-ATPase and FXYD proteins.** *J. Biol. Chem.* 279: 38895–38902.

Li H, Zhu H, Xu CJ, Yuan J. (1998) **Cleavage of BID by caspase-8 mediates the mitochondrial damage in the Fas pathway to apoptosis.** *Cell* 94**:** 491–501.

Li J, Zelenin S, Aperia A, Aizman O. (2006) **Low doses of ouabain protect from serum deprivation-triggered apoptosis and stimulate kidney cell proliferation via activation of NF-kappaB.** *J Am Soc Nephrol*. 17: 1848-1857.

Li M, Martin A, Wen C, Turner SW, Lewis LK, Whithworth JA. (1995) **Long-term ouabain administration does not alter blood pressare in conscious Sprague-Dawley rats.** *Clin. Exp. Pharmacol. Physiol.* 22: 919-923.

Li PF, Dietz R, von Harsdorf R (1999) **p53 regulates mitochondrial membrane potential through reactive oxygen species and induces cytochrome c-independent apoptosis blocked by Bcl-2.** *EMBO J* 18:6027–6036.

Li S, Wattenberg EV. (1998) **Differential activation of mitogen-activatedprotein**

kinases by palytoxin and ouabain, two ligands for the Na/K-ATPase. *Toxicol Appl Pharmacol* 151: 377–384

Liang C, Feng P, Ku B, Dotan I, Canaani D, Oh BH *et al.* (2006) **Autophagic and tumour suppressor activity of a novel Beclin1-binding protein UVRAG.** *Nat Cell Biol.* 8: 688–696

Liang M, Cai T, Tian J, Qu W, Xie ZJ.(2006) **Functional characterization of Src-interacting Na/K-ATPase using RNA interference assay.** *J Biol Chem* 281: 19709–19719

Ling YH, Aracil M, Zou Y, Yuan Z, Lu B, Jimeno J, Cuervo AM, Perez-Soler R. (2011) **PM02734 (elisidepsin) induces caspase-independent cell death associated with features of autophagy, inhibition of the Akt/mTOR signaling pathway, and activation of death-associated protein kinase** *Clin Cancer Res.* 17: 5353-66.

Lingrel JB, Kuntzweiler T. (1994) **Na^+, K^+-ATPase.** *J. Biol. Chem.* 269: 19659–19662.

Lingrel JB, Orlowski J, Shull MM, Price EM (1990) **Molecular genetics of Na,K-ATPase. Prog. Nucleic Acid Res. Mol. Biol.** 38: 37–89. |

Liu J, Xie Z. (2010) **The sodium pump and cardiotonic steroids-induced signal transduction protein kinases and calcium-signaling microdomain in regulation of transporter trafficking.** *Biochimica et Biophysica Acta* 1802: 1237–1245

Lockshin RA, Williams CM. (1964) **Programmed cell death – II. Endocrine potentiation of the breakdown of the intersegmental muscles of silkmoths.** *J Insect Physiol* 10: 643–649.

Lu CX, Fan TJ, Hu GB, Cong RS. (2003). **Apoptosis-inducing factor and apoptosis.** *Sheng Wu Hua Xue Yu Sheng Wu Wu Li Xue Bao (Shanghai)* 35: 881-885.

Lubarski I, Pihakaski-Maunsbach K, Karlish SJ, Maunsbach AB, Garty H (2005) **Interaction with the Na,K-ATPase and tissue distribution of FXYD5 (related to ion channel).** *J. Biol. Chem.* 280: 37717–37724.

Lum JJ, Bauer DE, Kong M, Harris MH, Li C, Lindsten T, Thompson CB. (2005) **Growth factor regulation of autophagy and cell survival in the absence of apoptosis.**

Cell 120: 237-248.

Luo S, Rubinsztein DC (2010) **Apoptosis blocks Beclin 1-dependent autophagosome synthesis: an effect rescued by Bcl-xL.** *Cell Death Differ* 17: 268–277

Luo X, Budihardjo I, Zou H, Slaughter C, Wang X. (1998) **Bid, a Bcl-2 interacting protein, mediates cytochrome *c* release from mitochondria in response to activation of cell surface death receptors.** *Cell* 94: 481–490.

Lytton J, Lin JC, Guidotti G. (1985) **Identification of two molecular forms of (Na,K)-ATPase in rat adipocytes. Relation to insulin stimulation of the enzyme**. *J Biol Chem* 260:1177–1184.

Magyar CE, Wang j, Azuma KK, McDonough AA. (1995) **Reciprocal regulation of cardiac Na,K-ATPase and Na/Ca exchanger: hypertension, thyroid hormone, development**. *Am. J. Physiol., Cell Physiol*. 269: C675–C682.

Maiuri MC, Le Toumelin G, Criollo A, Rain JC, Gautier F, Juin P, Tasdemir E, Pierron G, Troulinaki K, Tavernarakis N, Hickman JA, Geneste O, Kroemer G. (2007) **Functional and physical interaction between Bcl-X(L) and a BH3-like domain in Beclin-1.** *EMBO J* 26:2527–2539

Maiuri MC, Zalckvar E, Kimchi A, Kroemer G. (2007) **Self-eating and self-killing: crosstalk between autophagy and apoptosis.** *Nat Rev Mol Cell Biol.* 8: 741–752

Mammucari C, Milan G, Romanello V, Masiero E, Rudolf R, Del Piccolo P, Burden SJ, Di Lisi R, Sandri C, Zhao J, Goldberg AL, Schiaffino S, Sandri M. (2007) **FoxO3 controls autophagy in skeletal muscle in vivo.** *Cell Metab.* 6: 458-471.

Manna SK, Sreenivasan Y, Sarkar A. (2006) **Cardiac glycoside inhibits IL-8-induced biological responses by downregulating IL-8 receptors through altering membrane fluidity**. *J. Cell Physiol.* 207, 195–207

Manunta P, Ferrandi M. (2004). **Different effects of marinobufagenin and endogenous ouabain**. .*J Hypertens*. 22: 257-259

Manunta P, Hamilton BP, Hamlyn JM. (2006) **Salt intake and depletion increase circulating levels of endogenous ouabain in normal men.** *Am J Physiol Regul Integr*

Comp Physiol 290: R553–R559

Manunta P, Hamilton J, Rogowski AC, Hamilton BP, Hamlyn JM. (2000). **Chronic hypertension induced by ouabain but not digoxin in the rat: antihypertensive effect of digoxin and digitoxin.** *Hypertens Res.*;23: 77-85.

Manunta P, Stella P, Rivera R, Ciurlino D, Cusi D, Ferrandi M, Hamlyn JM, Bianchi G. (1999). **Left ventricular mass, stroke volume, and ouabain-like factor in essential hypertension.** *Hypertension* 34: 450-456.

Manunta P., Rogowski A.C., Hamilton B.P. and Hamlyn J.M. (1994). **Ouabain-induced hypertension in the rat: relationships among plasma and tissue ouabain and blood pressure.** *Journal of Hypertension* 12: 549–560**.**

Martinez-Ruiz G, Maldonado V, Ceballos-Cancino G, Grajeda JP, Melendez-Zajgla J (2008) **Role of Smac/DIABLO in cancer progression.** *J Exp Clin Cancer Res* 27:48-49

Marzo I, Brenner C, Zamzami N, Jürgensmeier JM, Susin SA, Vieira HL, Prévost MC, Xie Z, Matsuyama S, Reed JC, Kroemer G. (1998) **Bax and adenine nucleotide translocator cooperate in the mitochondrial control of apoptosis.** *Science* 281:2027–2031

Mathew R, Karp CM, Beaudoin B, Vuong N, Chen G, Chen HY, Bray K, Reddy A, Bhanot G, Gelinas C, Dipaola RS, Karantza-Wadsworth V, White E. (2009) **Autophagy suppresses tumorigenesis through elimination of p62.** *Cell* 137: 1062–1075

McConkey DJ, Lin Y, Nutt LK, Ozel HZ, Newman RA. (2000) **Cardiac glycosides stimulate Ca^{2+} increases and apoptosis in androgen-independent, metastatic human prostate adenocarcinoma cells.** *Cancer Res.* 60, 3807–3812.

McDonough AA, Geering K, Farley R. (1990) **The sodium pump needs its subunit.** *FASEB J.* 4: 1598–1605.

McDonough AA, Zhang Y, Shin V, Frank SJ. (1996) **Subcellular distribution of sodium pump isoform subunits in mammalian cardiac myocytes.** *Am. J. Physiol., Cell Physiol.* 270: C1221–C1227.

McGrail KM, Phillips JM, Sweadner KJ. (1991) **Immunofluorescent localization of**

three Na,K-ATPase isozymes in the rat central nervous system: both neurons and glia can express more than one Na,K-ATPase. *J Neurosci* 11**:**381–391.

Mijatovic T, Mathieu V, Gaussin JF, De Ne`ve N, Ribaucour F, Van Quaquebeke E, Dumont P, Darro F, Kis R. (2006a) **Cardenolide-induced lysosomal membrane permeabilization demonstrates therapeutic benefits in experimental human non-small cell lung cancers.** *Neoplasia* 8: 402– 412

Mijatovic T, Op De Beeck A, Van Quaquebeke E, Dewelle J, Darro F, de Launoit Y, Kiss R. (2006b) **The cardenolide UNBS1450 is able to deactivate nuclear factor "B-mediated cytoprotective effects in human non-small cell lung cancer cells.** *Mol Cancer Ther* 5: 391–399

Mijatovic T, Roland I, Van Quaquebeke E, Nilsson B, Mathieu A, Van Vynckt F, Darro F, Blanco G, Facchini V, Kiss R. (2007) **The α1 subunit ofthe sodium pump could represent a novel target to combat non-small cell lung cancers.** *J. Pathol*. 212: 170–179.

Minakata Y, Suzuki S, Grygorczyk C, Dagenais A, Berthiaume Y. (1998) **Impact of beta-adrenergic agonist on Na+ channel and Na+-K+-ATPase expression in alveolar type II cells.** *Am. J. Physiol*. 275: L414–L422.

Mizushima N, Klionsky DJ (2007) **Protein turnover via autophagy: implications for metabolism.** *Annu Rev Nutr.* 27:19-40.

Mizushima N, Levine B (2010) **Autophagy in mammalian development and differentiation.** *Nat Cell Biol* 12:823–830.

Mizushima N, Yoshimori T, Levine B. (2010) **Methods in mammalian autophagy research.** *Cell* 140: 313-326.

Mizushima N.(2007) **Autophagy: Process and function.** *Genes Dev.* 21: 2861–2873.

Mobasheri A, Avila J, Cozar-Castellano I, Brownleader MD, Trevan M, Francis MJ, Lamb JF, Martín-Vasallo P. (2000) **Na/K-ATPase isozyme diversity; comparative biochemistry and physiological implications of novel functional interactions.** *Biosci Rep* 20**:**51–91.

Mobasheri A, Avila J, Cozar-Castellano I, Brownleader MD, Trevan M, Francis MJ, Lamb JF, Martin-Vasallo MP. (2000) **Na+,K+-ATPase isozyme diversity; comparative biochemistry and physiological implications of novel functional interactions.** *Biosci. Rep*. 20: 51–91.

Moscat J, Diaz-Meco MT (2009) **p62 at the crossroads of autophagy, apoptosis, and cancer.** *Cell* 137: 1001–1004

Mosman T (1983) **Rapid colorimetric assay for cellular growth and survival: application to proliferation and cytotoxicity assays.** *J Immunol.* 65: 55–63

Mueller-Ehmsen J, Juvvadi P, Thompson CB, Tumyan L, Croyle M, Lingrel JB, Schwinger RH, McDonough AA, Farley RA. (2001) **Ouabain and substrate affinities of human Na!-K!-ATPase alpha(1)beta(1), alpha(2)beta(1), and alpha(3)beta(1) when expressed separately in yeast cells.** *Am J Physiol Cell Physiol* 281:C1355–C1364.

Neri G, De Toni R, Tortorella C, Rebuffat P, Bova S, Cargnelli G, Petrelli L, Spinazzi R, Nussdorfer GG. (2006) **Ouabain chronic infusion enhances the growth and steroidogenic capacity of rat adrenal zona glomerulosa: the possible involvement of the endothelin system.** *Int J Mol Med*. 18: 315-319.

Newman RA, Yang P, Pawlus AD, Block KI. (2008) **Cardiac Glycosides as Novel Cancer Therapeutic Agents.** *Mol Interv* 8: 36-49

Nezis IP, Simonsen A, Sagona AP, Finley K, Gaumer S, Contamine D, Rusten TE, Stenmark H, Brech A. (2008) **Ref(2)P, the Drosophila melanogaster homologue of mammalian p62, is required for the formation of protein aggregates in adult brain.** *J Cell Biol* 180: 1065–1071

Noble CG, Dong JM, Manser E, Song H. (2008) **Bcl-xL and UVRAG cause a monomer-dimer switch in Beclin1.** *J Biol Chem.* 283: 26274–26282

Ohsumi Y, Mizushima N. (2004) **Two ubiquitin-like conjugation systems essential for autophagy.** *Semin Cell Dev Biol*. 15: 231–236

Olivera WG, Ciccolella DE, Barquin N, Ridge KM, Rutschman DH, Yeates DB, SznajderJI. (2000) **Aldosterone regulates Na,K-ATPase and increases lung edema**

clearance in rats. *Am. J. Respir. Crit. Care Med*. 161: 567–573.

Paglin S, Hollister T, Delohery T, Hackett N, McMahill M, Sphicas E, Domingo D, Yahalom J. (2001) **A novel response of cancer cells to radiation involves autophagy and formation of acidic vesicles.** *Cancer Res*. 61: 439-444.

Pamnani MB, Chen S, Yuan CM, Haddy FJ. (1994). **Chronic blood pressure effects of bufalin, a sodium–potassium ATPase inhibitor, in rats.** *Hypertension* **23**: 106–109.

Pankiv S, Clausen TH, Lamark T, Brech A, Bruun JA, Outzen H, Øvervatn A, Bjørkøy G, Johansen T. (2007) **p62/SQSTM1 binds directly to Atg8/LC3 to facilitate degradation of ubiquitinated protein aggregates by autophagy.** *J Biol Chem* 282: 24131–24145

Pathak S, Multani AS, Narayan S, Kumar V, Newman RA. (2000) **Anvirzel, an extract of Nerium oleander, induces cell death in human but not murine cancer cells.** *Anticancer Drugs* 11: 455–463.

Patterson RL, Boehning D, Snyder SH. (2004) **Inositol 1, 4, 5-trisphosphate receptors as signal integrators.** *Annu. Rev. Biochem*. 73: 437–465.

Pattingre S, Tassa A, Qu X, Garuti R, Liang XH, Mizushima N, Packer M, Schneider MD, Levine B.(2005) **Bcl-2 antiapoptotic proteins inhibit Beclin 1-dependent autophagy.** *Cell* 122:927–939

Pelicano H, Feng L, Zhou Y, Carew JS, Hileman EO, Plunkett W, Keating MJ, Huang P. (2003) **Inhibition of mitochondrial respiration: a novel strategy to enhance drug-induced apoptosis in human leukemia cells by a reactive oxygen species-mediated mechanism.** *J Biol Chem.* 278: 37832-37839.

Peng M, Huang L, Xie Z, Huang WH, Askari A. (1996) **Partial inhibition of Na/K-ATPase by ouabain induces the Ca^{2+}-dependent expression of early response genes in cardiac myocytes**. *J Biol Chem* 271: 10372– 10378

Pennarun B, Meijer A, de Vries EG, Kleibeuker JH, Kruyt F, de Jong S (2010) **Playing the DISC: turning on TRAIL death receptor-mediated apoptosis in cancer.** *Biochim Biophys Acta* 1805:123–140

Pesce L, Guerrero C, Comellas A, Ridge K, Sznajder J. (2000) **Beta agonists regulate**

Na,K-ATPase via novel MAPK/ERK and rapamycin-sensitive pathways. *FEBS Lett.* 486: 310–314.

Pidgeon GB, Richards AM, Nicholls MG, Charles CJ, Rademaker MT, Lynn KL, Bailey RR, Lewis LK, Yandle TG. (1996) **Chronic ouabain infusion does not cause hypertension in sheep**. *Am. J. Physiol.* 270: E386-392.

Pierdomenico SD, Bucci A, Manunta P, Rivera R, Ferrandi M, Hamlyn JM, Lapenna D, Cuccurullo F, Mezzetti A. (2001). **Endogenous ouabain and hemodynamic and left ventricular geometric patterns in essential hypertension.** *Am J Hypertens.* 14: 44-50.

Pierre SV, Sottejeau Y, Gourbeau JM, Sa´nchez G, Shidyak A, Blanco G. (2008) **Isoform-specificity of Na,K-ATPase-mediated ouabain signaling**. *Am J Physiol Renal Physiol* 294: F859–F866.

Poüs C, Codogno P. (2011) **Lysosome positioning coordinates mTORC1 activity and autophagy.** *Nat Cell Biol.* 13: 342-344.

Prassas I, Diamandis EP. (2008) **Novel therapeutic applications of cardiac glycosides** *Nature reviews* 7:926-935

Pugazhenthi S, Miller E, Sable C, Young P, Heidenreich KA, Boxer LM, Reusch JE. (1999) **Insulin-like growth factor-I induces bcl-2 promoter through the transcription factor cAMP-response element-binding protein.** *J. Biol. Chem.* 274: 27529–27535

Raghavendra PB, Sreenivasan Y, Manna SK.(2007) **Oleandrin induces apoptosis in human, but not in murine cells: dephosphorylation of Akt, expression of FasL, and alteration of membrane fluidity.** *Mol Immunol. 44: 2292-2302.*

Rajasekaran SA, Ball WJ, Bander NH, Liu H, Pardee JD, Rajasekaran AK (1999) **Reduced expression of beta-subunit of Na,K-ATPase in human clear-cell renal cell carcinoma.** *J. Urol*. 62: 574–580.

Razani B, Woodman SE, Lisanti MP. (2002) **Caveolae: from cell biology to animal physiology.** *Pharmacol. Rev.* 54: 431–467.

Rebecchi JM, Pentyala SN. (2000) **Structure, function, and control of phosphoinositide- specific phospholipase C.** *Physiol. Rev.* 80: 1291–1335.

Reuter H, Pott C, Goldhaber JI, Henderson SA, Philipson KD, Schwinger RHG. (2005) **Na^+/Ca^{2+} exchange in the regulation of cardiac excitation-contraction coupling.** *Cardiovasc Res* 67: 198–207

Riccio A, Ahn S, Davenport CM, Blendy JA, Ginty DD. (1999) **Mediation by a CREB family transcription factor of NGF-dependent survival of sympathetic neurons.** *Science* 286: 2358–2361

Ridge K, Dada L, Lecuona E, Bertorello A, Katz A, Mochly-Rosen D, Sznajder J.(2002) **Dopamine-induced exocytosis of the Na,K-ATPase is dependent on the activation of protein kinase C delta and epsilon**. *Mol. Biol. Cell* 13: 1381–1389. |

Ridge KM, Olivera WG, Saldias F, Azzam A, Horowitz S, Rutschman DH, Dumasius V, Factor P, Sznajder JI. (2003) **Alveolar type 1 cells express the alpha2 Na,K-ATPase, which contributes to lung liquid clearance.** *Circ. Res*. 92: 453–460. |

Rosen H, Glukhman V, Feldmann T, Fridman E, Lichtstein D. (2004) **Cardiac steroids induce changes in recycling of the plasma membrane in human NT2 cells.** *Mol. Biol. Cell* 15: 1044–1054. |

Rosenfeldt MT, Ryan KM. (2009) **The role of autophagy in tumour development and cancer therapy.** *Expert Rev Mol Med.* 11:e36.

Rossi G, Manunta P, Hamlyn JM, Pavan E, De Toni R, Semplicini A, Pessina AC. (1995). **Immunoreactive endogenous ouabain in primary aldosteronism and essential hypertension: relationship with plasma renin, aldosterone and blood pressure levels.** *J Hypertens* 13: 1181-1191.

Rossoni LV, Salaices M, Marìn J, Vassallo DV, Alonso MJ. (2002). **Alterations in phenylephrine-induced contractions and the vascular expression of Na+,K+-ATPase in ouabain-induced hypertension.** *Br. J. Pharmacol.* 135: 771-781.

Roy S, Debnath J. (2010) **Autophagy and tumorigenesis.** *Semin Immunopathol*. 32: 383–396

Russo JJ, Sweadner KJ. (1993) **Na/K-ATPase subunit isoform pattern modification by mitogenic insulin concentration in 3T3–L1 preadipocytes.** *Am J Physiol* 264:C311–

C316.

Sakai H, Suzuki T, Maeda M, Takahashi Y, Horikawa N, Minamimura T, Tsukada K, Takeguchi N. (2004) **Up-regulation of Na/K-ATPase alpha 3-isoform and down-regulation of the alpha 1-isoform in human colorectal cancer**. *FEBS Lett*. 565: 151–154.

Sakai H, Suzuki T, Maeda M, Takahashi Y, Horikawa N, Minamimura T, Tsukada K, Takeguchi N. (2004) **Up-regulation of Na/KATPase alpha 3-isoform and down-regulation of the alpha 1-isoform in human colorectal cancer.** *FEBS Lett.* 563: 151–154.

Sakai H, Suzuki T, Maeda M, Takahashi Y, Horikawa N, Minamimura T, Tsukada K, Takeguchi N. (2004) **Up-regulation of Na(+),K(+)-ATPase alpha 3-isoform and down-regulation of the alpha1-isoform in human colorectal cancer.** *FEBS Lett*. 563: 151-154.

Salvesen GS, Dixit VM. (1997) **Caspases: intracellular signaling by proteolysis.** *Cell* 91: 443-446.

Saunders R, Scheiner-Bobis G. (2004) **Ouabain stimulates endothelin release and expression in human endothelial cells without inhibiting the sodium pump**. *Eur J Biochem.* 271: 1054-62

Savill J, Fadok V (2000) **Corpse clearance defines the meaning of cell death.** *Nature* 407:784–788

Scheiner-Bobis G. (2002) **The sodium pump. Its molecular properties and mechanics of ion transport.** *Eur. J. Biochem.* 269: 2424–2433.

Scherz-Shouval R, Weidberg H, Gonen C, Wilder S, Elazar Z, Oren M (2010) **p53-dependent regulation of autophagy protein LC3 supports cancer cell survival under prolonged starvation.** *Proc Natl Acad Sci USA* 107: 18511–18516

Schinzel A, Kaufmann T, Borner C. (2004**) Bcl-2 family members: integrators of survival and death signals in physiology and pathology** . *Biochim. Biophys. Acta*, 1644: 95–105.

Schoner W, Scheiner-Bobis G (2007) **Endogenous and exogenous cardiac glycosides: their roles in hypertension, salt metabolism, and cell growth** *Am J Physiol Cell Physiol* 293:C509-C536.

Schoner W, Scheiner-Bobis G. (2005). **Endogenous cardiac glycosides: hormones using the sodium pump as signal transducer.** *Semin Nephrol.* 25(5):343-51.

Schwinger RHG, Wang J, Frank K, Muller-Ehmsen J, Brixius K, McDonough AA, Erdmann E. (1999) **Reduced sodium pump a1-, a3-, and b1-isoform protein levels and Na,K-ATPase activity but unchanged Na/Ca exchanger protein levels in human heart failure.** *Circulation* 99: 2105–2112.

Scovassi AI, Torriglia A (2003**) Activation of DNA-degrading enzymes during apoptosis.** *Eur J Histochem* 47:185–194

Seglen PO, Gordon PB. (1982) **3-Methyladenine: specific inhibitor of autophagic/lysosomal protein degradation in isolated rat hepatocytes.** *Proc Natl Acad Sci U S A.* 79: 1889-1892.

Shamraj O, Grupp I, Grupp G, Melvin D, Gradoux N, Kremers W, Linqrel J, De Pover A. (1993) **Characterization of Na/K-ATPase, its isoforms, and the inotropic response to ouabain in isolated failing hearts.** *Cardiovasc Res* 72: 2229–22237

Shamraj OI, Lingrel JB. (1994) **A putative fourth Na,K-ATPase α-subunit gene is expressed in testis.** *Proc Natl Acad Sci U S A* 91:12952–12956.

Sharabani-Yosef O, Bak A, Langzam L, Lui Z, Nir U, Braiman L, Sweadner KJ, Sampson SR. (1999) **Rat skeletal muscle in culture expresses the alpha1 but not the alpha2 protein subunit isoform of the Na+/K+ pump.** *J. Cell. Physiol*. 180: 236–244.

Shen SS, Hamamoto ST, Bern HA, Steinhardt RA. (1978) **Alteration of sodium transport in mouse mammary epithelium associated with neoplastic transformation.** *Cancer Res.* 38: 1356–1361.

Shimizu S, Kanaseki T, Mizushima N, Mizuta T, Arakawa-Kobayashi S, Thompson CB, Tsujimoto Y. (2004) **Role of Bcl-2 family proteins in a non-apoptotic programmed cell death dependent on autophagy genes.** *Nat Cell Biol.* 6: 1221-1228.

Simonsen A, Tooze SA. (2009) **Coordination of membrane events during autophagy by multiple class III PI3-kinase complexes.** *J Cell Biol*. 186: 773–782

Skou JC. (1957) **The influence of some cations on an adenosinetriphosphatase from peripheral nerves.** *Biochim. Biophys. Acta* 23: 394–401

Skou JC. (1992) **The Na-K pump.** *News Physiol. Sci.* 7: 95–100.

Slee EA, Zhu H, Chow SC, MacFarlane M, Nicholson DW, Cohen GM. (1996) **Benzyloxycarbonyl-Val-Ala-Asp (OMe) fluoromethylketone (Z-VAD.FMK) inhibits apoptosis by blocking the processing of CPP32.** *Biochem J.* 315: 21-24.

Smith JA, Madden T, Vijjeswarapu M, Newman R A.(2001) **Inhibition of export of fibroblast growth factor-2 (FGF-2) from the prostate cancer cell lines PC3 and DU145 by Anvirzel and its cardiac glycoside component, oleandrin.** *Biochem. Pharmacol*. 62: 469–472

Srinivasula SM, Ashwell JD (2008**) IAPs: what's in a name?** *Mol Cell.* 30:123–135.

Stenkvist B, Bengtsson E, Eklund G, Eriksson O, Holmquist J, Nordin B, Westman-Naeser S. (1980) **Evidence of a modifying influence of heart glycosides on the development of breast cancer.** *Anal. Quant. Cytol*. 2: 49–54.

Stenkvist B, Pengtsson E, Dahlquist B, Eriksson O, Jarkrans T, Nordin B. (1982) **Cardiac glycosides and breast cancer, revisited.** *N. Engl. J. Med.* 306: 484.

Stenkvist B, Westman-Naeser S, Holmquist J, Nordin B, Bengtsson E, Vegelius J, Eriksson O Fox FH. (1978) **Computerized nuclear morphometry as an objective method for characterizing human cell populations.** *Cancer Res.* 38:4688–4697

Stenkvist B. (1999) **Is digitalis a therapy for breast carcinoma?** *Oncol. Rep*. 6: 493–496.

Subramaniam S, Unsicker K. (2006) **Extracellular signal-regulated kinase as an inducer of non-apoptotic neuronal death.** *Neuroscience* 138: 1055–1065

Suzuki S, Zuege D, Berthiaume Y. (1995) **Sodium-independent modulation of Na(+)-K(+)-ATPase activity by beta-adrenergic agonist in alveolar type II cells.** *Am. J.*

Physiol. 268: L983–L990.

Svensson A, Azarbayjani F, Backman U, Matsumoto T, Christofferson R. (2005) **Digoxin inhibits neuroblastoma tumor growth in mice.** *Anticancer Res.* 25: 207–212.

Sweadner KJ (1989) **Isozymes of the Na+/K+-ATPase.** *Biochim. Biophys. Acta* 988: 185–220.

Sznajder JI, Factor P, Ingbar DH. (2002) **Invited review: lung edema clearance: role of Na(+)-K(+)-ATPase.** *J. Appl. Physiol* 93: 1860–1866.

Tasdemir E, Maiuri MC, Galluzzi L, Vitale I, Djavaheri-Mergny M, D'Amelio M, Criollo A, Morselli E, Zhu C, Harper F, Nannmark U, Samara C, Pinton P, Vicencio JM, Carnuccio R, Moll UM, Madeo F, Paterlini-Brechot P, Rizzuto R, Szabadkai G, Pierron G, Blomgren K, Tavernarakis N, Codogno P, Cecconi F, Kroemer G. (2008**) Regulation of autophagy by cytoplasmic p53.** *Nat Cell Biol* 10: 676–687

Therien AG, Blostein R. (2000) **Mechanisms of sodium pump regulation** *Am. J. Physiol*. 279: C541–C566.

Thornberry NA, Lazebnik Y. (1998) **Caspases: enemies within.** *Science* 281: 1312-1316.

Tian J, Cai T, Yuan Z, Wang H, Liu L, Haas M, Maksimova E, Huang XY, Xie ZJ. (2006) **Binding of Src to Na/K-ATPase forms a functional signaling complex.** *Mol Biol Cell* 17: 317–326

Tian J, Gong X, Xie Z. (2001**) Signal-transducing function of Na/K-ATPase is essential for ouabain's effect on [Ca^{2+}]i in rat cardiac myocytes.** *Am J Physiol Heart Circ Physiol* 281: H1899–H1907

Tian J, Li X, Liang M, Liu L, Xie JX, Ye Q, Kometiani P, Tillekeratne M, Jin R, Xie Z. (2009) **Changes in sodium pump expression dictate the effects of ouabain on cell growth.** *J Biol Chem.* 284: 14921-14929.

Tian J, Liu J, Garlid KD, Shapiro JI, Xie Z.(2003) **Involvement of mitogenactivated protein kinases and reactive oxygen species in the inotropic action of ouabain on cardiac myocytes. A potential role for mitochondrial KATP channels.** *Mol Cell Biochem* 242: 181–187

Torriglia A, Lepretre C (2009) **LEI/L-DNase II: interplay between caspase-dependent and independent pathways.** *Front Biosci* 14:4836–4847

Torriglia A, Perani P, Brossas JY, Altairac S, Zeggai S, Martin E, Tréton J, Courtois Y, Counis MF. (2000) **A caspase-independent cell clearance program. The LEI/L-DNase II pathway.** *Ann N Y Acad Sci*. 926: 192-203.

Trevisi L, Pighin I, Bazzan S, Luciani S. (2006) **Inhibition of 3-(4,5-dimethylthiazol-2-yl)-2,5-diphenyltetrazolium bromide (MTT) endocytosis by ouabain in human endothelial cells.** *FEBS Lett*. 580: 2769-2773.

Trevisi L, Visentin B, Cusinato F, Pighin I, Luciani S. (2004) **Antiapoptotic effect of ouabain in human umbilical vein endothelial cells.** *Biochem Biophys Res Commun* 321: 716–721

Urayama O, Shutt H, Sweadner KJ. (1989) **Identification of three isozyme proteins of the catalytic subunit of the Na,K-ATPase in rat brain**. *J Biol Chem* 264**:**8271–8280.

Van Quaquebeke E, Simon G, Andre A, Dewelle J, Yazidi M EI, Bruyneel F, Tuti J, Nacoulma O, Guissou P, Decaestecker C, Braekman JC, Kiss R, Darrot F. (2005) **Identification of a novel cardenolide (2-oxovoruscharin) from *Calotropis procera* and the hemisynthesis of novel derivatives displaying potent in vitro antitumor activities and high in vivo tolerance: structure-activity relationship analyses.** *J Med Chem* 48: 849–856

Vande Walle L, Lamkanfi M, Vandenabeele P (2008) **The mitochondrial serine protease HtrA2/Omi: an overview.** *Cell Death Differ* 15:453–460

Vander Heiden MG, Chandel NS, Williamson EK, Schumacker PT, Thompson CB (1997) **Bcl-xL regulates the membrane potential and volume homeostasis of mitochondria.** *Cell* 91:627–637

Viola G, Bortolozzi R, Hamel E, Moro S, Brun P, Castagliuolo I, Ferlin MG, Basso G. (2012) **MG-2477, a new tubulin inhibitor, induces autophagy through inhibition of the Akt/mTOR pathway and delayed apoptosis in A549 cells.** *Biochem Pharmacol.* 83: 16-26.

Wade OL. (1986) **Digoxin 1785-1985. I. Two hundred years of digitalis.** *J. Clin. Hosp. Pharm*. 11: 3-9

Wang H, Haas M, Liang M, Cai T, Tian J, Li S, Xie Z. (2004) **Ouabain assembles signaling cascades through the caveolar Na/K-ATPase.** *J. Biol. Chem*. 279: 17250–17259.

Wang H, Haas, M, Cai, T, Xie, Z. (2003). **Sodium pump as a signal transducer: A role of caveolae.** *Biophysical J*. 83: 268a.

Wang Y, Dawson VL, Dawson TM (2009) **Poly(ADP-ribose) signals to mitochondrial AIF: a key event in parthanatos.** *Exp Neurol* 218:193–202

Wang ZB, Liu YQ, Cui YF. (2005) **Pathways to caspase activation.** *Cell Biol Int.* 29: 489-496.

Watabe M, Ito K, Masuda Y, Nakajo S, Nakaya, K. (1998) **Activation of AP-1 is required for bufalin-induced apoptosis in human leukemia U937 cells.** *Oncogene* 16 , 779–787.

Watabe M, Kawazoe N, Masuda Y, Nakajo S, Nakaya K. (1997) **Bcl-2 protein inhibits bufalin-induced apoptosis through inhibition of mitogen-activated protein kinase activation in human leukemia U937 cells.** *Cancer Res.* 57, 3097–3100.

Watabe M, Masuda Y, Nakajo S, Yoshida T, Kuroiwa Y, Nakaya, K. (1996) **The cooperative interaction of two different signaling pathways in response to bufalin induces apoptosis in human leukemia U937 cells.** *J. Biol. Chem*. 271: 14067-14073

Waters CM, Ridge KM, Sunio G, Venetsanou K, Sznajder JI. (1999) **Mechanical stretching of alveolar epithelial cells increases Na^+-K^+-ATPase activity.** *J. Appl. Physiol*. 87: 715-721.

Weidemann H. (2005) **Na/K-ATPase, endogenous digitalis-like compounds and cancer development—A hypothesis.** *Front. Biosci*. 10: 2165–2176.

Weinander R, Anderson C, Morgenstern R. (1994) **Identification of N-acetylcysteine as a new substrate for rat liver microsomal glutathione transferase. A study of thiol ligands.** *J. Biol. Chem.* **269: 71-76**

Wilson BE, Mochon E, Boxer LM. (1996) **Induction of bcl-2 expression by phosphorylated CREB proteins during B-cell activation and rescue from apoptosis.** *Mol. Cell. Biol.* 16: 5546–5556

Wilson IG (1997) **Inhibition and facilitation of nucleic acid amplification**. *Applied and Environmental Microbiology, 63: 3741-3751.*

Wirawan E, Vande Walle L, Kersse K, Cornelis S, Claerhout S, Vanoverberghe I, Roelandt R, De Rycke R, Verspurten J, Declercq W, Agostinis P, Vanden Berghe T, Lippens S, Vandenabeele P. (2010) **Caspase-mediated cleavage of Beclin-1 inactivates Beclin-1-induced autophagy and enhances apoptosis by promoting the release of proapoptotic factors from mitochondria.** *Cell Death Dis.* 1:e18.

Withering W. (1985) **An account of the foxglove, and some of its medical uses with practical remark on dropsy and other diseases.** *Robinson, London* p 207

Xiao AY, Wei L, Xia S, Rothman S, Yu SP. (2002) **Ionic mechanism of ouabain-induced concurrent apoptosis and necrosis in individual cultured cortical neurons.** *J. Neurosci.* 22, 1350–1362.

Xie CM, Chan WY, Yu S, Zhao J, Cheng CH. (2011) **Bufalin induces autophagy-mediated cell death in human colon cancer cells through reactive oxygen species generation and JNK activation.** *Free Radic Biol Med.* 51: 1365-1375.

Xie Z, Askari A.(2002) **Na/K-ATPase as a signal inducer.** *Eur J Biochem* 269: 2434–2439

Xie Z, Klionsky DJ. (2007) **Autophagosome formation: Core machinery and adaptations.** *Nat Cell Biol.* 9: 1102–1109.

Xie Z, Kometiani P, Liu J, Li J, Shapiro JI, Askari A. (1999) **Intracellular reactive oxygen species mediate the linkage of Na/K-ATPase to hypertrophy and its marker genes in cardiac myocytes.** *J Biol Chem* 274: 19323–19328

Xie Z. and Cai T. (2003) **Na+-K+-ATPase-mediated signal transduction: from protein interaction to cellular function.** *Mol. Interv.* 3: 157-168.

Yang P, Menter DG, Cartwright C, Chan D, Dixon S, Suraokar M, Mendoza G, Llansa N,

Newman RA. (2009) **Oleandrin-mediated inhibition of human tumor cell proliferation: importance of Na,K-ATPase alpha subunits as drug targets.** *Mol Cancer Ther*. 8: 2319-28.

Yang Z, Klionsky DJ (2010**) Eaten alive: a history of macroautophagy.** *Nat Cell Biol* 12:814–822.

Youle RJ, Strasser A. (2008) **The BCL-2 protein family: opposing activities that mediate cell death.** *Nat. Rev. Mol. Cell Biol*.**9:** 47–59.

Yousefi S, Perozzo R, Schmid I, Ziemiecki A, Schaffner T, Scapozza L, Brunner T, Simon HU. (2006) **Calpain-mediated cleavage of Atg5 switches autophagy to apoptosis.** *Nat Cell Biol* 8: 1124–1132

Yu CL, Xie ZJ, Askari A, Modyanov NN. (1997) **Enzymatic properties of human Na,K-ATPase α1β3 isozyme.** *Arch. Biochem. Biophys.* 345: 143–149

Yu L, Alva A, Su H, Dutt P, Freundt E, Welsh S, Baehrecke EH, Lenardo MJ. (2004) **Regulation of an ATG7-beclin 1 program of autophagic cell death by caspase-8.** *Science* 304: 1500-1502.

Yuan CM, Manunta P, Hamlyn JM, Chen S, Bohen E, Yeun J, Haddy FJ, Pamnani MB. (1993). **Long term ouabain produces hypertension in rats.** *Hypertension* **22:** 178–187.

Yudowski GA, Efendiev R, Pedemonte CH, Katz AI, Berggren PO, Bertorello AM. (2000) **Phosphoinositide-3 kinase binds to a proline-rich motif in the Na,K-ATPase α-subunit and regulates its trafficking.** *Proc Natl Acad Sci USA* 97: 6556–6561

Zahler R, Brines M, Kashgarian M, Benz EJ, Gilmore-Hebert M. (1992) **The cardiac conduction system in the rat expresses the !2 and !3 isoforms of the Na/K ATPase.** *Proc Natl Acad Sci U S A* **89:**99–103.

Zalckvar E, Berissi H, Mizrachy L, Idelchuk Y, Koren I, Eisenstein M, Sabanay H, Pinkas-Kramarski R, Kimchi A. (2009) **DAP-kinase-mediated phosphorylation on the BH3 domain of beclin 1 promotes dissociation of beclin 1 from Bcl-XL and induction of autophagy.** *EMBO Rep* 10: 285–292

Zha J, Harada H, Yang E, Jockel J, Korsmeyer SJ. (1996**). Serine phosphorylation of**

death agonist BAD in response to survival factor results in binding to 14-3-3 not BCL-X(L). *Cell*.87: 619-628.

Zhang J, Lee MY, Cavalli M, Chen L, Berra-Romani R, Balke CW, Bianchi G, Ferrari P, Hamlyn JM, Takahiro I, Lingrel JB, Matteson DR, Wier WG, Blaustein MP. (2005) **Sodium pump α2-subunits control myogenic tone and blood pressure in mice.** *J Physiol* 569: 243–256

Zhang Z, Devarajan P, Dorfman AL, Morrow JS. (1998) **Structure of the ankyrin-binding domain of alpha-Na, K-ATPase.** *J. Biol. Chem.* 273: 18681–18684.

Zhong Y, Wang QJ, Li X, Yan Y, Backer JM, Chait BT *et al.* (2009) **Distinct regulation of autophagic activity by Atg14L and Rubicon associated with Beclin 1-phosphatidylinositol-3-kinase complex.** *Nat Cell Biol.* 11: 468–476

Zhou F, Yang Y, Xing D. (2011) **Bcl-2 and Bcl-xL play important roles in the crosstalk between autophagy and apoptosis.** *FEBS J* 278:403–413

Zhou X, Jiang G, Zhao A, Bondeva T, Hirrszel P, Balla T. (2001) **Inhibition of Na,K-ATPase activates PI3 kinase and inhibits apoptosis in LLC-PK1 cells.** *Biochem. Biophys. Res. Commun.* 285,46-51.

Acknowledgement

I am especially grateful to my supervisor, dott. ssa Lucia Trevisi. I began under her guide my adventure in the field of pharmacology in Autum 2007.

Thanks to Prof. Pietro Giusti for giving me the opportunity to taking up this experience.

I would also like to thank Prof Paola Patrignani. I spend a lot of months of my PhD in her laboratory and she always given me valuable comments and suggestion.

Thanks to Federico for the help with cytofluorimetric experiment and to all of the technical staff for the nice talking.

These years of study for the Ph.D have been also cheered up by the friends with common passions and interests. In particular I would like to thank Emanuela, Chiara, Andrea, Vera, Daniele, Luisa. Thank you also to Giulia, Elisa, Vera, Valentina, Melania, Luigia, Annalisa, Stefania, Paoletta.

A constant, illuminanting presence during the preparation of the Thesis has been Luca. He has lived with me this experience, being very supportive and giving words of encouragement.

Finally I would like to thank my family for the continuing love and support during these years.